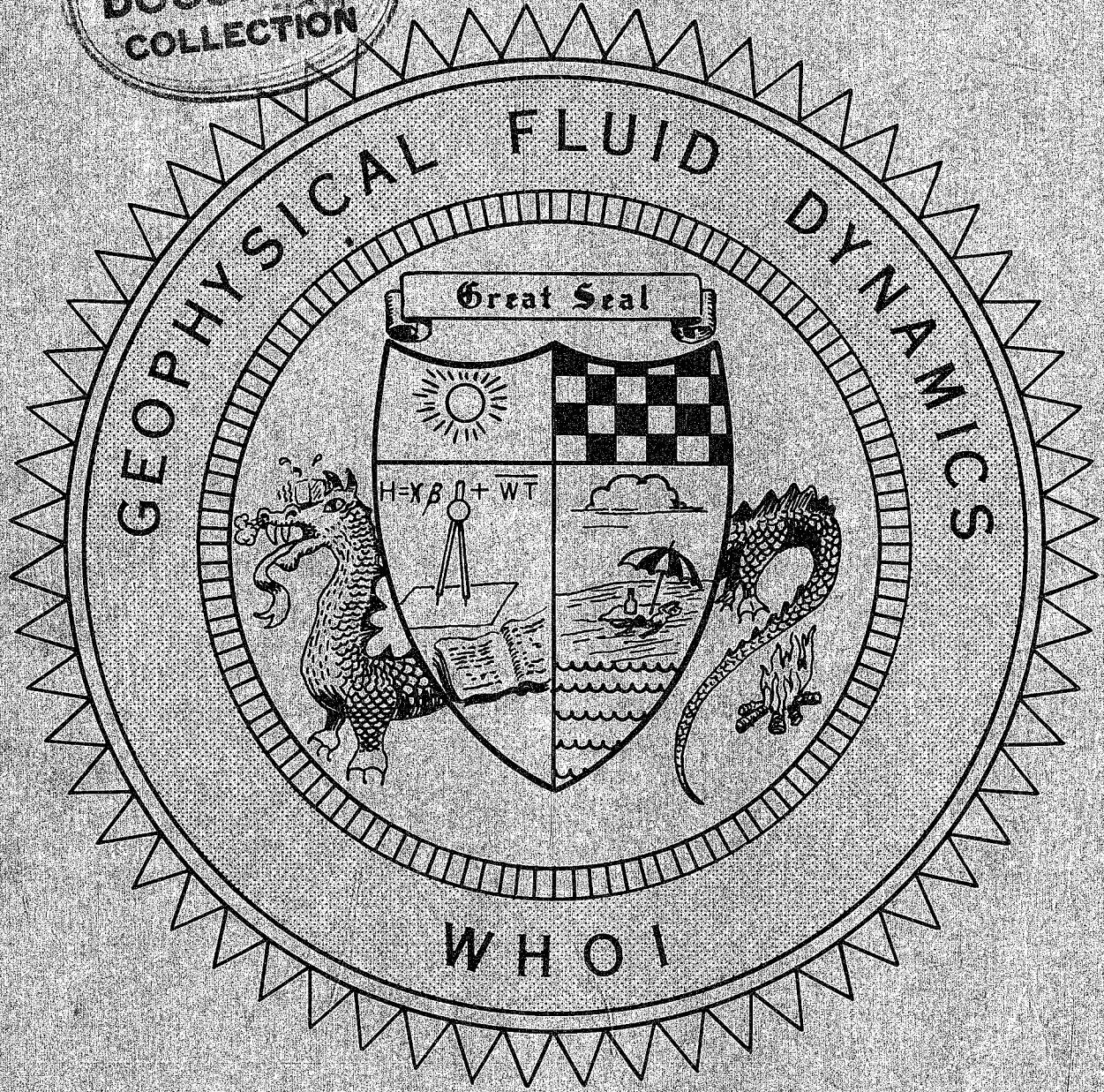


69-41
1969 *Copy 1*

VOLUME I

WHOI
DOCUMENT
COLLECTION



COURSE LECTURES
AND
ABSTRACTS OF SEMINARS

Notes on the 1969
Summer Study Program
in
GEOPHYSICAL FLUID DYNAMICS
at

The WOODS HOLE OCEANOGRAPHIC INSTITUTION



Reference No. 69-41

Contents of the Volumes

Volume I Course Lectures and Abstracts of Seminars

Volume II Fellowship Lectures

1969

Participants and Staff Members

Anderson, James L.	Stevens Institute of Technology
Backus, George	University of California at San Diego
Busse, Friedrich	University of California at Los Angeles
Eichenbaum, B.R.	New York University
Gough, Douglas O.	Institute of Space Studies, N.Y.U.
Harrison, Edward R.	University of Massachusetts
Keller, Joseph B.	New York University
Kraichnan, Robert H.	Peterborough, New Hampshire
Longuet-Higgins, Michael	Oregon State University
Malkus, Willem V.R.	University of California at Los Angeles
Mestel, Leon	Cambridge University, England
Prendergast, Kevin	Columbia University
Reiss, Edward L.	Courant Institute, N.Y.U.
Spiegel, Edward A.	New York University
Toomre, Alar	Massachusetts Institute of Technology
Toomre, Juri	Institute of Space Studies, N.Y.U.
Zahn, Jean-Paul	Institute of Space Studies, N.Y.U.

Fellows

Auré, Jean-Luc	Astrophysics	Inst.d'Astrophysics, Paris, France
Barker, Terrance G.	Geophysics	Massachusetts Institute of Technology
Buschi, Joseph M.	Physics	New York University
Defouw, Richard J.	Astronomy	California Institute of Technology
Gans, Roger F.	Geology	University of California, Los Angeles
McKee, William D.	Geophysical Fl.Dynamics	Cambridge University, England
Mészáros, Pedro	Astronomy	University of California at Berkeley
Perdang, Jean	Physics	University of Liege, Belgium
Trasco, John D.	Astronomy	Columbia University

Editor's Preface

The principal theme of this eleventh Summer Program has been Astrophysical Fluid Dynamics. As in the past, we have explored the region of overlap in technique and theory of our summer theme and other aspects of Fluid Dynamics. An interesting example of this overlap is the application of the physics of salt-finger instability, a significant oceanographic process, to instabilities due to differential rotation in the sun, a critical problem in stellar evolution.

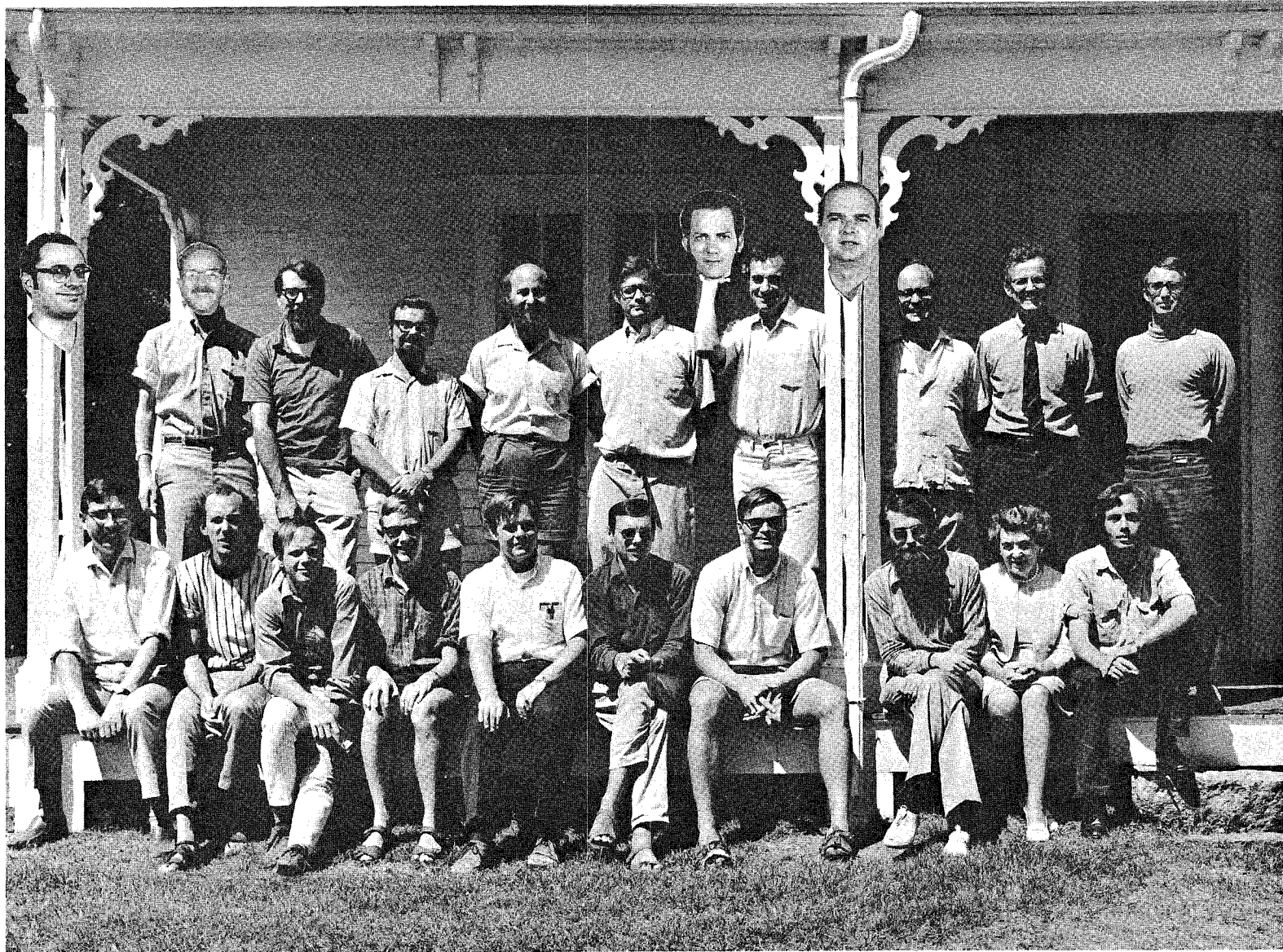
Drs. Spiegel, Prendergast, Keller, Toomre and Zahn introduced Staff and Fellows to topics ranging from waves in the galactic disk to non-linear perturbation theory. This volume contains a restatement by the Fellows of these introductory lectures. A stated purpose of these lectures was to provide an interesting class of unsolved problems and techniques to attack them. I fear this grand purpose was achieved only in part, for enthusiastic scientists often drift from pedagogy to proselytization.

Following these notes, abstracts of the summer research seminars are recorded. These were prepared by their authors as extended abstracts, to clearly indicate novel content and appropriate references. The editor finds, the reader will find, that this goal is difficult to achieve.

Mrs. Mary Thayer has done all the work in assembling and reproducing the lectures. We are all indebted to her for her navigational skills as we beat along each summer course.

We are also indebted to the National Science Foundation for financial support and to the Woods Hole Oceanographic Institution for encouragement and shelter.

Willem V.R. Malkus



Standing (left to right): Buschi (posted), Stern, Prendergast, Gough, Keller, Kraichnan, Spiegel (being supported by Veronis), Toomre (pillared), Harrison, Backus, Malkus.
Seated: Zahn, Defouw, Gans, McKee, Trasco, Perdang, Barker, Auré, Thayer, Mészáros.

CONTENTS OF VOLUME I

Course Lectures and Seminars

	Page No.
Perturbation Theory (I) Dr. Joseph B. Keller	1
Perturbation Theory (II) Dr. Joseph B. Keller	15
A Scaling and Expansion of Equations of Motion to yield the Boussinesq Equations Dr. Willem V.R. Malkus	23
Self-Gravitating Stellar Systems Dr. Kevin H. Prendergast	29
Structure of Barred Spirals Dr. Kevin H. Prendergast	34
Machine Simulation of Galactic Evolution Dr. Kevin H. Prendergast	43
Fluid Dynamical Phenomena in the Sun Dr. Edward A. Spiegel	48
Decrease in the Rotation Rate of the Sun Dr. Edward A. Spiegel	61
Waves in Galactic Disks Dr. Alar Toomre	66
Worlds in Collision (Almost) Dr. Alar Toomre	72
Total Effects in Double Stars Dr. Jean-Paul Zahn	83

CONTENTS OF VOLUME I (continued)

ABSTRACTS

	Page No.
Abstracts	101
Geophysical Inverse Problems	103
Dr. George E. Backus	
The Optimal Structure of Turbulent Transport Processes	104
Dr. Freidrich Busse	
Differential Rotation in Stellar Convection Zones	107
Dr. Freidrich Busse	
An Approach to Thermal Convection	108
Dr. Douglas O. Gough	
Baryon Inhomogeneity in the Early Universe	109
Dr. Edward R. Harrison	
Report on the Boeing Turbulence Symposium	110
Dr. Robert H. Kraichnan	
Convergents to Turbulence Functions	111
Dr. Robert H. Kraichnan	
The Generation of Longshore Currents	113
Dr. Michael Longuet-Higgins	
On Multi-variable Asymptotic Expansions	115
Dr. Edward L. Reiss	
Acoustic Waves in Rapidly Varying Inhomogeneous Fluids	122
Dr. Edward L. Reiss	
Time-dependent Cellular Convection	126
Dr. Juri Toomre	
Magnetic Braking and the Oblique Rotator Model	129
Dr. Leon Mestel	

Additional Seminars

Relativistic Radiative Transfer Theory

James L. Anderson

High Resolution Time-Dependent Observations of the Solar Spectrum

(thesis defense) B.R.Eichenbaum

Magnetic Braking and the Oblique Rotator

Leon Mestel

PERTURBATION THEORY (I)

Joseph B. Keller

Definitions

Perturbation theory is the study of a function $u(\varepsilon)$ in the neighborhood of a point ε_0 .

A function $u(\varepsilon)$ is a point in a Hilbert space \mathcal{H} . The concept of neighborhood is to be understood in the following sense: If $h > 0$, the open set $N(\varepsilon_0, h) = (\varepsilon_0 - h, \varepsilon_0 + h)$ is called a neighborhood with center ε_0 and radius h . Knowing a solution $u(\varepsilon)$ of a given problem for a special value $\varepsilon = \varepsilon_0$, the aim of perturbation theory is to extend this solution to the neighborhood $N(\varepsilon_0, h)$. One distinguishes two kinds of perturbation theories, the regular and the singular perturbation theory.

Regular or Ordinary Perturbation Theory

ε_0 is a regular point of $u(\varepsilon)$ i.e. $u(\varepsilon)$ is continuous and admits of derivatives of all orders at $\varepsilon = \varepsilon_0$. In that case the function $u(\varepsilon)$ may be represented by a Taylor expansion

$$u(\varepsilon) = \sum_{k=0}^n \frac{\varepsilon^k}{k!} \left[\frac{\partial^k}{\partial \varepsilon^k} u \right]_{\varepsilon=0} + R_n(\varepsilon) \quad (1)$$

$R_n(\varepsilon)$ being the remainder. In this expression we have translated the regular point ε_0 to the origin.

Making use of the Landau notations

$$\begin{aligned} f(\varepsilon) = o[g(\varepsilon)] &\iff \lim_{\varepsilon \rightarrow 0} f(\varepsilon)/g(\varepsilon) = 0 \\ f(\varepsilon) = O[g(\varepsilon)] &\iff \lim_{\varepsilon \rightarrow 0} |f(\varepsilon)/g(\varepsilon)| \leq B \end{aligned} \quad (2)$$

B being a positive constant, the remainder has the property

$$R_n(\varepsilon) = o(\varepsilon^n) \quad (*)$$

A special case arises if $u(\varepsilon)$ is an analytic function of ε (analytic case). By definition, $u(z)$ is analytic in Ω if its complex derivative $u'(z)$ exists at every point of Ω . The existence of $u'(z)$ implies its continuity; Cauchy's integral formula implies the existence of the complex derivatives of all orders. In the analytic case, the Taylor series is always convergent for $|\varepsilon - \varepsilon_0| < \varepsilon_1$, ε_1 being a sufficiently small positive constant.

For practical purposes, the analyticity of $u(\varepsilon)$, or the convergence of the series (1) is not required. It is sufficient to know that the remainder $R_n(\varepsilon)$ is "sufficiently small".

Singular Perturbation Theory (Asymptotics)

ε_0 is a singular point of $u(\varepsilon)$, i.e. $u(z)$ being considered as a complex-valued function defined in Ω , it is not analytic at $z = \varepsilon_0$, but analytic in an open annulus $A(\varepsilon_0, r_1, r_2)$ of radii $r_1, r_2 > 0$. (The singularity is a pole of order n if $(z - \varepsilon_0)^n u(z)$ is analytic in ε_0 ; it is an essential singularity if for any n $(z - \varepsilon_0)^n u(z)$ remains non-analytic at $z = \varepsilon_0$).

Regular Perturbation Theory

Position of the problem

The solution $u(\varepsilon)$ of the following general system

(*) The remainder may be written in one of the following forms

$$R_n(\varepsilon) = \frac{\varepsilon^{n+1}}{n!} \int_0^1 dt (1-t)^n \left[\frac{\partial^{n+1}}{\partial \varepsilon^{n+1}} u \right]_{\varepsilon t} = \begin{cases} \frac{\varepsilon^{n+1}}{(n+1)!} \left[\frac{\partial^{n+1}}{\partial \varepsilon^{n+1}} u \right]_{\varepsilon \theta} & \text{(Lagrange)} \\ \frac{\varepsilon^{n+1}}{n!} (1-\theta)^n \left[\frac{\partial^{n+1}}{\partial \varepsilon^{n+1}} u \right]_{\varepsilon \theta} & \text{(Cauchy)} \\ \theta \in (0,1) \end{cases}$$

$$F(\varepsilon, u(\varepsilon)) = 0 \quad (3)$$

is to be found in $N(0, h)$ where F is a generally non-linear operator, depending on ε . The operator F is supposed to be regular in ε and in u , so that the derivatives of all orders $F_u(\varepsilon, u(\varepsilon)), F_\varepsilon(\varepsilon, u(\varepsilon)), \dots, F_{u u \dots \varepsilon \varepsilon \dots}(\varepsilon, u(\varepsilon))$ exist in some neighborhood $N(0, h)$. The existence of a solution u_0 of (3) is postulated for $\varepsilon = 0$, and is assumed to be known explicitly.

In a practical problem it is generally not possible to know a priori if the conditions of applicability of the regular perturbation theory are fulfilled i.e. if $\varepsilon = 0$ is a regular point of $u(\varepsilon)$. This information can only be obtained a posteriori: if one finds that the n^{th} derivative of $u(\varepsilon)$ does not exist, one concludes that $\varepsilon = 0$ is a singular point of $u(\varepsilon)$.

Solution

The solution $u(\varepsilon)$ in $N(0, h)$ is given by a Taylor expansion at the point $\varepsilon = 0(1)$. One thus needs the derivatives $[\partial^k / \partial \varepsilon^k u]_{\varepsilon=0}$, which are readily obtained by successive differentiations of (3) with respect to ε .

1st derivative:

$$F_\varepsilon(\varepsilon, u(\varepsilon)) + F_u(\varepsilon, u(\varepsilon)) u_\varepsilon(\varepsilon) = 0 \quad (4)$$

This equation is a linear, non-homogeneous equation in the first derivative of the solution u_ε . If we assume that the operator $F_u(\varepsilon, u(\varepsilon))$ is regular at $\varepsilon = 0$, we may write

$$u_\varepsilon(0) = -F_u^{-1}(0, u_0) F_\varepsilon(0, u_0) \quad (5)$$

u_0 being the solution at $\varepsilon = 0$. This shows that if $F_\varepsilon(0, u_0) = 0$, then

$u_\varepsilon = 0$. The only way to obtain a non-zero u_ε is to assume that the

$F_u(0, u_0)$ operator is singular. We recall that a linear operator L

defined in a Hilbert space \mathcal{H} is said to be regular if it does not admit of zero eigenvalues. Thus

$$\forall \varphi \in \mathcal{H} \rightarrow L\varphi \neq 0$$

2nd derivative: Applying $\partial^2/\partial \varepsilon^2$ on (3), one obtains a linear equation in

$$u_{\varepsilon\varepsilon}(\varepsilon): F_u(\varepsilon, u(\varepsilon))u_{\varepsilon\varepsilon} + F_{uu}(\varepsilon, u(\varepsilon))(u_\varepsilon)^2 + 2F_{u\varepsilon}(\varepsilon, u(\varepsilon))u_\varepsilon + F_{\varepsilon\varepsilon}(\varepsilon, u(\varepsilon)) = 0$$

Under the previous assumption of regularity of the linear operator $F_u(\varepsilon, u(\varepsilon))$ at $\varepsilon=0$, this equation may be solved

$$u_{\varepsilon\varepsilon}(0) = -F_u^{-1}(0, u_0) \left\{ F_{uu}(0, u_0)(u_\varepsilon(0))^2 + 2F_{u\varepsilon}(0, u_0)u_\varepsilon(0) + F_{\varepsilon\varepsilon}(0, u_0) \right\} \quad (6)$$

All the quantities of the right-hand side are known from (5).

kth derivative: Applying $\partial^k/\partial \varepsilon^k$ on (4) one finds

$$F_u(\varepsilon, u(\varepsilon)) \underbrace{u_{\varepsilon\varepsilon\dots\varepsilon}}_k + \mathcal{F} = 0$$

where \mathcal{F} contains derivatives of u of order $k-1$ at most, which are known

from the previous steps of calculation. The latter equation thus gives

$u_{\varepsilon\varepsilon\dots\varepsilon}(0)$ provided $F_u(0, u(0))$ is regular. One concludes that this method completely determines the coefficients in the Taylor expansion (1), provided the linear operator $F_u(0, u(0))$ is invertible.

As one may notice, this technique is considerably simpler than the usual perturbation technique, in which the expansion (1) is introduced in equation (3), and the coefficients of the different powers of ε are put equal to zero.

In the illustrative examples, we make use of the following notation:

$$\text{if } f \equiv f(\varepsilon), f^0 \equiv f(0), \dot{f} \equiv \left[\frac{\partial f}{\partial \varepsilon} \right]_{\varepsilon=0} \quad (7)$$

Examples

1) Acoustic approximation in gas dynamics

Let ρ , s , u_i , p be the mass density, the entropy density, the velocity components, and the pressure. The relevant equations of gas dynamics may be written

$$\rho_t + (\rho u_i)_{x_i} = 0 \quad (\text{continuity equation})$$

$$u_{i_t} + u_j u_{i x_j} + \frac{1}{\rho} p_{x_i} = 0 \quad (\text{momentum equation})$$

$$s_t + (s u_i)_{x_i} = 0 \quad (\text{entropy equation})$$

$$p = p(\rho, s) \quad (\text{equation of state})$$

where the subscripts t and x_i denote partial differentiation with respect to time and spatial coordinates, and where the convention of summation over repeated subscripts i has been used.

These equations are of the form $F(u) = 0$, with

$$u = (u_i, \rho, p, s)$$

The expansion parameter ϵ is assumed to occur only in the boundary conditions, and in the initial conditions.

Suppose that

$$u_0 = (u_i^0, \rho^0, p^0, s^0)$$

is a solution of the system of equations. For initial conditions that differ slightly from u_0 , the equations governing the first approximation (Eq.4) are explicitly

$$\dot{\rho}_t + (\dot{\rho} u_i^0)_{x_i} + (\rho^0 \dot{u}_i)_{x_i} = 0$$

$$\dot{u}_{i_t} + \dot{u}_j u_{i x_j}^0 + u_j^0 \dot{u}_{i x_j} + \frac{1}{\rho^0} \dot{p}_{x_i} - \frac{1}{(\rho^0)^2} \dot{\rho} p_{x_i}^0 = 0$$

$$\dot{s}_t + (\dot{s} u_i^0)_{x_i} + (s^0 \dot{u}_i)_{x_i} = 0$$

$$\dot{p} - p_\rho^0(\rho^0, s^0) \dot{\rho} - p_s^0(\rho^0, s^0) \dot{s} = 0$$

which correspond to the usual acoustic equations. The dotted quantities represent the acoustic variables, whereas the undotted variables describe the basic flow. The latter equations are of the form (4) with

$$u_\varepsilon = (\dot{u}_i, \dot{p}, \dot{p}, \dot{s})$$

$$F_u(0, u_0) = \begin{pmatrix} \delta_{ij} \frac{\partial}{\partial t} + (u_i^0)_{,x_j} + u_j^0 \frac{\partial}{\partial x_j} & -\frac{1}{(\rho^0)^2} p_{x_i}^0 & \frac{1}{\rho^0} \frac{\partial}{\partial x_i} & 0 \\ (\rho^0)_{,x_j} & \frac{\partial}{\partial t} + \frac{\partial}{\partial x_i} u_i^0 & 0 & 0 \\ \frac{\partial}{\partial x_j} s^0 & 0 & 0 & \frac{\partial}{\partial t} + \frac{\partial}{\partial x_i} u_i^0 \\ 0 & -p_p^0 & 1 & -p_s^0 \end{pmatrix}$$

$$F_\varepsilon(0, u_0) = 0$$

2) Vibrating String

Let λ be the Lagrangian variable labelling the points of the string, and assume that the linear density is a function of the position λ . The displacement \underline{x} is a function of λ and of time t . Thus

$$\rho = \rho(\lambda) ; \underline{x} = \underline{x}(\lambda, t)$$

The equation of motion of the string is given by

$$\left. \begin{aligned} \rho \underline{x}_{tt} &= (T \underline{\tau})_{,\lambda} \\ T &= T(|\underline{x}_{,\lambda}|) \\ \underline{\tau} &= \underline{x}_{,\lambda} / |\underline{x}_{,\lambda}| \end{aligned} \right\}$$

where the elastic properties of the string are described by the tension T , and $\underline{\tau}$ is the tangent at the point λ .

As a particular solution this system admits

$$\underline{x}^0 = \lambda \underline{l}$$

\underline{l} being the unit vector along the Ox direction. Indeed

$$\left[\left(T(|\underline{x}_{,\lambda}|) \frac{\underline{x}_{,\lambda}}{|\underline{x}_{,\lambda}|} \right)_{,\lambda} \right]_{\underline{x}=\underline{x}^0} = (T(1) \underline{l})_{,\lambda} = 0$$

The equations describing the vibrating string are of the form (3), with $u = \underline{x}$.

The expansion parameter (ε) is supposed to enter in the initial conditions.

If $u_0 = \underline{x}^0$ corresponds to the case $\varepsilon = 0$, the derivative $\dot{\underline{x}}$ is given by Eq. (4)

$$\dot{\rho} \dot{x}_{tt}^{\circ} + \rho \dot{x}_{tt}^{\circ} = \left\{ T'(|x_{\Delta}^{\circ}|) \frac{x_{\Delta}^{\circ}}{|x_{\Delta}^{\circ}|} \frac{\partial}{\partial \varepsilon} |x_{\Delta}^{\circ}| + T(|x_{\Delta}^{\circ}|) \frac{1}{|x_{\Delta}^{\circ}|} \dot{x}_{\Delta}^{\circ} - T(|x_{\Delta}^{\circ}|) \frac{x_{\Delta}^{\circ}}{|x_{\Delta}^{\circ}|} \frac{\partial}{\partial \varepsilon} |x_{\Delta}^{\circ}| \right\}_{\Delta}$$

where the prime in $T'(|x_{\Delta}^{\circ}|)$ indicates a derivative with respect to the argument $|x_{\Delta}^{\circ}|$. The first term of the left-hand side vanishes as x° is independent of τ . Replacing x° by $\Delta \dot{L}$ we obtain the following linearized string equation

$$\rho^{\circ} \dot{x}_{tt}^{\circ} = \left\{ T'(1) \dot{L} \frac{\partial}{\partial \varepsilon} |x_{\Delta}| + T(1) \dot{x}_{\Delta} - T(1) \dot{L} \frac{\partial}{\partial \varepsilon} |x_{\Delta}| \right\}_{\Delta}$$

Projecting successively on a plane normal to \dot{L} , and on the direction \dot{L} , we derive equations for the transverse ($x_j, j = 2, 3$), and for the longitudinal displacements (x_1).

transverse displacements

$$\rho^{\circ} \dot{x}_{jtt} = T(1) \dot{x}_{j\Delta\Delta}$$

This equation describes ordinary wave propagation with phase velocity $c = (T(1)/\rho^{\circ})^{1/2}$.

longitudinal displacements

$$\rho^{\circ} \dot{x}_{1tt} = T'(1) \frac{\partial}{\partial \varepsilon} |x_{\Delta}| - T(1) \frac{\partial}{\partial \varepsilon} |x_{\Delta}| + T(1) \dot{x}_{1\Delta}$$

One readily sees that the underlined terms cancel. Indeed

$$|x| = (x \cdot x)^{1/2}$$

$$\frac{\partial}{\partial \varepsilon} |x| = \frac{1}{2} (x \cdot x)^{-1/2} 2 \dot{x} \cdot x$$

$$\frac{\partial}{\partial \varepsilon} |x_{\Delta}| = \frac{1}{2} (x_{\Delta} \cdot x_{\Delta})^{-1/2} 2 \dot{x}_{\Delta} \cdot x_{\Delta} = \dot{x}_{\Delta} \cdot \dot{L} = \dot{x}_{1\Delta}$$

Thus

$$\rho^{\circ} \dot{x}_{1tt} = T'(1) \dot{x}_{1\Delta\Delta}$$

which describes the longitudinal wave propagation.

In the first order approximation the transverse and the longitudinal motions are decoupled.

Difficulties of the Method

The technique ceases to be applicable in the following cases:

a) $F_u(0, u(0))$ is singular

In this case one has to make use of a modified perturbation theory.

b) Non-uniformity in time, space, or in some other parameter

In this case the perturbation solution is significant in a certain domain D of t, x or another parameter p, whereas the perturbation terms are unbounded if t, x, p \notin D. A well-known example of this behavior of a perturbation solution is the occurrence of secular terms in oscillating systems, which lead to a significant solution only for sufficiently small values of t. This phenomenon will be called secularity.

The modified perturbation theory may get rid of this effect.

3. Example of secularity: solution of $du(t, \epsilon)/dt = i\epsilon u(t, \epsilon); u(0, \epsilon) = u^0$ by means of the perturbation technique

According to (3) we have $F(\epsilon, u(\epsilon)) \equiv (d/dt - i\epsilon)u(\epsilon) = 0$

zeroth approximation: $F(0, u_0) = 0$ or $u(0, t) = u_0(t) = u^0$

1st approximation: $F_u(0, u_0)\dot{u} + F_\epsilon(0, u_0) \equiv d/dt \dot{u} - i\epsilon u^0 = 0$
 $\dot{u}(t) \equiv i u^0 t$

Thus the solution may be written

$$u(t, \epsilon) = u^0 + \epsilon i u^0 t + R_2(\epsilon)$$

For fixed t $\lim_{\epsilon \rightarrow 0} R_2(\epsilon) = 0, \forall t$

However this solution is not uniform at infinity. Comparing with the exact solution, the remainder has the following form

$$R_2(\epsilon, t) = u^0 e^{i\epsilon t} - (u^0 + i\epsilon u^0 t) = O(\epsilon^2 t^2)$$

showing that the truncation error depends on time.

Perturbation methods were first devised by Lagrange and Delaunay, for problems of celestial mechanics. In the discussion of the three-body problem, considered as a Kepler problem perturbed by a third mass, one meets

with one of the difficulties listed above; in our formalism, the linear operator $F_u(0, u_0)$ becomes singular if one looks for periodic solutions, or the phenomenon of secularity occurs if one studies the initial value problem. Historically, this is the first problem in which non-uniformity appears. In order to avoid secularity, Poincaré and Lindstedt established a method which will be generalized in the following section.

Modified Perturbation Theory

The leading idea in the Poincaré-Lindstedt technique consists in considering the period of the non-perturbed Kepler problem as being modified by the perturbation due to the third body. In addition to the usual characteristic parameters, one also has to expand the frequency in terms of the perturbation parameter.

The general perturbation problem may be treated in essentially the same way. We introduce in Eq.(3) an additional function $\lambda(\epsilon)$ which plays the role of the period in the three-body problem.

Thus

$$F(\epsilon, u(\epsilon), \lambda(\epsilon)) = 0 \quad (8)$$

with $u(0) = u_0$ being a known function satisfying $F(0, u_0, \lambda_0) = 0$
 $\lambda_0 = \lambda(0)$.

To find a solution of (8), $u(\epsilon)$, in the neighborhood $N(0, h)$, we make use of the expansion (1) and determine the coefficients of the expansion as described above:

zeroth approximation: $u(\epsilon) = u_0$

first approximation: $F_u(\epsilon, u(\epsilon), \lambda(\epsilon))u_\epsilon + F_\lambda(\epsilon, u(\epsilon), \lambda(\epsilon))\lambda_\epsilon + F_\epsilon(\epsilon, u(\epsilon)) \quad (9)$

$$F_u(0, u_0, \lambda_0)u_\epsilon = -F_\lambda(0, u_0, \lambda_0)\lambda_\epsilon - F_\epsilon(0, u_0, \lambda_0) \quad (10)$$

In the case under consideration, the operator $F_u(o, u_o, \lambda_o)$ is singular. Let $F_u^+(o, u_o, \lambda_o)$ be its adjoint, defined by

$$(\xi, F_u \zeta) = (F_u^+ \xi, \zeta), \quad \xi, \zeta \in \mathcal{H}$$

where we have omitted the arguments of F_u . Then we have

$$\exists \Psi \in \mathcal{H} : F_u^+(o, u_o, \lambda_o) \Psi = 0 \quad (11)$$

as a consequence of the definition of a singular operator. Applying the eigenfunction Ψ on (9) and taking the inner product, one has

$$(\Psi, F_u u_\varepsilon) = -(\Psi, F_\lambda \lambda_\varepsilon) - (\Psi, F_\varepsilon)$$

The left hand side vanishes as

$$(\Psi, F_u u_\varepsilon) = (F_u^+ \Psi, u_\varepsilon) = 0$$

by Eq.(11). Thus

$$\lambda_\varepsilon = -(\Psi, F_\varepsilon(o, u_o, \lambda_o)) / (\Psi, F_\lambda(o, u_o, \lambda_o)) \quad (12)$$

λ being not affected by the operators in \mathcal{H} , it behaves like a constant in the inner product. As the choice of λ is arbitrary, (Ψ, F_λ) may always be assumed to be non-zero.

With the value of λ_ε given by (11), Eq.(10) may be solved, for instance by means of an eigenfunction expansion. The solution u_ε thus obtained depends linearly on an arbitrary parameter, and hence is not unique.

If $F_u(o, u(o), \lambda(o))$ has $m > 1$ zero eigenvalues, a set of m functions of $\varepsilon, \lambda_1(\varepsilon), \lambda_2(\varepsilon), \dots, \lambda_m(\varepsilon)$ must be chosen, leading to m solvability conditions of the form (12). The solution u_ε depends linearly on m arbitrary parameters.

These parameters are fixed by additional conditions, as appears clearly in the following illustrative examples:

4) Duffing equation for the vibrating string

$$u_{tt} - u_{xx} = f(u), \quad x \in [0, \pi]$$

$$u(0, t) = u(\pi, t) = 0; \quad f(0) = 0$$

If $f(u) = 0$, this equation admits periodic solutions. Assuming that periodic solutions exist also if $f(u) \neq 0$, the perturbation method allows us to find these solutions.

The periodicity condition is the following

$$u(x, t) = u(x, t + 2\pi/\omega), \quad \text{period} = 2\pi/\omega$$

By the substitution $t \rightarrow \omega t$ this problem can be written in the form

$$\begin{aligned} \omega^2 u_{tt} - u_{xx} &= f(u) \\ u(x, t) &= u(x, t + 2\pi) \end{aligned}$$

We now consider ε as the parameter fixing the initial amplitude of the system. If $\varepsilon = 0, u(x, t; 0) = u_0 = 0$ is regarded as the zeroth-order solution.

1st approximation

As the operator F_u will be singular in this problem, we have to choose an additional parameter $\lambda(\varepsilon)$ which may be taken as

$$\lambda(\varepsilon) = \omega(\varepsilon)^2$$

The first order approximation is given by (9):

$$\lambda \dot{u}_{tt} - \dot{u}_{xx} - f'(u) \dot{u} + \dot{\lambda} u_{tt} = 0$$

Evaluating the coefficients at $\varepsilon = 0$, the perturbation $\dot{\lambda}$ disappears:

$$\lambda^0 \dot{u}_{tt} - \dot{u}_{xx} - f'(0) \dot{u} = 0$$

This equation is of the form $F_u \dot{u} = 0$, showing that $F_u(0, u_0, \lambda_0)$ is a singular operator. As the formal adjoint operator (i.e. without reference to the boundary conditions) of a linear differential operator

$$L = \sum_{i=0}^n a_i(x_1, x_2, \dots, x_m) \frac{\partial^{n-i}}{\partial x_1^{v_1^i} \partial x_2^{v_2^i} \dots \partial x_m^{v_m^i}}, \quad v_1^i + v_2^i + \dots = n-i$$

is given by

$$L^+ = \sum_{i=0}^n (-1)^i \frac{\partial}{\partial x_1} \frac{\partial^{n-i}}{\partial x_1^{v_1^i} \dots \partial x_m^{v_m^i}} a_i(x_1, x_2, \dots, x_m)$$

one notices that $F_u(0, u_0, \lambda_0)$ is formally self-adjoint (i.e. without reference to the boundary conditions). The latter being symmetric $F_u(0, u_0, \lambda_0) = F_u^+(0, u_0, \lambda_0)$

in the sense of the definition given above, the inner product being defined by

$$(\xi, F_u \zeta) = \int_{[0, \pi] \times [0, 2\pi]} dx dt \quad \xi^* \left(\lambda^0 \frac{\partial^2}{\partial t^2} - \frac{\partial^2}{\partial x^2} - f'(0) \right) \zeta$$

To find an eigenfunction Ψ corresponding to the zero eigenvalue of $F_u^+(0, u_0, \lambda_0)$

we note that the perturbation equation is invariant under translations in time and space. Thus we may use a Fourier expansion in time and space for

Ψ . Shifting the time origin in order to have $u(x, t, \varepsilon) = 0$ at $t = 0$, we find

$$\Psi = \sin kt \sin jx$$

k and j being integers as a consequence of the periodicity and boundary conditions. The parameter λ^0 is given by the dispersion relation

$$-\lambda^0 k^2 + j^2 - f'(0) = 0$$

As λ^0 has to be positive in order to preserve the oscillatory motion, the latter equation imposes the condition $j^2 \geq f'(0)$. If we fix k and j , we are left with one auxiliary parameter $\lambda(\varepsilon)$. We remark that the first approximation does not allow us to find a frequency shift $\dot{\lambda}$, as $\dot{\lambda}$ does not occur in the relevant equation.

The self-adjointness of F_u implies that F_u and F_u^+ have the same set of eigenfunctions (differing possibly by a multiplicative constant). Thus in general $\dot{u} = A\Psi$.

2nd approximation

Applying $\partial/\partial\varepsilon$ on (9) we find

$$\lambda \ddot{u}_{tt} - \ddot{u}_{xx} - f'(u) \ddot{u} - f''(u) (\dot{u})^2 + 2\dot{\lambda} \dot{u}_{tt} + \ddot{\lambda} u_{tt} = 0$$

At $\varepsilon = 0$ we have

$$\lambda^0 \ddot{u}_{tt} - \ddot{u}_{xx} - f'(0) \ddot{u} - f''(0) (\dot{u})^2 = -2\dot{u}_{tt} \dot{\lambda}$$

which is of the form

$$F_{uu} (\dot{u})^2 + F_u \ddot{u} = -F_{\lambda u} \dot{u} \dot{\lambda}$$

Applying Ψ and taking the inner product we obtain

$$-(\Psi, F_{uu} (\dot{u})^2) - (\Psi, F_u \ddot{u}) = (\Psi, F_{\lambda u} \dot{u}) \dot{\lambda}$$

where the underlined quantity vanishes on account of the definition of the singularity of F_u^+

$$(\Psi, F_u \ddot{u}) = (F_u^+ \Psi, \ddot{u}) = 0$$

Thus

$$\dot{\lambda} = -(\Psi, F_{uu} (\dot{u})^2) / (\Psi, F_{\lambda u} \dot{u})$$

As $\dot{u} = \Psi$, the numerator of this expression becomes

$$(\Psi, F_{uu} (\dot{u})^2) = -f''(0) A^2 \int_{[0, \pi] \times [0, 2\pi]} dx dt \sin^2 kt \sin^3 jx = 0$$

and $\dot{\lambda} = 0$.

The second order approximation \ddot{u} is then given by

$$F_u \ddot{u} = -F_{uu} (\dot{u})^2$$

or

$$(\lambda^0 \frac{\partial^2}{\partial t^2} - \frac{\partial^2}{\partial x^2} - f'(0)) \ddot{u} = f''(0) A^2 (1 - \cos 2kt - \cos 2jx + \cos 2kt \cos 2jx)$$

The homogeneous solution, \ddot{u}_H , and a particular solution, \ddot{u}_I , of the inhomogeneous equation are given by

$$\ddot{u}_H = \sin jx (C \sin kt + D \cos kt)$$

$$\ddot{u}_I = -\frac{A^2 f''(0)}{4} \left[\frac{1}{f'(0)} - \frac{\cos 2kt}{4k^2 \lambda^0 + f'(0)} + \frac{\cos 2jx}{4j^2 - f'(0)} + \frac{\cos 2kt \cos 2jx}{4k^2 \lambda^0 - 4j^2 + f'(0)} \right]$$

with $\lambda^0 = \omega^2(0)$.

The solution of the Duffing equation to the second order approximation becomes

$$u(x, t; \varepsilon) = 0 + \varepsilon A \sin jx \sin kt + \frac{\varepsilon^2}{2} (\ddot{u}_H + \ddot{u}_I) + O(\varepsilon^3)$$

The integration constants A, C and D are so far arbitrary. By defining ε as in example 9, two of them however may be eliminated.

3rd approximation

Applying $\partial^2 / \partial \varepsilon^2$ on (9), and putting $\varepsilon = 0$, one obtains an equation in $\ddot{\lambda}(0)$. Multiplying this equation by Ψ and taking the inner product, the singular operator F_u is eliminated and we are left with an equation in $\ddot{\lambda}$

$$\ddot{\lambda}(\psi, 3 F_{\lambda\lambda u} \dot{u}) = (\psi, \chi)$$

where χ is a quantity expressed in terms of the previous approximations.

Explicitly

$$\begin{aligned} \ddot{\lambda} &= \int_{[0, \pi] \times [0, 2\pi]} dx dt (f'''(0) \dot{u}^4 + 3f''(0) \dot{u}^2 \ddot{u}) / 3 \int_{[0, \pi] \times [0, 2\pi]} dx dt \dot{u} \ddot{u}_{tt} \\ &= -\frac{3A^2}{16\kappa^2} f'''(0) + \frac{A}{8\kappa^2} f''(0) \left[\frac{19}{10f'(0)} - \frac{1}{4j^2 - f'(0)} + \frac{1}{4j^2 - 3f'(0)} \right] \end{aligned}$$

and

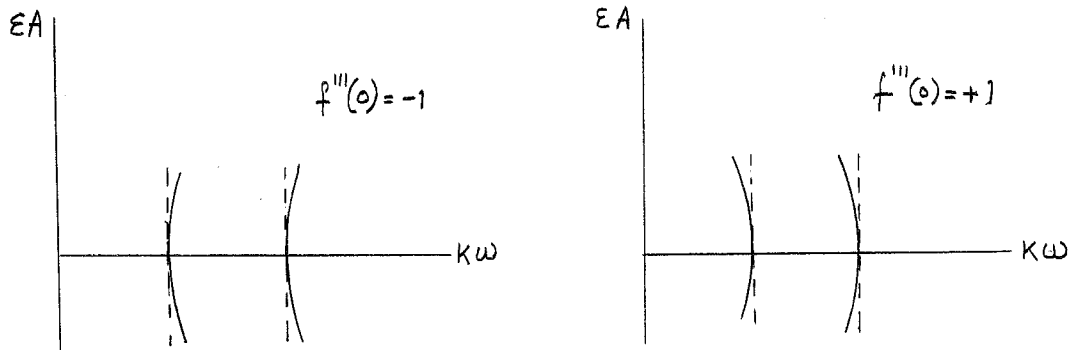
$$\omega^2(\varepsilon) = \frac{j^2 - f'(0)}{\kappa^2} + O(\varepsilon) + \frac{\varepsilon^2}{2!} \ddot{\lambda} + O(\varepsilon^3)$$

As ε appears as a measure of the amplitude, the latter equation shows that the period is amplitude-dependent in the non-linear domain of ε .

The amplitude-frequency relation is displayed in the following diagram, for the numerical values

$$f'(0) = \frac{1}{2}; \quad f''(0) = 0; \quad f'''(0) = -1, +1$$

The dotted lines show the frequency in the linear theory



Notes submitted by
Jean Perdang

PERTURBATION THEORY (II)

Joseph B. Keller

5) Longitudinal Vibration of a String

Using the same definitions as in example (2), the equation of motion may be written

$$\omega^2 \rho(s) x_{tt} = [T(x_s)]_s$$

We look for periodic solutions subject to the boundary conditions

$$\begin{aligned} x(0, t) = 0 \quad x(L, t) = L \\ x(s, t + 2\pi) = x(s, t) \end{aligned}$$

It is necessary to use the modified perturbation theory i.e. to set $\omega = \omega(\epsilon)$.

The zero order solution is $x(s, t, 0) = s$
 $\omega_0 = 1$

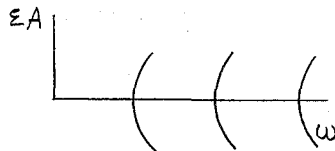
The first order results give $x(s, t, \epsilon) = s + \epsilon A \sin t f_j(s)$
 $\omega(\epsilon) = \omega_j$

where f_j is an eigenvector of the homogeneous system and ω_j is the corresponding eigenfrequency. To the next higher order the solution may be written

formally as

$$\begin{aligned} x(s, t, \epsilon) = s + \epsilon A \sin t f_j(s) + \frac{\epsilon^2}{2} \ddot{x}(0) \\ \omega(\epsilon) = \omega_j + 0 \cdot \epsilon + \frac{\epsilon^2}{2} \ddot{\omega}(0) \end{aligned}$$

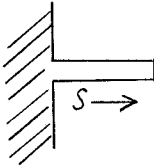
The amplitude-frequency relation is given by



where the curves cross the axis of zero amplitude at the eigenfrequencies of the linear problem. This diagram illustrates why it is necessary to use modified perturbation theory. Use of any perturbation scheme implies following a solution as ϵ increases. But there may exist no branch at an arbitrarily chosen ω and so it is necessary to allow ω to vary in order to

locate the point where the branch exists.

6) Vibration of a beam



Let S be the Lagrangian variable along the beam. Then for constant density (ρ), the equations may be written

$$\omega^2 \rho x_{tt}(s,t) = (N \cos \theta + V \sin \theta)_s$$

$$\omega^2 \rho y_{tt}(s,t) = (N \sin \theta - V \cos \theta)_s$$

where N and V are the longitudinal and the vertical stresses respectively.

The Euler-Bernoulli theory gives the relations

$$V = -M_s = B \theta_{ss}$$

where B is a constant and θ is defined by $x_s = \cos \theta$ and $y_s = \sin \theta$. The boundary conditions are

$$x = y = \theta = 0 \text{ at } s = 0$$

$$N = V = M = 0 \text{ at } s = L$$

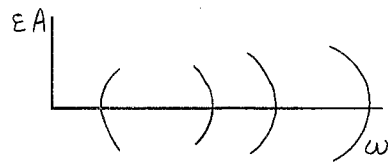
Modified P.T. is used giving

$$\omega_j^2 = \rho^{-1} B \lambda_j^4 \left[1 + \frac{(EA)^2}{2} \left\{ 3 \int_0^L \phi_j^2 (\phi_j')^2 ds - \lambda_j^4 \int_0^L \left(\int_0^s \phi_j^2 ds' \right)^2 ds \right\} / \int_0^L (\phi_j')^2 ds + O(\epsilon^3) \right]$$

where $\lambda_j = \omega_j^2$.

The term in ϵ is absent as it is in any time-reversible problem.

The amplitude-frequency diagram is



So the frequency of the first mode is increased while those of the higher modes are decreased as the amplitude increases.

7) Vibrations of gas in a container (Isentropic, irrotational motion).

Let φ be the velocity potential i.e. $u_i = \varphi_{x_i}$ then Bernoulli's equation is written as

$$\omega \varphi_t + \frac{1}{2} \varphi_{x_i} \varphi_{x_i} + \int_{p_0}^p \frac{dp}{\rho(p)} = 0$$

The equation of motion is given by

$$\rho(\rho(\rho)) \Delta \varphi - \rho_{tt} = 2 \varphi_{x_i} \varphi_{x_i t} + \varphi_{x_i} \varphi_{x_j} \varphi_{x_i x_j}$$

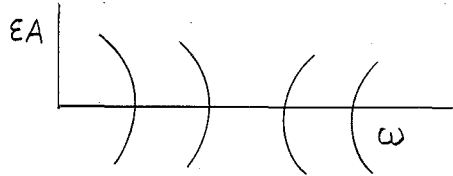
where $\rho_\rho \equiv \frac{\partial \rho}{\partial \rho}$ is the sound speed. Rigid boundaries are assumed $\frac{\partial \varphi}{\partial n} = 0$ and periodic solutions are looked for.

A zero order solution is given by

$$\varphi_0 = 0 \quad \rho = \rho_0 \quad \text{where } \rho_0 \text{ is a constant.}$$

The first order results were discussed in example (1). The results to second order are shown in an amplitude-frequency diagram for the case

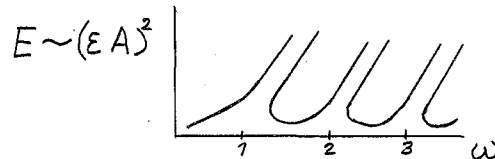
$\rho(\rho) = B\rho^\gamma$, ($\gamma = 1.4$) for a sphere of radius R



8) Forced vibration of a string

$$u_{tt} - u_{xx} = f(\omega) + \epsilon \cos \omega t \sin x$$

The results to second order for $f(u) = -u^2$ with the force applied at one end are given by



The solution thus displays a jump phenomenon as the frequency is altered.

9) Temperature distribution due to a non-linear heat source

$$\Delta T = \lambda S(T)$$

(where λ is usually one but here will be used as the variable parameter in the modified P.T.)

The boundary condition is

$$\frac{\partial T}{\partial n} = \alpha (T - T_0) \quad (\text{Newton's Law of cooling})$$

$$\text{and } S(T_0) = 0$$

An initial solution is $T(x, 0) = T_0$

The first order equations are then

$$\Delta \dot{T} - \lambda_0 S'(T_0) \dot{T} = 0$$

$$\frac{\partial \dot{T}}{\partial n} - \alpha \dot{T} = 0$$

This is a standard eigenvalue problem with the solution

$$\lambda_0 = \lambda_n$$

$$\dot{T}(x) = A \varphi_n(x) \quad \text{where } \varphi_n \text{ is a normalized eigenfunction.}$$

Defining $\varepsilon = \int \varphi_n (T - T_0) dx$ and differentiating this with respect to ε gives

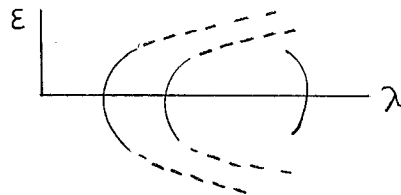
$$1 = \int \varphi_n \dot{T} dx = A \int \varphi_n \varphi_n dx$$

$$\Rightarrow A = 1$$

Further differentiation yields

$$\int \varphi_n T^{(j)} dx = 0 \quad j = 2, 3, \dots$$

The second order results are shown in the following diagram



As noted above λ is arbitrarily introduced i.e. in the actual problem $\lambda \equiv 1$ but it is necessary to vary λ to reach a solution branch. Since there are a number of solutions at a given eigenvalue, it is of interest to consider the stability of the solutions. To do this for the present problem we consider $T(x, t, \varepsilon, \eta)$ i.e. change $T(x, \varepsilon)$ by a small amount measured by η . Then $T(x, t, \varepsilon, \eta) = T(x, t, \varepsilon, 0) + \eta T_\eta(x, t, \varepsilon, 0) + o(\eta^2)$ where $T(x, t, \varepsilon, 0) = T(x, \varepsilon, 0)$ i.e. the steady state solution found above.

The time dependent problem can now be written

$$-\gamma T_t + \Delta T = \lambda S(T)$$

$$\frac{\partial T}{\partial \eta} = \alpha (T - T_0), \quad S(T_0) = 0$$

$$T(x, 0, \epsilon, \eta) = g(x, \epsilon, \eta)$$

where

$$g(x, \epsilon, 0) = T(x, \epsilon)$$

The first order equations are

$$-\gamma T_{\eta t} + \Delta T_{\eta} = \lambda S'(T) T_{\eta}$$

$$\frac{\partial T_{\eta}}{\partial \eta} - \alpha T_{\eta} = 0$$

$$T_{\eta}(x, 0, \epsilon, 0) = g_{\eta}(x, \epsilon, 0)$$

As the coefficients in these equations are independent of time, we can use

separation of variables

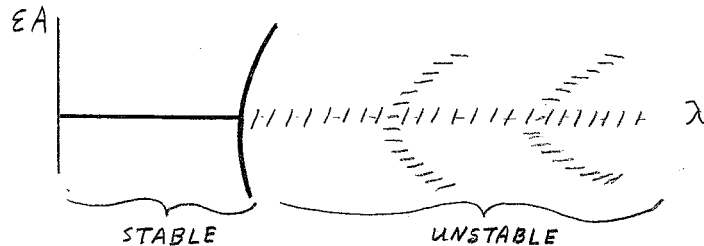
$$T_{\eta} = u(x, \epsilon) e^{\beta(\epsilon)t}$$

substituting in the first order equations gives

$$-\gamma \beta(\epsilon) u + \Delta u = \lambda S'(T(x, \epsilon)) u$$

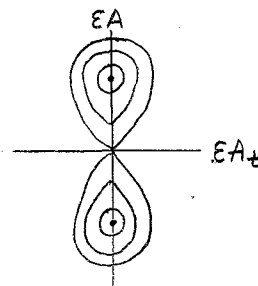
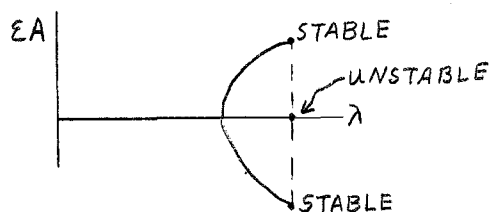
$$\frac{\partial u}{\partial \eta} - \alpha u = 0$$

β is now a parameter in the modified perturbation theory. The results for the case $S''(T_0) = 0$, $\frac{S'''(T_0)}{S'(T_0)} < 0$ and $S'(T_0) < 0$ show that all the modes except the first are unstable



To solve the initial value problem, it is necessary to use a superposition of modes $e^{\beta t}$ all of which blow up (except for the first mode).

Taking a cut in the above diagram at a constant λ might show, for example



Thus the solutions would ultimately move to a stable branch.

II. SINGULAR PERTURBATION THEORY (ASYMPTOTICS)

One of the methods used in this case will be demonstrated by considering the problem of a self-sustained oscillation.

$$u_{tt} - u_{xx} + u = \epsilon f(u, u_t, \epsilon)$$

$$0 \leq x \leq \pi$$

$$0 \leq t$$

subject to the boundary conditions

$$u(0, t) = u(\pi, t) = 0$$

$$u(x, 0) = g(x, \epsilon)$$

$$u_t(x, 0) = h(x, \epsilon)$$

We will consider the special case

$$f = f_0 = u_t - \frac{1}{3} u_t^3$$

which gives negative damping for small velocities and positive damping for high velocities which implies the existence of a limit cycle for the motion (for small ϵ this will approach a circle).

Modified P.T. gives infinitely many periodic solutions

$$u_n(x, t, \epsilon) = \frac{4}{\sqrt{3(1+n^2)}} \sin n x \cos \omega_n(\epsilon) t$$

$$+ \epsilon \dot{u}_n + O(\epsilon^2)$$

$$\omega_n(\epsilon) = (1+n^2)^{1/2} + \frac{1}{2} \ddot{u}_n(0) \epsilon^2 + O(\epsilon^3)$$

We are interested in determining which mode is actually excited by given initial conditions. The method used is known as the "two time method".

We define two new variables

$$\begin{aligned} \tau &= \varepsilon t \\ \sigma &= \omega(\varepsilon)t \end{aligned}$$

then $u(x, t, \varepsilon) = v(x, \sigma, \tau, \varepsilon)$

$$\begin{aligned} \text{and } \frac{\partial v}{\partial t} &= \frac{\partial v}{\partial \tau} \frac{\partial \tau}{\partial t} + \frac{\partial v}{\partial \sigma} \frac{\partial \sigma}{\partial t} \\ &= \varepsilon v_{\tau} + \omega(\varepsilon) v_{\sigma} \end{aligned}$$

Substituting into the original equations gives

$$\omega^2 v_{\sigma\sigma} - v_{xx} + v = -2\varepsilon\omega v_{\sigma\tau} - \varepsilon^2 v_{\tau\tau} + \varepsilon f(v, \omega v_{\sigma} + \varepsilon v_{\tau}, \varepsilon)$$

$$v(0, \sigma, \tau, \varepsilon) = v(\pi, \sigma, \tau, \varepsilon) = 0$$

$$v(x, 0, 0, \varepsilon) = g(x, \varepsilon)$$

$$\omega v_{\sigma}(x, 0, 0, \varepsilon) + \varepsilon v_{\tau}(x, 0, 0, \varepsilon) = h(x, \varepsilon)$$

Next regular modified P.T. is applied.

Setting $\omega(0) = 1$, $\omega_{\varepsilon}(0) = 0$ we obtain for the zero order equations

$$\begin{aligned} v_{\sigma\sigma}^0 - v_{xx}^0 &= 0 \\ v^0(0, \sigma, \tau) &= v^0(\pi, \sigma, \tau) = 0 \\ v^0(x, 0, 0) &= g(x, 0) \\ v_{\sigma}^0(x, 0, 0) &= h(x, 0) \end{aligned}$$

This is a standard eigenvalue problem with the solution

$$v^0(x, \sigma, \tau) = \sum_{n=1}^{\infty} \left\{ A_n(\tau) \cos(1+n^2)^{1/2} \sigma + B_n(\tau) \sin(1+n^2)^{1/2} \sigma \right\} \sin nx$$

The initial conditions fix $A_n(0)$ and $B_n(0)$

$$A_n(0) = \frac{2}{\pi} \int_0^{\pi} g(x, 0) \sin nx \, dx$$

$$B_n(0) = \frac{2}{(1+n^2)^{1/2} \pi} \int_0^{\pi} h(x, 0) \sin nx \, dx$$

The first order equations are obtained by differentiating the original equations with respect to ε and setting $\varepsilon = 0$. If we write $\left. \frac{\partial v}{\partial \varepsilon} \right|_{\varepsilon=0} = v'$,

we obtain

$$v'_{\sigma\sigma} - v'_{xx} + v' = -2v_{\sigma\tau}^0 + f(v^0, v_{\sigma}^0, 0)$$

$$v' = 0 \text{ at } 0, \pi$$

$$v' = g_{\varepsilon}(x)$$

$$\omega_0 v'_{\sigma} + v_{\tau}^0 = h_{\varepsilon}(x)$$

We assume v' is bounded and operate on the equations with

$$\lim_{T \rightarrow \infty} \frac{1}{T} \int_0^T d\sigma \int_0^\pi dx \begin{cases} \cos(1+n^2)^{1/2} \sigma \sin nx \\ \sin(1+n^2)^{1/2} \sigma \sin nx \end{cases}$$

The result is

$$\frac{dA_n}{dT} + \lim_{T \rightarrow \infty} \frac{2}{\pi(1+n^2)^{1/2} T} \int_0^T \int_0^\pi f(v, v_\sigma, \sigma) \sin nx \sin(1+n^2)^{1/2} \sigma dx d\sigma = 0$$

$$\frac{dB_n}{dT} + \lim_{T \rightarrow \infty} \frac{2}{\pi(1+n^2)^{1/2} T} \int_0^T \int_0^\pi f(v, v_\sigma, \sigma) \sin nx \cos(1+n^2)^{1/2} \sigma dx d\sigma = 0$$

If we now use the assumption $f = f_0 = u_\pm - \frac{1}{3} u_\pm^3$, these equations reduce to

$$2 \frac{dA_n}{dT} = A_n + \frac{1}{16} (n^2+1) A_n (A_n^2 + B_n^2) - \frac{A_n}{4} \sum_{k=1}^{\infty} (k^2+1) (A_k^2 + B_k^2)$$

$$2 \frac{dB_n}{dT} = B_n + \frac{1}{16} (n^2+1) B_n (A_n^2 + B_n^2) - \frac{B_n}{4} \sum_{k=1}^{\infty} (k^2+1) (A_k^2 + B_k^2)$$

We define

$$y_n(\tau) = \frac{n^2+1}{16} (A_n^2 + B_n^2)$$

and $Y = \max_K y_K(0)$

Then the solution of the system of equations shows that if

$$y_k(0) < Y, \quad y_k(\tau) \rightarrow 0$$

and if $y_k(0) = Y, \quad y_k(\tau) \rightarrow \frac{1}{4q-1}$

where q is the number of modes for which $y_k(0) = Y$. The stability analysis of this solution shows that it is unstable unless $q = 1$.

Notes submitted by

John D. Trasco

A SCALING AND EXPANSION OF EQUATIONS OF MOTION TO YIELD THE
BOUSSINESQ EQUATIONS

Willem V.R. Malkus

The equations governing macroscopic fluid motion are those of conservation of mass

$$\frac{D}{Dt} \rho = -\rho \nabla \cdot \underline{v}, \quad (1)$$

conservation of momentum

$$\rho \frac{D}{Dt} \underline{v} = -\nabla p + \nabla \cdot \underline{\mathbb{P}} + \underline{F} \quad (2)$$

and conservation of energy

$$\rho \frac{D}{Dt} (C_v T) = -\rho \nabla \cdot \underline{v} + \nabla \cdot \underline{q} + \Phi + Q \quad (3)$$

Here, ρ is the density, \underline{v} the velocity, p the pressure, $\underline{\mathbb{P}}$ the viscous stress tensor, \underline{F} the body force, C_v the specific heat at constant volume, T the temperature, Φ the rate of viscous dissipation, \underline{q} the molecular heat flux, and Q the molecular heat source (or sink). $\frac{D}{Dt}$ is the substantial derivative.

The goal is to produce an expansion scheme for the dependent variables for which the lowest order terms yield the Boussinesq approximation to the governing equations (1-3). The Boussinesq equations are valid under certain conditions (to be discussed later), which will prejudice our choice of expansion parameters and scaling factors. The scaling employed is not unique, but is constructed so that the equations can describe slow, non-linear flow in shallow fluid layers.

We begin by writing the stress tensor $\underline{\mathbb{P}}$ in the form applicable to a dilute gas:

$$P_{ij} = \mu \left(\frac{\partial}{\partial x_j} v_i + \frac{\partial}{\partial x_i} v_j \right) - \frac{2}{3} \mu \frac{\partial}{\partial x_k} v_k \delta_{ij} \quad (4)$$

$$q_i = k \frac{\partial}{\partial x_j} T \quad (5)$$

$$\Phi = \frac{1}{2} \mu \left(\frac{\partial}{\partial x_j} v_i + \frac{\partial}{\partial x_i} v_j \right)^2 - \frac{2}{3} \mu \left(\frac{\partial v_k}{\partial x_k} \right)^2 \quad (6)$$

The cartesian tensor notation is used here and later in the text when convenient. The equation of state for a dilute gas is

$$\rho(P, T) = \frac{p}{RT} \quad (7)$$

Equations (4), (5), (7) are correct when the gradients of χ and $\log T$ are small compared to the reciprocal of the mean free path of the gas molecules.

The accuracy of the Boussinesq equations depends on the degree to which the following is true:

- a. for convective motions the fluid behaves as though the density were constant except in the equation of state and the force term involving gravity;
- b. the fluid behaves as though it were incompressible, the density varying only as a consequence of changes in temperature;
- c. the mechanical dissipation rate, Φ , makes a negligible contribution to the heat equation;
- d. the fluid parameters μ , k , and C_v are constants.

When (a-d) hold, the governing equations (1)-(3), with (4)-(7) are

$$\nabla \cdot \underline{v} = 0 \quad (8)$$

$$\rho_n \frac{Dx}{Dt} = -\nabla p + \mu \nabla^2 \underline{v} + \rho(T) g \hat{k} \quad (9)$$

$$\rho_n C_v \frac{D}{Dt} T = -k \nabla^2 T \quad (10)$$

where ρ_n is the density at some reference temperature T_n , and \hat{k} is a unit vector in the direction that gravity acts. Requirements (a-d) imply a small density contrast, vanishingly small compressibility, and velocities very small compared to the speed of sound. In the light of these conditions, one expects that the Boussinesq equation will hold for small values of the distance (d) between heating plates, or small temperature differ-

ence (ΔT). We are thus motivated to write the dependent variables as expansions in ΔT and d .

Continuing with the dilute gas, and requiring that the nine parameters ($d, \Delta T, C_v, \mu, k, g, P_n, T_n$, and R) be constant, we construct five independent non-dimensional combinations of the nine parameters. We wish to choose two of the combinations so that they become vanishingly small as d and ΔT become vanishingly small, the numerical value of the other non-dimensional combinations being held fixed.

The reference field will be hydrostatic

$$\frac{\partial \rho_a(z)}{\partial z} = -g \rho_a(z) \quad (11)$$

ρ_a and P_a are not determined until T_a is chosen. To that end, choose T_a to satisfy an adiabatic gradient

$$\frac{\partial T_a}{\partial z} = -g/c_p \quad (12)$$

In addition to simplifying the equations, this choice retains the advective non-linearity in the heat equation (3).

$$\text{Let } \tilde{\rho} = \rho - \rho_a, \tilde{p} = p - P_a, \text{ and } \tilde{T} = T - T_a \quad (13)$$

Then only terms involving departures from ρ_a, P_a, T_a are retained in (3). Equations (7), (11), and (12) describe an "adiabatic" hydrostatic

field. Now $\frac{T_a}{T_n} = (1 - \eta \frac{z}{d}) = f; \left(\frac{P_a}{P_n}\right)^s = f; \frac{P_a}{P_n} = \frac{P_a}{P_n}, \frac{T_n}{T_a} = f\left(\frac{1-s}{s}\right)$

where $T_n = T_a(z=0), P_n = P_a(z=0), \rho_n = \rho_a(z=0),$ and

$$\eta \equiv \frac{gd}{c_p T_n}$$

$$s = \frac{R}{c_p}$$

The number η — the ratio of depth d to adiabatic depth $\frac{c_p T_n}{g}$ — proportional to d and will serve as an expansion parameter. The number s

will be fixed. We need three more parameters. Let

$$\begin{aligned} \nu &= \frac{\mu(T_n)}{\rho_n} && \text{"kinematic viscosity"} \\ \kappa &= \frac{k(T_n)}{\rho_n c_p} && \text{"thermometric conductivity"} \\ \sigma &= \frac{\nu}{\kappa} && \text{"Prandtl number"} \end{aligned}$$

σ will be thought of as fixed. We choose the fourth non-dimensional number and second expansion parameter to be proportional to the difference in $T - T_a$ from one boundary to the other, and define

$$\varepsilon = \frac{\Delta \bar{T}}{T_n}; \quad \Delta \bar{T} = \Delta T - \Delta T_a$$

$\Delta T_a = \eta T_n$ is the temperature difference across the gas which would result from the adiabatic "lapse rate" g/c_p . Note also that

$$\frac{\Delta T}{T_n} = \varepsilon + \eta$$

The final non-dimensional number is the Rayleigh number

$$R_G = \frac{g d^3 \Delta \bar{T}}{\nu \kappa T_n}$$

We now scale the variables. As noted earlier, this procedure is arbitrary, but we will require that the momentum and heat equations remain coupled as η and $\varepsilon \rightarrow 0$. This will enable the lowest order equations to describe convection. Thus,

$$\begin{aligned} \underline{x} &= d \underline{x}'; \quad \underline{\mu} = [\mu(T_n)] \underline{\mu}'; \quad \underline{k} = [k(T_n)] \underline{k}' \\ \underline{\bar{T}} &= [\varepsilon T_n] \underline{T}'; \quad \underline{\bar{p}} = [\varepsilon \rho_n] \underline{p}' \\ \underline{v} &= [\nu] \underline{v}'; \quad \underline{\bar{p}} = [\rho_n \nu^2] \underline{p}'; \quad \underline{t} = \left[\frac{d}{\nu}\right] \underline{t}' \end{aligned}$$

All primed quantities are non-dimensional, and if scaled for the convection problem, will be of order unity.

For motion produced by buoyancy, a characteristic velocity is terminal velocity of free fall, through the distance d , of a fluid element with the maximum buoyancy, i.e.

$$V = \left(\frac{g d \Delta \tilde{T}}{T_n} \right)^{1/2}$$

or

$$V = (\varepsilon \eta)^{1/2} c$$

where $c = \sqrt{c_p T_e}$ is the sound speed. The corresponding time scale is $\frac{d}{V} = \left(\frac{d}{\varepsilon g} \right)^{1/2}$. Thus ε, η small compared to one corresponds to V small compared to c . Also, one anticipates that the initial terms in the expansion will not describe flows resulting from any time-dependent boundary conditions of shorter period than the time scale $\left(\frac{d}{\varepsilon g} \right)^{1/2}$. Hence, acoustic and acoustic-like fields of motion should be based on equations generated by a different scaling and expansion than that here.

Using the variables defined by (13) and the scaling (14), the equations (1)-(3) become

$$\frac{D}{Dt'} \ln(1 + \varepsilon f^{-m} \rho') = -\nabla' \cdot \underline{v}' + \eta m f^{-1} w' \quad (15)$$

$$(f^m + \varepsilon \rho') \frac{D \underline{v}'}{Dt'} = -\rho' \hat{k} - \nabla p' + \left(\frac{\sigma}{R_g} \right)^{1/2} \nabla' \cdot \mathbb{P} \quad (16)$$

$$\varepsilon (f^m + \varepsilon \rho') \frac{DT'}{Dt'} = \varepsilon \left(\frac{1}{R_g \sigma} \right)^{1/2} \nabla' \cdot k' \nabla T' + \eta \left[\left(\frac{1}{\sigma R_g} \right)^{1/2} \frac{\partial k'}{\partial z'} \right] + \varepsilon \eta \left[w' \rho' + \frac{D \rho'}{Dt'} + \left(\frac{\sigma}{R_g} \right)^{1/2} \Phi' \right] \quad (17)$$

where $w' = \hat{k} \cdot \underline{v}'$, $m \equiv \frac{1-s}{s}$ and \mathbb{P} , Φ' are as in (4) and (6), but unprimed quantities replaced by primed quantities. For an adiabatic reference field

$$\frac{DT}{Dt} = \frac{D\tilde{T}}{Dt} - \rho_a g w, \quad (18)$$

which becomes

$$\rho' = \frac{\eta \rho' - s f^m T'}{s(f + \varepsilon T')} \quad (19)$$

We now write the dependent variables in the form

$$G' = \sum_{i,j=0}^{\infty} G'_{ij} \varepsilon^i \eta^j. \quad (20)$$

G' is any one of the variables T' , ρ' , \underline{v}' , ρ' , μ' , and k' .

Substitute (20) into Eqs. (15), (16), (17), and (19) and order the equations

in powers of ϵ and η . We then have

$$\rho'_{00} = -T'_{00} \quad (21)$$

$$\nabla' \cdot \underline{V}'_{00} = 0 \quad (22)$$

$$\frac{D_{00}}{Dt} \underline{V}'_{00} = -\rho'_{00} \hat{k} + \left(\frac{\sigma}{R_G}\right)^{1/2} \nabla' \cdot \nabla' \underline{V}'_{00} - \rho'_{00} \quad (23)$$

$$\frac{D_{00}}{Dt} T'_{00} = \left(\frac{1}{R_G \sigma}\right)^{1/2} \nabla' \cdot \nabla' T'_{00} \quad (24)$$

where $\frac{D_{00}}{Dt} = \frac{\partial}{\partial t'} + \underline{V}'_{00} \cdot \nabla'$ and $k'_{00} = \mu'_{00} = 1$ from (14).

Equations (22)-(24) are identical to (8)-(10), with the assumption that ρ , p , and T be interpreted as departures from the adiabatic hydrostatic field - which was our original goal. In addition, we are capable of producing equations of higher order in ϵ and η to test the validity of the Boussinesq set. Equations (22)-(24) retain the advective non-linearity of the substantial derivative. However, the advective terms do not appear in equations of higher order. This facilitates computation of higher terms. The compressibility of the gas appears in these equations only through the implicit relation of the primed fields to the adiabatic hydrostatic reference field. The thermal expansion of the gas plays an important part through the term $-\rho'_{00} k'$. This separation of the effects of compressibility and thermal expansion is a dynamic consequence of the requirement that the zeroth order terms of the ϵ , η expansion be capable of describing convection (i.e., coupled momentum and heat equations).

The arbitrary nature of the preceding analysis should be emphasized. However, many physical processes fall within the realm of validity of these equations.

Notes submitted by
Terrance G. Barker

SELF-GRAVITATING STELLAR SYSTEMS

Kevin H. Prendergast

Galaxies are self-gravitating systems of stars and interstellar material. Gas dynamics is important in the study of the interstellar gas. Even in the absence of interstellar gas, however, the study of galaxies is appropriate in a course on stellar fluid dynamics since a galaxy is essentially a rarefied gas of stars. Galactic dynamics is similar to the study of fluid flow at large Knudsen number (mean free path is larger than scale of system).

We now review the outstanding observational features of galaxies and then turn to the theoretical treatments.

Hubble Classification

Hubble classified galaxies according to their visual forms. Galaxies for which isophotes are ellipses are called ellipticals. Elliptical (E) galaxies contain very little interstellar material. They are further classified according to the eccentricity of their isophotes so that a spherical galaxy is called an E0 while the most eccentric elliptical (axial ratio $\approx 1/3$) is E7.

Galaxies with spiral arms are subdivided into two categories, the ordinary spirals (S) and the barred spirals (SB). Except for the details of the spiral arms, the former are axisymmetric while the latter are characterized by a bar which passes through the center of the galaxy. Spiral galaxies are called Sa if their arms are compact and contain few H II regions. Sc galaxies have open arms with many H II regions. Sb galaxies (of which our galaxy may be an example) are intermediate between Sa and Sc. The

barred spirals are similarly subdivided into groups SBa, SBb, SBc.

The SO galaxies represent the link between elliptical and spiral galaxies and have nuclei which are redder than the disk (like spirals but unlike ellipticals, which are composed entirely of population II stars).

The Hubble classification scheme contains two "junk piles". The so-called irregulars are galaxies with no discernable symmetry. The peculiar galaxies are galaxies which, except for some anomalous feature, would ordinarily be in one of the other categories. For example, an elliptical galaxy with an H II region would be called peculiar.

Morgan Classification

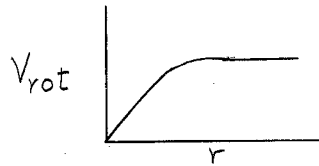
Morgan took integrated spectra of galaxies and found that by looking at a photograph of a galaxy it is possible to predict its integrated spectral type. In particular, galaxies with the greatest central concentration of brightness have the latest integrated spectral type. Thus E galaxies have spectral type k while Sa and SBa galaxies have spectral type g. Sc and SBc galaxies have spectral type f while the irregulars are of spectral type a. (Note that small letters are used to denote spectral types for galaxies.) While the matching of morphological type with spectral type is not as clean-cut as implied here, the correlation is, in fact, very good.

Rotational Velocities

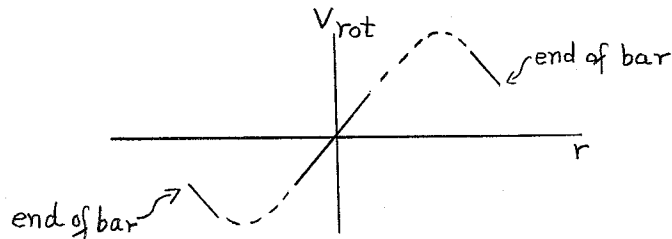
By measuring the Doppler shift of spectral lines as a function of position, it is possible to deduce the rotational velocities of galaxies (apart from projection effects) as a function of distance from the center. For the case of E galaxies only a small part of the full rotation curve is

obtainable since the brightness of the galaxy fades rapidly with distance from the center (i.e., the brightness is centrally concentrated).

A typical rotation curve for an Sc galaxy looks like this:



A typical rotation curve for an SBc galaxy looks like this:



The full rotation curve corresponds to the bar. While the inner portion of the bar rotates like a solid body, the bar as a whole is not in solid-body rotation.

We now discuss theoretical models for galaxies.

Ellipticals

The basic equations are the Boltzmann equation

$$\frac{\partial f}{\partial t} + u_i \frac{\partial f}{\partial x_i} - \frac{\partial \psi}{\partial x_j} \frac{\partial f}{\partial u_j} = \frac{\delta f}{\delta t} \Big|_{coll}$$

and Poisson's equation

$$\nabla^2 \psi = 4 \pi G \rho$$

The distribution function $f(\underline{r}, \underline{u})$ is defined so that $f(\underline{r}, \underline{u}) d\underline{r} d\underline{u}$ is proportional to the number of stars contained by an elemental six-dimensional cube $d\underline{r} d\underline{u}$ at the point $\underline{r}, \underline{u}$ in phase space. The quantity ψ is the gravitational potential. The Boltzmann and Poisson equations are coupled by the ψ term in the former and by the fact that the density which

appears in the latter is

$$\rho = m \int f d\underline{u},$$

where m is the stellar mass and the integration is carried over all of velocity space.

We shall presume the existence of a steady state. In addition we shall neglect the collisional term on the right side of the Boltzmann equation. This is possible since the relaxation time for binary collisions between stars is very long in an E galaxy. However, collisions must be included in the study of star clusters and in galaxies which contain massive clouds of interstellar gas.

Thus the equations used to describe an elliptical galaxy are the Vlasov equation,

$$u_i \frac{\partial f}{\partial x_i} - \frac{\partial \psi}{\partial x_j} \frac{\partial f}{\partial u_j} = 0$$

and the Poisson equation, $\nabla^2 \psi = 4\pi G m \int f d\underline{u}$,

The Vlasov equation is solved by an arbitrary function of its integrals. For a time-independent potential, one integral is the energy.

$$E = \frac{1}{2} |\underline{u}|^2 + \psi(r).$$

If there is axisymmetry, another integral is the z-component of angular momentum,

$$J_z = (\underline{r} \times \underline{u}) \cdot \hat{k}.$$

Thus an arbitrary function of E and J_z will solve the Vlasov equation. However, such a solution is not the most general since the Vlasov equation has six, not just two, integrals. However, we must know the details of the potential ψ before we can compute the third integral. The remaining integrals are not isolating and are therefore not of interest.

We may construct a model of an E galaxy as follows:

1. We pick a particular form for f , for example,

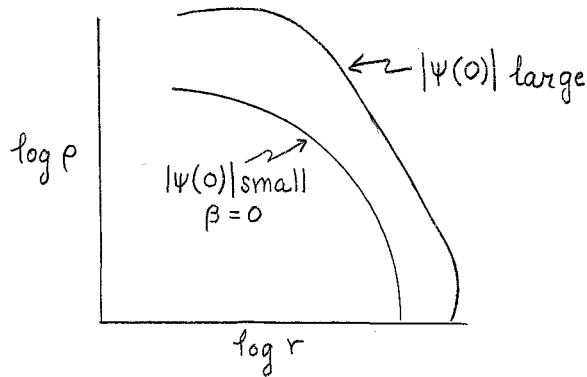
$$f = \begin{cases} a e^{\alpha^2 E + \beta J_z} & \text{if } E \leq E_0 < 0 \\ 0 & \text{otherwise} \end{cases}$$

2. We then compute $\rho = m \int f d\underline{u}$, which will be a function of Ψ .

3. Next we insert ρ into Poisson's equation and solve for Ψ , subject to the boundary conditions that $\Psi \rightarrow 0$ as $r \rightarrow \infty$ and that Ψ be well-behaved at the origin. The solution is achieved by iteration. That is, we solve successive equations of the form $\nabla^2 \Psi^{(n+1)} = C^{(n)} \rho(r, \Psi^{(n)})$, where C^n is chosen so that integration over all space gives the same total mass each time.

4. Substituting the solution Ψ from part (3) into the solution ρ of part (2), we obtain ρ as a function of position.

Typical results of this calculation are shown in the following figure:



The theoretical results can be compared with observation if we assume that the mass to light ratio is independent of position so that variations in brightness can be ascribed to variations in mass density. The observed brightness curve for the elliptical NGC 3379 has been matched by a theoretical density curve with a large value of $|\psi(0)|$. It is found that $\rho(r)$ is nearly independent of β , which is in accord with the observation that the

brightness curve is nearly independent of the eccentricity (i.e., it is nearly the same for E0 and E7 Galaxies).

For a given value of $\psi(0)$, there is a maximum value of β beyond which models of E galaxies cannot be constructed owing to the large angular momentum. This occurs at an axial ratio of 1/3, which is the axial ratio of E7 galaxies.

Apparently, the recipe for model construction given above successfully accounts for the observed features of elliptical galaxies. However, the present analysis leaves open the following questions. Why do ellipticals belong to a one-parameter (eccentricity) sequence? This feature has been built into the theoretical models by the arbitrary choice of the distribution function (β is the only free parameter since α^2 can be removed by appropriate scaling). The answer to this question seems to be that collisionless relaxation, which is studied by computer simulations of the N-body problem (see below), controls the form of the distribution function.

Notes submitted by
Richard J. Defouw

STRUCTURE OF BARRED SPIRALS (II)

Kevin H. Prendergast

(o) A neat, self-consistent model of barred spirals, akin to that developed for the ellipticals, is not obtainable. However, many of the gross features of barred spirals can be rationalized. In what follows the observer will almost always dwell in a rotating coordinate system in which the density of the galaxy is independent of time. Such a choice seems to conflict with the observed rotation curves for barred spirals, but it will be shown that there is no conflict.

In such a coordinate system one can write equations of motion,

$$-\nabla \left\{ \psi + \frac{1}{2} \Omega^2 \varpi^2 \right\} = \begin{cases} \frac{d^2 \underline{r}}{dt^2} + 2 \underline{\Omega} \times \frac{d \underline{r}}{dt} ; \text{ stars} \\ \frac{\partial \underline{u}}{\partial t} + \underline{u} \cdot \nabla \underline{u} + 2 \underline{\Omega} \times \underline{u} ; \text{ gas} \end{cases}$$

where Ω is the rotation rate, ψ the gravitational potential and ϖ the cylindrical radial coordinate. $\psi + \frac{1}{2} \Omega^2 \varpi^2$ will be denoted by V and called the potential. An equipotential map in the plane of the galaxy completes the preliminaries (see Fig.1, in which points a are saddle points and points b are maxima.)

(i) Gradient wind approximation: As a first attempt to discover trajectories suppose that particles (either stars or gas particles) move along the equipotentials at a rate just fast enough to balance the Coriolis force and the pressure gradient. The arrows in Fig.1 show the flow lines. Note that in the region of the bar there is flow in the same sense as the rotation. This vanishes on the curve passing through a's and increases toward the center. In a non-rotating coordinate system this produces an apparent rotation curve, (Fig.1a), the center and ends of which resemble strongly the observed curves for barred spirals. (If stars were to "leak" out of the saddle points, then they would have a sense of motion that would form arms which would have the correct sense with respect to the rotation curve.)

(ii) Consider more precisely the motion of stars well within the bar which have velocities small compared with ΩL initially. Suppose further that V is a uniform ellipsoid, so that $\nabla_i V = A_{ij} x_j$. The star's motion is governed by

$$\frac{d^2 \underline{r}}{dt^2} + 2 \underline{\Omega} \times \frac{d \underline{r}}{dt} = A_{ij} x_j$$

An equipotential map in the plane of the galaxy completes the preliminaries.

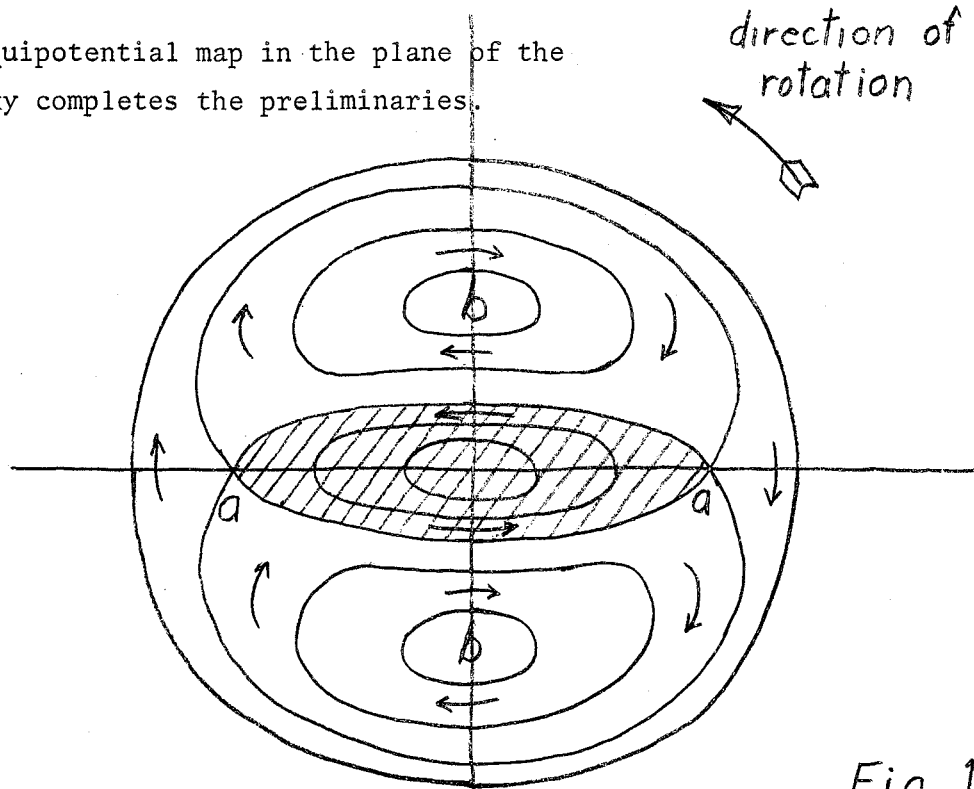


Fig. 1

Points a are saddle points and points b are maxima.

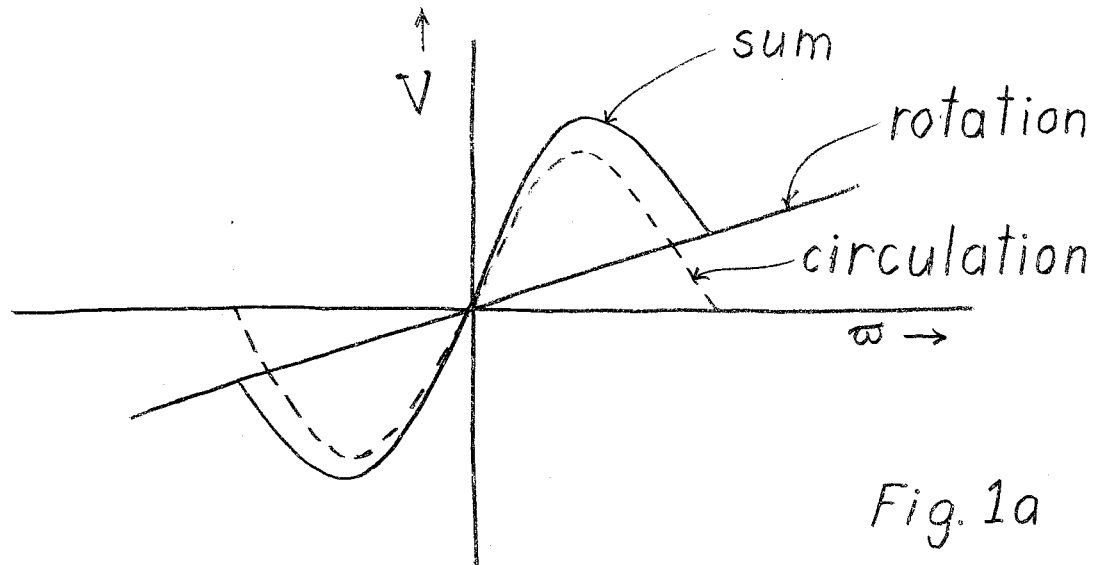


Fig. 1a

and the movement paths are



There is a direct electromagnetic analogy. The motion of a charged particle in a uniform magnetic field and a potential electric field is governed by

$$\frac{d^2 \underline{r}}{dt^2} + \frac{e}{c} \underline{\kappa} \times \frac{d\underline{r}}{dt} = e \underline{E} = -\nabla V_{elec.}$$

and the loops can be identified with Larmor motion about magnetic field lines, and the gross orbital motion with $\underline{E} \times \underline{B}$ drift.

(iii) It can be shown that one can relax the restriction on the nature of the potential function at high rotation rates and obtain star trajectories which are direct analogs of those described in (ii) above.

(iv) One can escape the restrictions above only numerically. Here the motion of a star with $\left| \frac{dr}{dt} \right|_0$ small, medium and large is considered.

(a) $\left| \frac{dr}{dt} \right|_0 \gg \Omega L$: Star escapes to infinity in a spiral (in the rotating system) or a straight line (in non-rotating system).

(b) $\left| \frac{dr}{dt} \right|_0 \sim \Omega L$ (see Fig.2),

In Fig.2 the a's and b's are the same as those marked on the equipotential diagram (Fig.1). This can be pictured physically as a star trying to execute the epicyclic motion of (ii) on a scale comparable to the size of the bar.

Figure 3 shows an actual SB_b^a for comparison with the model (Fig.2).

In such galaxies there is observed high random motion. That is, the gravitational potential is significantly balanced by "dynamic pressures" as distinct from centrifugal pressures. For a galaxy like that shown the dynamic pressure is of the order of the centrifugal pressure.

(c) $\left| \frac{dr}{dt} \right|_0 \ll \Omega L$, but with the star near the edge of the bar (Fig.4).

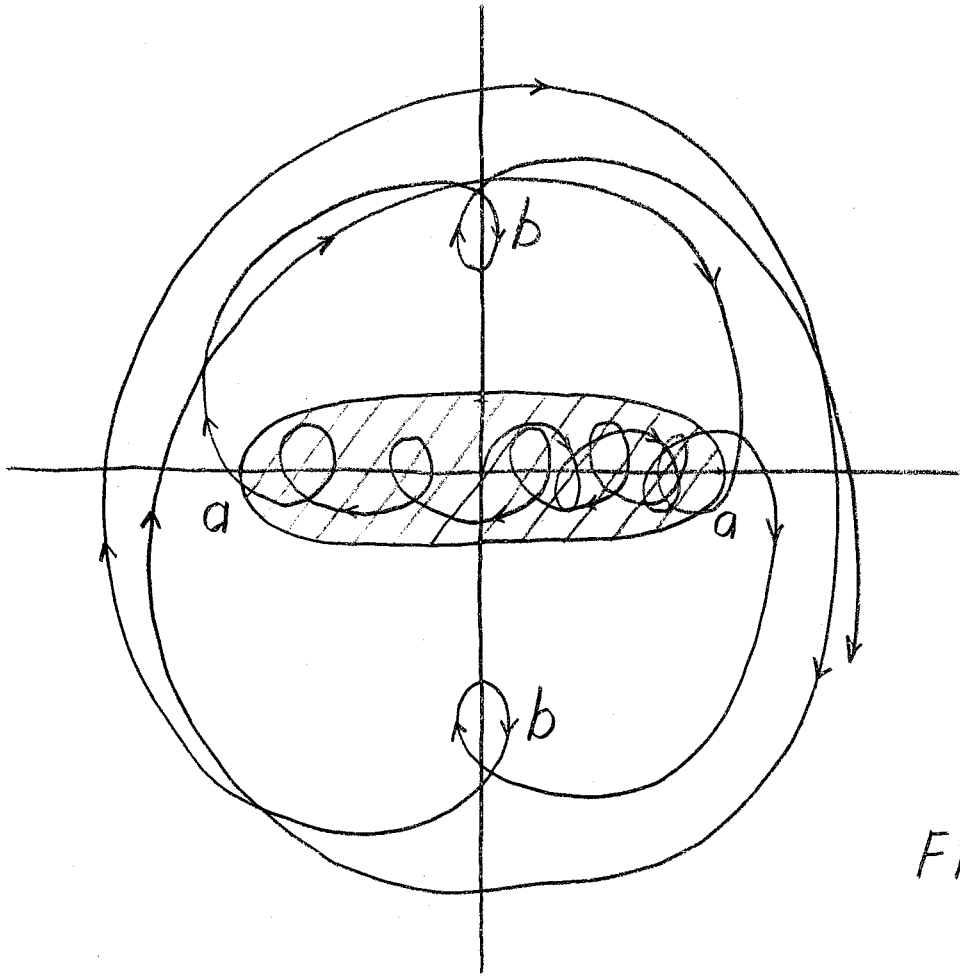


Fig. 2

Schematic SBa



Fig. 3

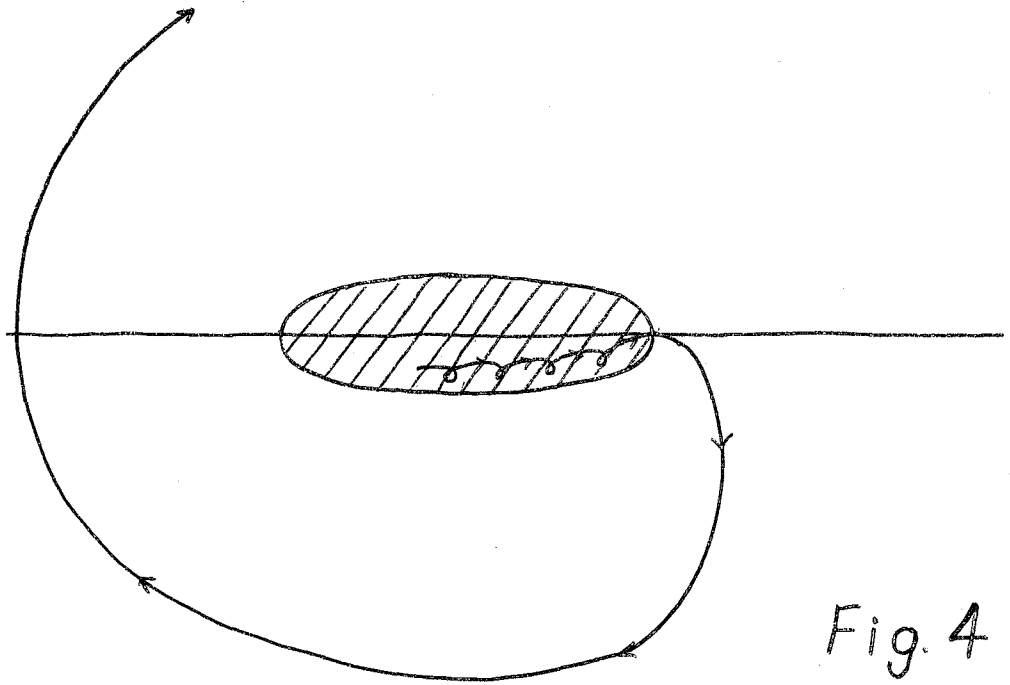


Fig. 4

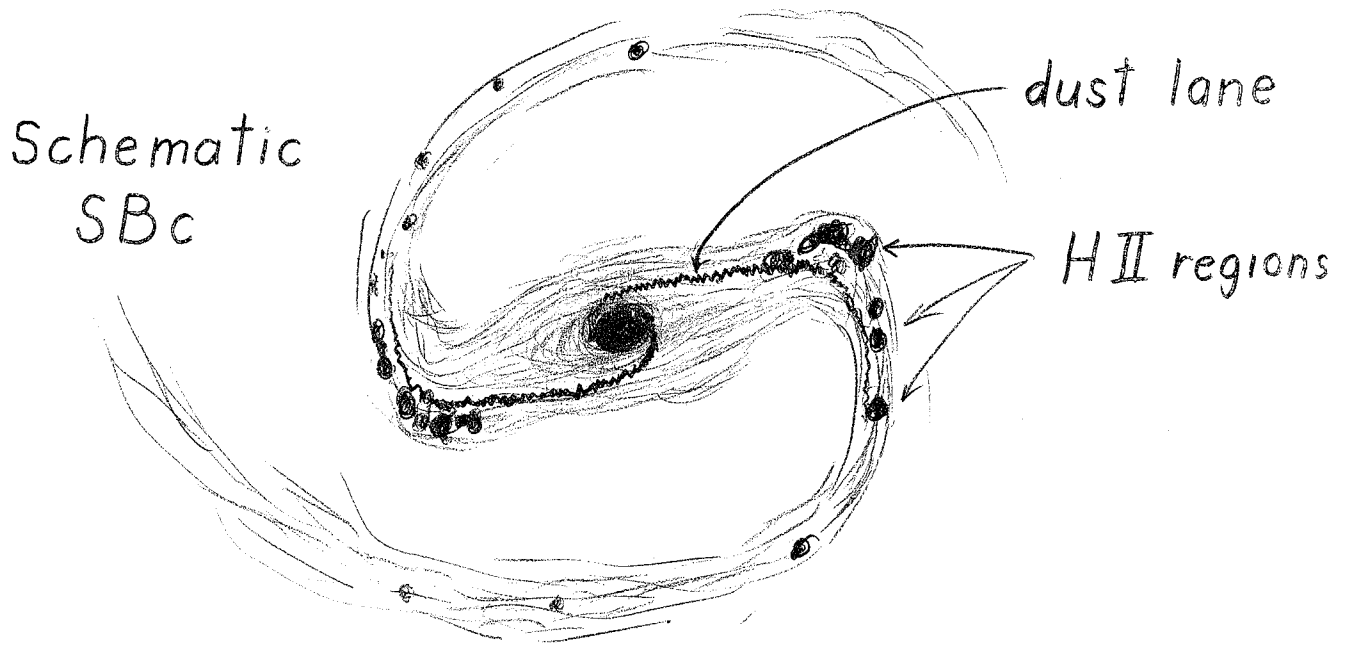


Fig. 5

In this case the star escapes because it is more constrained. It must remain on the equipotential until the force holding it there is very small. This gives it sufficient time to gain angular momentum comparable to that associated with ΩL , so that when it finally breaks its contact with the equipotential it can escape the entire system. (This picture is in the rotating coordinate system. However, if stars are escaping radially in the neighborhood of the ends of the bar, and the bar is turning, the integrated result in a non-rotating system will look like a single trajectory in the rotating system.)

An actual SBc is shown in Fig.5.

(d) Bearing in mind the picture in Fig.5, consider again V corresponding to a uniform ellipsoid and add dust. The exact solution gives streamlines as in Fig.6. The inner dashed line is the sonic locus. The dash-dot lines are characteristics. The outer-directed ones are asymptotic to the free surface, and the inner ones are reflected off the sonic locus. A shock would resemble these characteristic curves and the question arises naturally, are the dust lanes shock phenomena? The solution in the neighborhood of the saddle-point (x-point) is as in the figure. All the characteristics are asymptotic to a single line. This is suggestive of a shock. (Fig.6a).

To look more carefully attempt a similarity solution in the neighborhood of the x-point. (Fig.7). Map the end of the bar into a formal problem replacing the dividing streamline by a wall. Then put

$$u_{\sigma} = rV(\varphi) \quad v_{\varphi} = \sigma V(\varphi) \quad C^2 = r^2 Z(\varphi)$$

Solving the equations under these assumptions requires a shock. Without

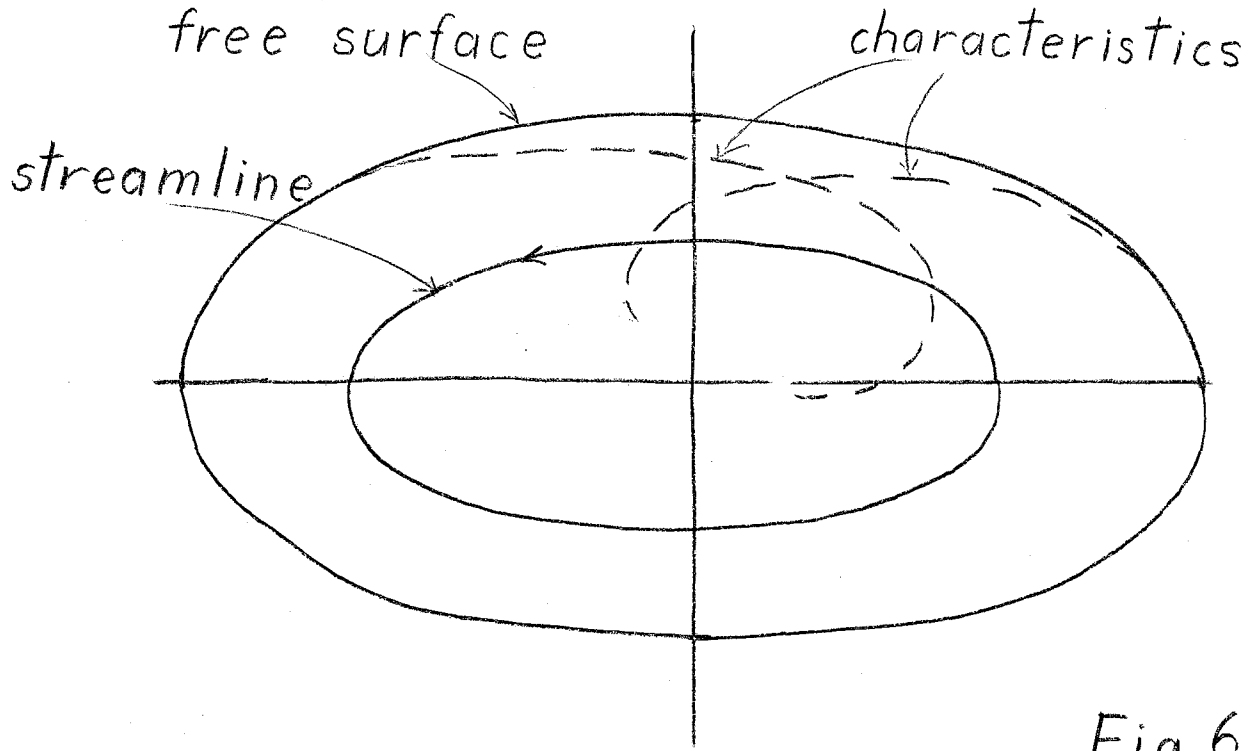


Fig. 6

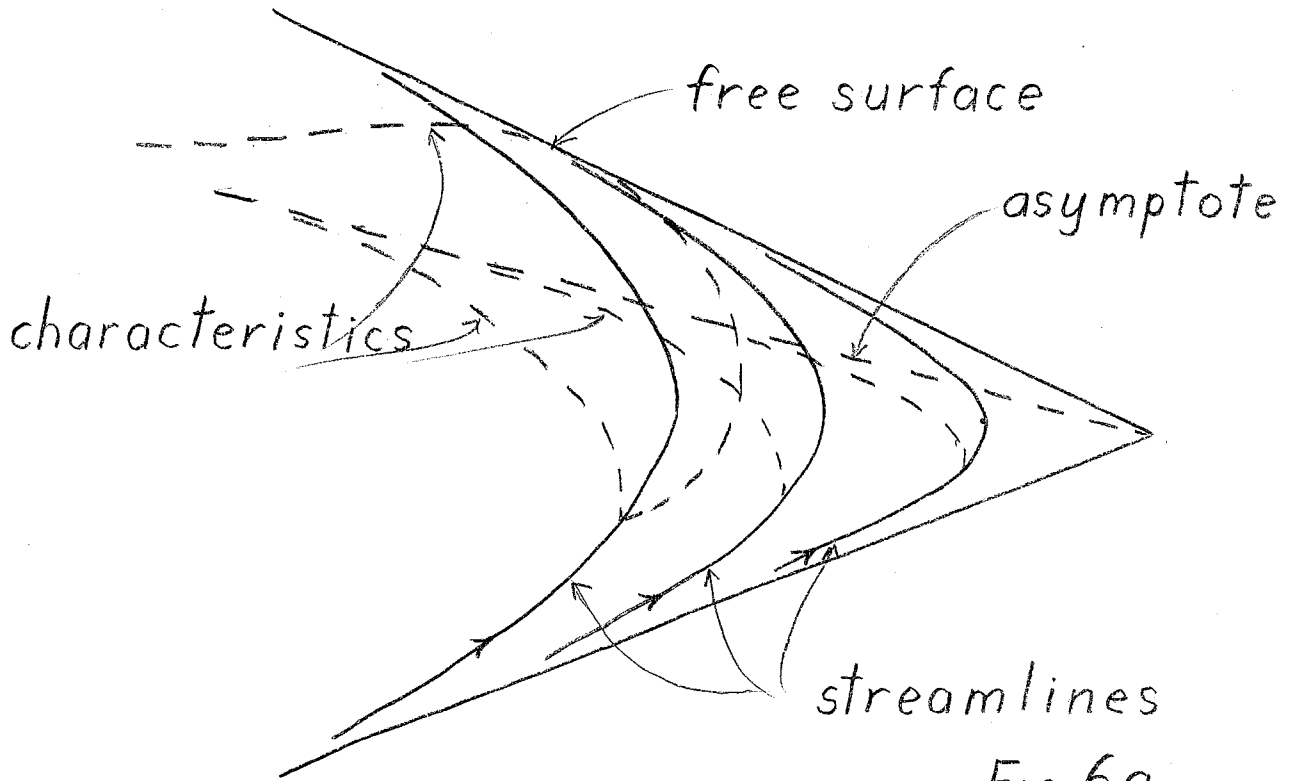


Fig. 6a

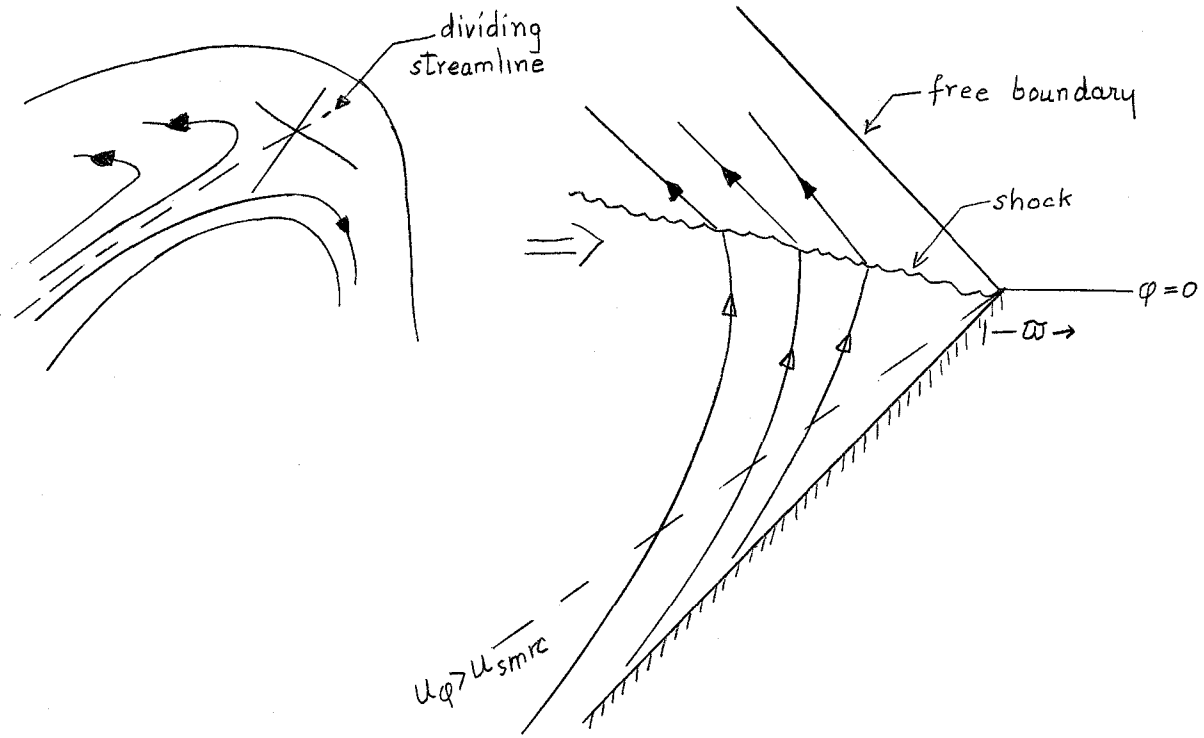
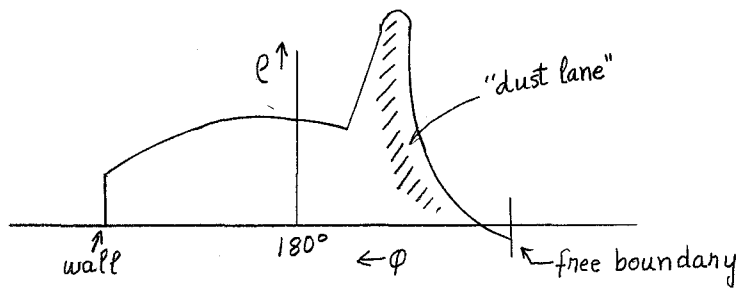


Fig.7

the shock the computed streamlines cross. One adds a shock and adjusts its location until the labelled free boundary is a free boundary. By this is meant that one runs out of density and velocity in the same place. A density map of such a solution looks like



and one can see that this calculation does rationalize the dust lanes.

Notes submitted by
Roger F. Gans

MACHINE SIMULATION OF GALACTIC EVOLUTION (III)

Kevin H. Prendergast

We now return to the question raised in the discussion of E galaxies, namely, what determines the form of the distribution function f ? In general, f can be any function of the integrals of the problem. However, relaxation processes reduce the number of possible forms for f . One form of relaxation is due to binary encounters, but the time scale for this process in a galaxy is longer than the age of galaxies. Relaxation through binary collisions therefore does not account for the apparent "relaxed" state of galaxies. A faster relaxation process is phase mixing (collisionless relaxation) and is probably the process we are looking for.

Some work on the statistical mechanics of collisionless systems has been performed by Lynden-Bell, who considered systems of distinguishable particles which obey an exclusion principle corresponding to the requirement that density in phase space is preserved (Liouville's theorem).

Another approach to the relaxation problem has been to simulate the process on a computer. A particularly simple problem is to determine the motion of parallel planar masses in the direction perpendicular to the planes. Since the force due to an infinite plane is independent of distance, one obtains the force on a given slab A simply by counting the number of slabs on either side of A. A more realistic problem is to actually compute the three-dimensional motion of N mass points. Owing to the greater complexity of this problem, present computers can follow the motion only for relatively small N (25-100). The formation of transient binary systems eats up computer time and obscures the physics one is really after.

Yet another problem which can be studied on a computer is the two-dimensional motion of a system of mass points. This problem is easier than the three-dimensional problem but avoids the artificiality of the one-dimensional motion of slabs. In order to reduce the effects of encounters, which tend to be important for small N (but not for actual galaxies of large N), one lets the gravitational potential from a point mass vary as $(r^2 + a^2)^{-1/2}$. The introduction of "a" reduces the effects of nearby approaches of stars but has little effect on the collective dynamics. We now discuss the two-dimensional problem in greater detail. First we describe a "game" formulation of the problem which has many advantages for machine computation. We then describe the results of such computations as displayed in the film shown by Dr. Prendergast.

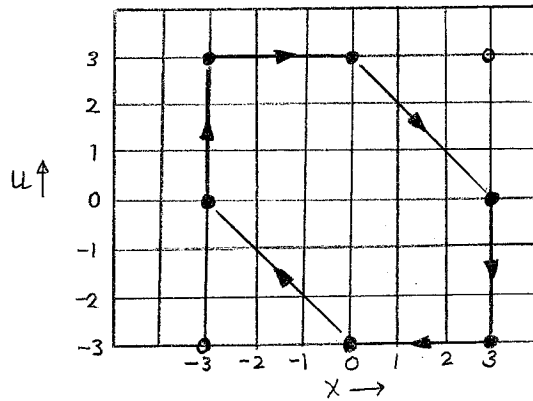
Notes submitted by
Richard J. Defouw

MACHINE SIMULATION OF GALACTIC EVOLUTION (2)

Kevin H. Prendergast

To model a collisionless galaxy on the machine requires either incredibly small round-off error, or a scheme which fixes the round-off error to be precisely the truncation error. This is because the round-off error acts like diffusion and any collisionless relaxation mechanism would be obscured by the round-off relaxation. Such a scheme can be done by "discretizing" everything in the problem.

Make a grid in a one-dimensional system. A particle in this grid has the velocity u corresponding to its u line number and feels a force $f(x)$



according to its x line number.

For an example, suppose $f(x) = -x$, and begin at $(-3, 3)$;

- (i) move 3 to right (ii) $f(0) = 0$, no move
- (iii) move 3 to right (iii) $f(3) = -3$, move down 3
- (v) move 0 (vi) $f(3) = -3$, move down 3
- (vi) move 3 to left (vii) $f(0) = 0$. . . etc.

The difference equations this process represents are:

$$u^{(n+\frac{1}{2})} - u^{(n-\frac{1}{2})} = f(x^{(n)})$$

$$x^{(n+1)} - x^{(n)} = u^{(n+\frac{1}{2})}$$

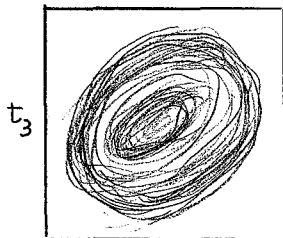
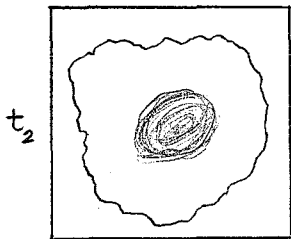
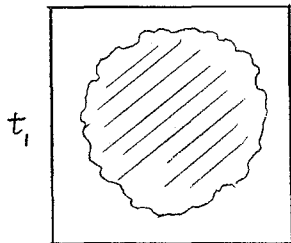
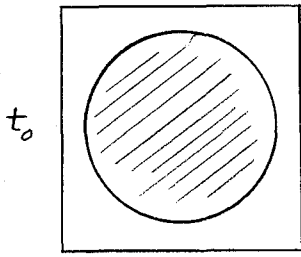
and the solutions have the properties:

- i) perfect periodicity
- ii) complete reversability
- iii) no orbits have common points
- iv) motion is area preserving, equivalent to Liouville Theorem. All

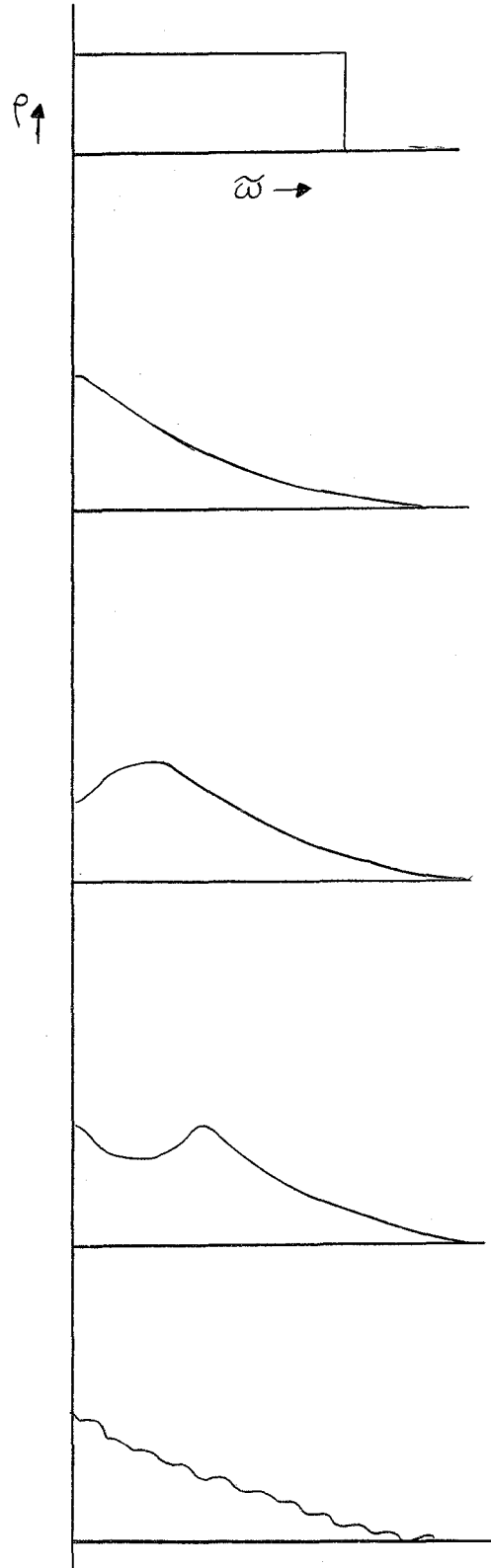
of these properties of Newtonian dynamics are built directly into the system.

Similar schemes can be used in N dimensions. By modification of f one can include interaction effects. (In the current state of the art the boundary conditions at the edge of the grid are taken to be periodicity conditions to make computation easier. This affects only particles near the edge, but makes their motion incorrect. This is to be rectified in the future.)

Plan view



Section



First computation: Pour particles into x-y space in an approximate circle, n particles/grid point. In u,v space assign each (x,y) grid point its tangential velocity corresponding to solid rotation and group the n particles at x_0, y_0 as closely to u_0, v_0 as possible. This provides a near equilibrium starting point. As the computation begins the fast particles ($\omega r t \Omega R$) escape, depleting the remaining material more in energy than mass, initiating a collapse. The collapse overshoots and "bounces". One gets central concentration and a very hot (high random motion) system.

To test the sensitivity of this process to the initial condition the configuration of the first computation, which will be called the "quiet circle" is replaced by a noisy circle, in which u_0, v_0 are randomly modified by adding -1, 0 or 1 in a random fashion to the initial positions in velocity space. Such a calculation does not maintain four-fold symmetry as the first did. The end point is an elliptical concentration with a pattern rotation rate less than the star rotation rate. Qualitatively the two calculations are quite similar.

Both of the above computations share the disadvantage of producing very hot systems. One wishes to produce galaxies with both hot and cold populations. One can make cold populations by artificial cooling. If this is done suddenly in the midst of a calculation, the assemblage after cooling will collapse because of the reduced dynamic pressure; the collapse will reheat the system and nothing has been gained. If, on the other hand, one cools at every step no order emerges from the calculation.

In a natural system of gas and stars, the gas, with good internal dissipation and radiation, will remain cool; stars will not. This suggests

a two-component system can be formed by starting with "gas" and using some technique to form "stars".

Such a technique is used to generate the film. A star formation law

$$\text{rate} = \propto \rho^2$$

is assumed, and at each time step the "gas" is cooled, if ρ is of the appropriate magnitude anywhere the correct number of "stars" is formed and the next time step is executed. The crucial point is that, for the remainder of the calculation, the "stars" that have been formed are not cooled.

The film showed separately the behavior of the "gas" and the "stars". The "gas" behaved in what this reviewer might call a galactic manner, but the "stars" were rather dull, clumping into a central concentration with moderately large random motion; one might say they were upstaged by the "gas".

There followed a discussion of the philosophy of the process described as scientific inquiry during which little was resolved.

Notes submitted by
Roger F. Gans

FLUID DYNAMICAL PHENOMENA IN THE SUN

Edward A. Spiegel

In considering the dynamics of the sun it is convenient to start with the simplest reasonable hypotheses regarding structure. We assume that the sun is basically in hydrostatic equilibrium so that we may write:

$$-\nabla p + \rho \nabla \phi = 0 \quad (1)$$

$$\nabla^2 \phi = -4\pi G \rho \quad (2)$$

where ρ is the density, p is the pressure and ϕ is the gravitational

potential. To Eqs. (1) and (2) we add the simplifying assumption that ρ is smooth at the center of the sun. Next we introduce an appropriate equation of state:

$$p = \frac{k}{\mu m_H} \rho T \quad (3)$$

where T is the temperature, k is the Boltzmann constant, m_H is the proton mass and μ is the mean molecular weight measured in proton masses.

Finally we assume that the system is in radiative equilibrium. Then using Eddington's approximation we obtain:

$$\underline{F} = -K \nabla T \quad (4)$$

where \underline{F} is the radiative flux and K is the radiative conductivity. The conductivity K in (4) is given by:

$$K = \frac{4}{3} \frac{acT^3}{\kappa\rho} \quad (5)$$

where a is the Stefan-Boltzmann constant, c is the velocity of light and κ is the Rosseland mean opacity.

Next we try to determine the conditions under which the assumed equilibrium is unstable. To do this we consider the following perturbation (cf. Fig.1). Let us displace a small element of matter upwards (toward the surface) by a small distance dr . Let the element expand adiabatically until the pressure inside the element is equal to the ambient pressure.

Then if the element starts moving back towards its original position the radiation equilibrium is stable whereas if it tends to move upward, the equilibrium is unstable. In the figure, the primed quantities represent states in the element while the unprimed quantities represent states in the surrounding regions.

Let the subscript 1 represent the initial states where we have:

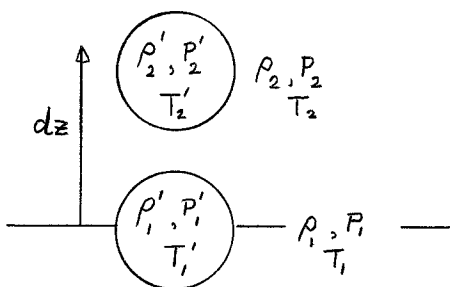


Fig.1

$$\rho'_1 = \rho_1, P'_1 = P_1 \text{ and } T'_1 = T_1 \quad (6)$$

After the perturbation we have:

$$P'_2 = P_2 \text{ and } \rho'_2 = \rho'_1 \left(\frac{P_2}{P'_1} \right)^{1/\gamma} \quad (7)$$

where we have used the adiabatic law

$$\rho = \text{constant} \times P^{1/\gamma} \quad (8)$$

and $\gamma = \frac{c_p}{c_v}$, the ratio of specific heats.

Clearly we have a stable equilibrium if $\rho'_2 > \rho_2$ since the pressure force has not been altered in the perturbation. From (6) and (7) we can determine the condition for stability in terms of ambient quantities:

$$\rho_1 \left(\frac{P_2}{P_1} \right)^{1/\gamma} > \rho_2 \quad (9)$$

Then using

$$\rho_2 - \rho_1 = \frac{d\rho}{dz} dz \text{ and } P_2 - P_1 = \frac{dP}{dz} dz \quad (10)$$

we obtain

$$\frac{1}{\gamma} \frac{1}{P} \frac{dP}{dz} > \frac{1}{\rho} \frac{d\rho}{dz} \quad (11)$$

where we have dropped the subscript 1. Then if we use Eq.(3) in the form

$$\rho = (c_p - c_v) \rho T \quad (12)$$

together with (8) we obtain, after some computation:

$$-\frac{dT}{dz} \Big|_{AD} > -\frac{dT}{dz} \quad (13)$$

where

$$\frac{dT}{dz} \Big|_{AD} \equiv \left(1 - \frac{1}{\gamma} \right) \frac{T}{P} \frac{dP}{dz} \text{ is the adiabatic gradient.} \quad (14)$$

The hydrostatic law (1) in the form

$$\frac{dP}{dz} = -\rho g \quad (15)$$

and Eq.(12) then enables us to replace (14) by:

$$\left. \frac{dT}{dz} \right|_{AD} = - \frac{g}{c_p} \quad (16)$$

Hence the stability condition can be written finally as follows:

$$\frac{F}{K} = |\nabla T| < \left. |\nabla T| \right|_{AD} = \frac{g}{c_p} \quad (17)$$

The corresponding instability condition is

$$\frac{F}{K} > \frac{g}{c_p} \quad (18)$$

and this is the famous Schwarzschild Criterion. Thus we expect instability when c_p is large or when K is small. For example, consider regions where there is a high concentration of single ionized hydrogen atoms (H_2^-). In such regions we would expect c_p to be large due to the absorption of energy by H_2^- . We would also have a large opacity (and hence a small K) due to this absorption. The Schwarzschild Criterion then tells us that we should expect convective instability in such regions.

Evidence for the existence of convective motions in the outer layers of the sun comes from a study of the granulation observed on the surface. This granulation consists of cell-like structures ranging in size from 300 km to 2000 km. They are observed as brightness fluctuations corresponding to temperature fluctuations of hundreds of degrees. Further evidence for the existence of convective motion arises in the analysis of spectroheliograms on the solar surface. In particular, the technique used by Leighton, Noyes and Simon¹ described below yields a wealth of data on convection in the photosphere and lower chromosphere.

The spectroheliograph used by the Leighton group to photograph velocity fields is represented schematically in Fig.2. It consists of a

¹Leighton, Noyes and Simon, Astrophysical Journal 135: 474-499 (1962).

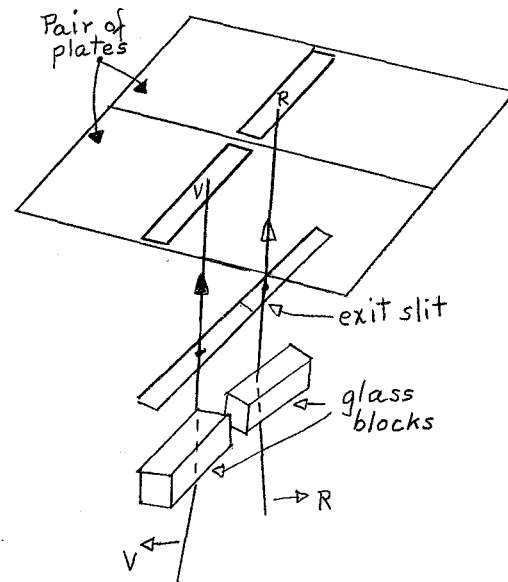
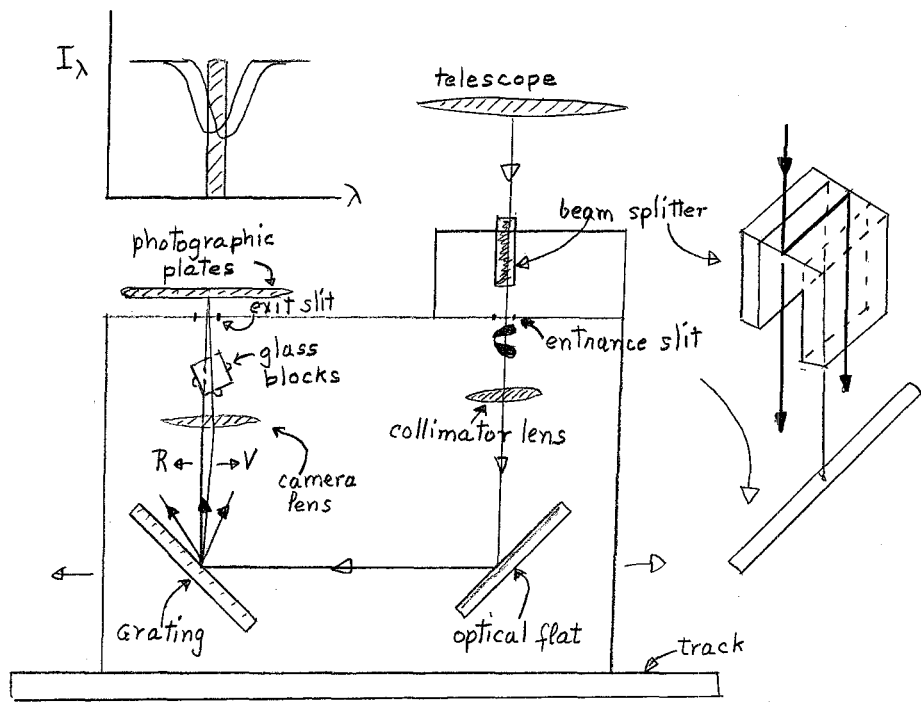


FIG. 2

moveable box containing optical equipment constructed and mounted in such a way that the entire solar disk in the image field of a telescope is scanned and photographed monochromatically in a sequence of vertical strips parallel to the solar rotation axis as the box is moved from left to right or vice versa. Light from the telescope reaches the entrance slit in two adjacent beams by the action of the beam splitter as shown in Fig. 2. The grating picks out a spectral line and the exit slit is centered precisely on the spectral lines when the glass blocks shown in the figure are un-tilted. The glass blocks are then tilted through equal angles but in opposite directions. As a result, one plate receives an image of the red side of the line and the other plate an image of the blue side of the line.

From the two plates we make a composite plate by superposing a positive transparency of one plate on the other negative. The result, after correction is made for the effects of rotation, is a uniform gray if there is no Doppler shift. If the line is Doppler shifted however, then the composite plate records only this shift, and density variations due to variations in intrinsic brightness cancel to a uniform gray (cf. Fig.3). Such a composite photograph is referred to as a singly cancelled plate.

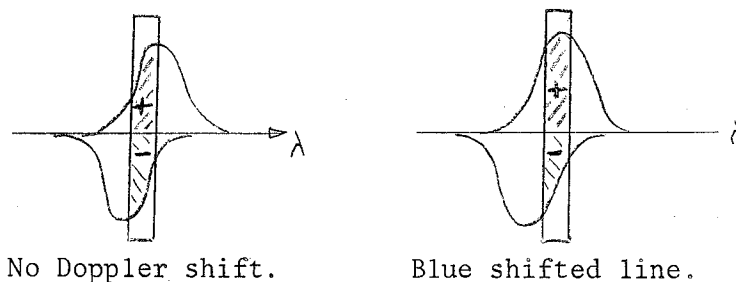


Fig.3

It gives a picture of the line of sight velocity fields on the solar disk.

Suppose that we scan the solar disk first in one direction and then immediately scan again in the opposite direction (the process takes about eight minutes). If we make two singly cancelled plates from the originals and then "subtract" the two composites in the same way we obtain a double cancellation or Doppler difference plate. If the velocity field changes during the eight minutes of scanning, then the difference plate records the accelerations in the solar atmosphere. (cf. Fig.4).

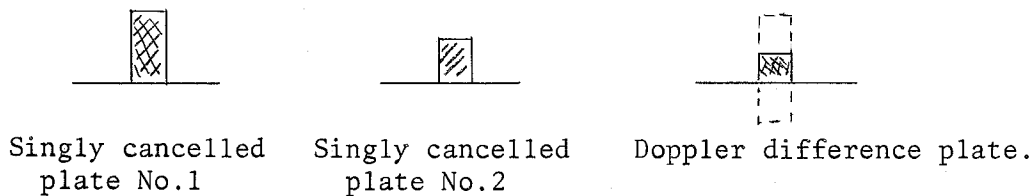


Fig.4

If there is no change in velocity field, the difference plate records a uniform gray.

We can also construct a Doppler sum plate as follows:

We scan first in one direction, tilt the blocks in the opposite sense and immediately scan in the opposite direction. If the two singly cancelled plates constructed from the originals are then "subtracted" again, the result is a fourfold enhancement of the Doppler shift on the originals (cf. Fig.5). The effect is to smear out small scales so as to bring out the larger scales more clearly.

Some of the results of such experiments may be summarized as follows:

1) Large "cells" of horizontally moving material are distributed roughly uniformly over the entire solar surface. The spacing between centers is of order 3×10^4 km, with r.m.s. velocities of outflow of 0.5 km/sec. Within

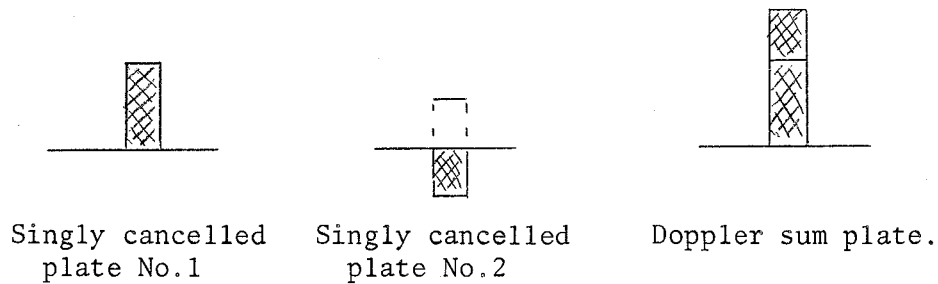


Fig.5

each cell the motion is outward from the center towards the boundaries.

Leighton et al. suggest that these "cells" are a surface manifestation of a "supergranulation" pattern of convective currents which come from relatively great depths inside the sun. These large scale motions appear most clearly in Doppler sum plates.

2) A study of the original plates in a given scan shows a correlation between local brightness fluctuations and vertical velocities. The correlation coefficient is ~ 0.5 . This suggests that the small scale granulation pattern is associated with mechanical transport of energy by convection.

3) A statistical analysis of difference plates reveals that the vertical velocities exhibit a repetitive motion with an autocorrelation time scale of about 300 seconds. The Leighton group interpret this as a wave-like propagation of energy upward from within the photosphere at a well-defined frequency and its dissipation into heat in the lower chromosphere.

4) A study of velocity fields in the H_{α} line enables us to observe structure in the chromosphere. One finds granular structures in the upper chromosphere with cells' size of order $3-4 \times 10^3$ km. At lower levels one finds predominantly downward motions which are concentrated in "tunnels" which presumably follow magnetic lines of force (c. Fig.10).

The following analysis represents a rough attempt to understand some of these phenomena.

In order to obtain some idea of the magnitudes of the scales of convective motion we must consider a modification of the flux equation. For this purpose we consider a small blob of mass m and volume V moving in the vertical direction as shown in Fig.6 below. Let $\bar{\rho}$, \bar{T} and \bar{p} represent horizontal averages of the corresponding quantities in the ambient region at the position z of the element, and let ρ , T , p be the density, temperature and pressure in the element itself. We may assume that the motions are subsonic so that we may set $\bar{p} = p$. The motion of the blob is governed by gravitational and buoyancy forces and, using the Boussinesq approximation we set

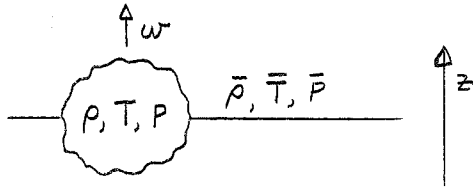


Fig.6

horizontal averages of the corresponding quantities in the ambient region at the position z of the element, and let ρ , T , p be the density, temperature and pressure in the element itself. We may assume that the motions are subsonic so that we may set $\bar{p} = p$. The motion of the blob is governed by gravitational and buoyancy forces and, using the Boussinesq approximation we set

$$\bar{\rho} \ddot{z} = -g(\rho - \bar{\rho}) \text{ and} \quad (19)$$

$$\rho - \bar{\rho} = -\frac{\bar{\rho}}{\bar{T}} (T - \bar{T}) \equiv -\bar{\rho} \alpha \theta \quad (20)$$

where we have set $\alpha \equiv \frac{\bar{\rho}}{\bar{T}}$ and $\theta \equiv T - \bar{T}$, (21)

This gives:

$$\ddot{z} = g \alpha \theta \quad (22)$$

Now the flux equation may be written as follows:

$$\rho c_p \frac{dT}{dt} - \frac{dp}{dt} = \nabla \cdot \underline{F} \quad (23)$$

where \underline{F} is the radiative flux.

Newton's law of cooling gives:

$$\nabla \cdot \underline{F} = -\bar{\rho} c_p g \theta \quad \text{where } [c_p] = T^{-1} \quad (24)$$

By the chain rule:

$$\frac{dT}{dt} = \frac{d\theta}{dt} + \frac{d\bar{T}}{dz} \dot{z} \quad (25)$$

and
$$\frac{dp}{dt} = \frac{d\bar{p}}{dt} \approx \frac{d\bar{p}}{dz} \bar{w} = -g \bar{p} w \quad (26)$$

where $\bar{w} \equiv \dot{z}$. (27)

Substitution of (24) through (27) in (23) gives as the new heat equation:

$$\dot{\theta} - \beta \bar{w} = -g \theta \quad (28)$$

where

$$\beta \equiv \left(-\frac{d\bar{T}}{dz} \right) - \frac{g}{c_p} \quad (29)$$

and is unknown at this point. However by the Schwarzschild criterion (18) we know that convection occurs in regions where $\beta > 0$. Therefore in order to determine the dominant convection scales we must obtain some estimate of the behaviour of the function $\beta(z)$ in the convective zone. In order to do this we use a self-consistent approximation starting with $\beta = \text{constant} > 0$ for the small scale motion of the blob through a distance l where we assume that

$$l \sim \text{size of blob} \sim \text{mean free path of blob} \sim \left(\frac{1}{\bar{p}} \frac{d\bar{p}}{dz} \right)^{-1} \quad (30)$$

With these assumptions we proceed to integrate (7) and (13) to obtain \bar{w} and θ from which we obtain the convective heat flux $F_c = \bar{p} c_p \bar{w} \theta$ as a function of β . Then from

$$\mathcal{F} = F_c - K \frac{d\bar{T}}{dz} \equiv \text{total flux} \quad (31)$$

where \mathcal{F} can be related to the constant luminosity L we obtain a differential equation for \bar{T} which we then integrate through the convective zone to get \bar{T} (and hence β) as a function of z . The result is shown schematically in Fig.7. This gives us the granulation and supergranulation scales of order 2000 km and 30,000 km respectively.

Using this result we can now proceed to the time integration of (22) and (28). Upon eliminating θ from (22) using (28) we obtain:

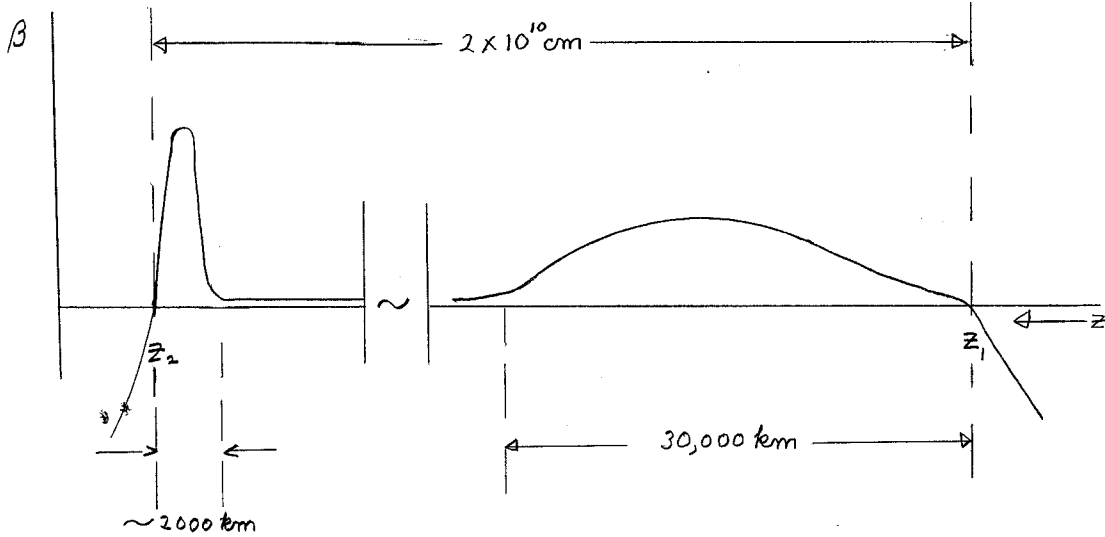


Fig.7

$$\ddot{z} + q\dot{z} - g\alpha\beta\dot{z} = 0 \quad (32)$$

A time integration then yields:

$$\dot{z} + qz + g\alpha\left(\bar{T} + \frac{g}{c_p}z\right) = \text{constant} \equiv g\alpha T_0 \quad (33)$$

We can think of (33) as the equation of a damped oscillator:

$$\ddot{z} + q\dot{z} + \frac{\partial U}{\partial z} = 0 \quad (34)$$

where

$$\frac{\partial U}{\partial z} \equiv g\alpha\left(\bar{T} - T_0 + \frac{g}{c_p}z\right) \quad (35)$$

represents the available potential energy. A sketch of the results both with and without damping is shown in Figs.8a and 8b. The time scale for the oscillation in Fig.8b corresponds to that observed in the analysis of difference plates.

Our interpretation of the granulation in the chromosphere may help to explain the tight correlation of the width W_0 of the ionized calcium line (cf. Fig.9) with the luminosity L of a star over a wide range of stars. In Fig.10 we have a schematic representation of the granular cells in the chromosphere. Let $\overline{v_c^2}$ be the mean square velocity in the chromo-

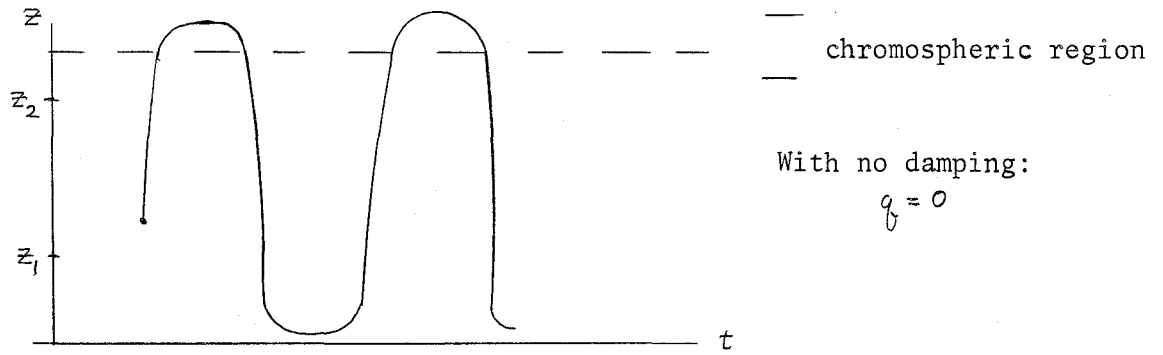


Fig.8a

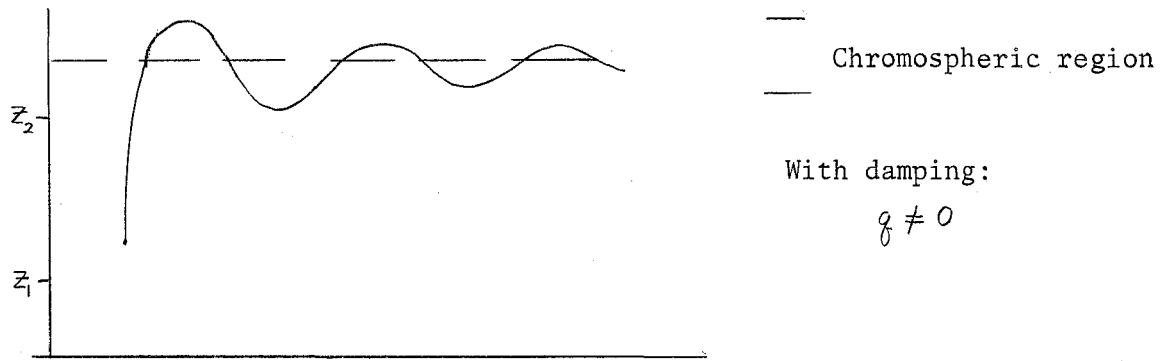
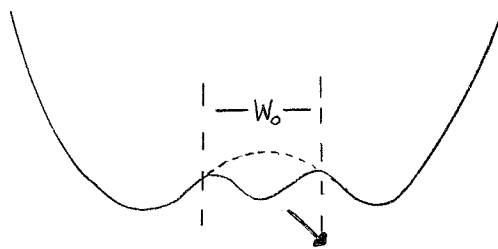


Fig.8b



Calcium emission line

Fig.9

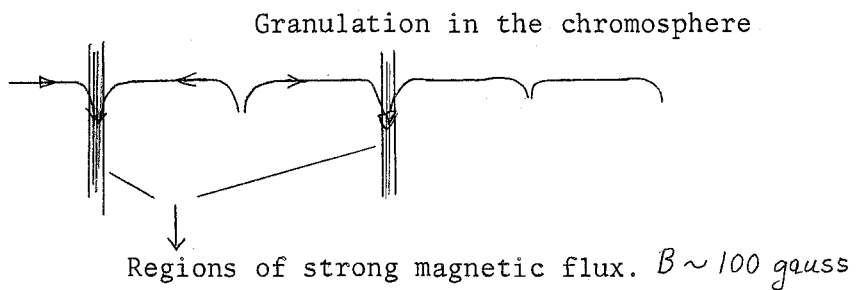


Fig.10

sphere. Then if W_0 is due principally to Doppler broadening we have:

$$W_0^2 \sim \overline{v_c^2} \quad (36)$$

Now suppose that emission occurs when dissipation of the motion becomes important. Then if $\overline{B^2}$ is the mean square field produced by the convective cells extending into the convection zone we would expect that

$$\frac{1}{2} \rho_c \overline{v_c^2} \sim \frac{\overline{B^2}}{8\pi} \sim \frac{1}{2} \rho_0 W_0^2 \quad (37)$$

$$\overline{v_c^2} \sim \frac{\overline{B^2}}{4\pi\rho_c} \equiv V_A^2 \sim W_0^2 \quad (38)$$

where ρ_c is the density in the chromosphere and V_A is the Alfvén speed.

But if the cells extend into the photosphere of density ρ_{ph} where the mean square velocity of convective motion is say $\overline{u^2}$, we may write:

$$\frac{1}{2} \rho_{ph} \overline{u^2} \sim \frac{1}{2} \rho_c \overline{v_c^2} \quad (39)$$

whence we obtain

$$W_0^2 \sim \frac{\rho_{ph}}{\rho_c} \overline{u^2} \quad (40)$$

Since $\overline{u^2}$ determines the flux (and hence the luminosity) of a star and since ρ_{ph}/ρ_c varies only weakly from star to star we are led to expect that indeed there should be a correlation between W_0 and L.

Reference

Leighton, Noyes and Simon, Astrophys.J. 135: 474-499 (1962).

Notes submitted by
Joseph M. Buschi

DECREASE IN THE ROTATION RATE OF THE SUN

Edward A. Spiegel

The best evidence for the decrease in the rotation rates of stars with time comes from an analysis of the Doppler broadening in the spectra of various stars having the same mass and chemical composition but different ages. The following table gives some results obtained in one such study (Kraft, Ap.J.). In the column labelled "Veq" we record typical equatorial velocities obtained for stars in a given system.

Stars	Age (in yrs)	Veq. (in km/sec)
Pleiades	$\sim 5 \times 10^7$	~ 20
Hyades	$\sim 5 \times 10^8$	~ 10
Sun	$\sim 5 \times 10^9$	~ 2

The solar wind has been proposed as an effective mechanism for decreasing the angular momentum of the sun. In order to see this, we compare the magnetic energy density $B_r/8\pi$ of the radial field B_r and the radial kinetic energy density $\frac{1}{2} \rho u_r^2$ of the wind. Consider a sphere of radius $r > R_\odot$ concentric with the sun. The flux of \underline{B} and the flux of mass are given respectively by:

$$F_B = 4\pi r^2 B_r = \text{constant} \quad (1)$$

$$F_M = 4\pi \rho r^2 u_r = \text{constant} \sim 10^{12} M_\odot / \text{yr.} \quad (2)$$

where F_B and F_M are known quantities independent of r .

Therefore

$$\frac{B_r^2/8\pi}{\frac{1}{2}\rho u_r^2} = \frac{4\pi \rho F_B^2}{F_M^2} \equiv \frac{\rho}{\rho_c} \quad \text{or:} \quad (3)$$

$$u_r^2 = \frac{\rho_c}{\rho} V_A^2 \quad \text{where } V_A \text{ is the Alfvén speed and } \rho_c \text{ a constant density.}$$

Hence for $r < R_A$ where R_A is such that $\frac{\rho}{\rho_c} \sim 1$ (i.e., $R_A \sim 15 R_\odot$) the field is strong enough to cause the wind to co-rotate with it. Hence the rate of change of the angular momentum J of the sun is given by:

$$\dot{J} = \dot{M} R_A^2 \Omega \quad (4)$$

where Ω is the angular velocity of rotation of the sun. Now we may express the angular momentum J as follows:

$$J = \alpha M_\odot R_\odot^2 \Omega \quad (5)$$

where α is a factor which depends on the density and rotational velocity distribution within the sun. If all of the solar mass rotates with the same angular velocity, then $\alpha \sim 1$. Using typical estimates of \dot{M} and R_A we obtain from (4) and (5) a time scale T for this process at present:

$$T = \frac{J}{\dot{J}} = \alpha \frac{M_\odot R_\odot^2}{\dot{M} R_A^2} \sim \alpha \times 5 \times 10^9 \text{ yrs.} \quad (6)$$

If we follow Dicke¹ and assume that the interior is still rotating much more rapidly than the surface layers we obtain a value of order 10^{-2} for α . However we suggest that this estimate is not correct because it is based on the assumption that the spin down of the solar interior is controlled by viscous diffusion. We propose that the interior spins down on a time scale much smaller than the viscous diffusion time proposed by Dicke. The basis of our proposal is that the principal mechanism for spin down is not viscous diffusion but more probably the Ekman-like pumping action of the convective zone. The following is a rough analysis of this process.

In Fig.1 we give a schematic representation of the kind of secondary flow pattern to be expected as a result of the suction of the interior fluid into the convection zone which is being slowed down by braking due to the

¹Dicke, R.H., 1967 The Astrophysical Journal 149: L121-127.

solar wind. We ignore the effect of stratification for the present.

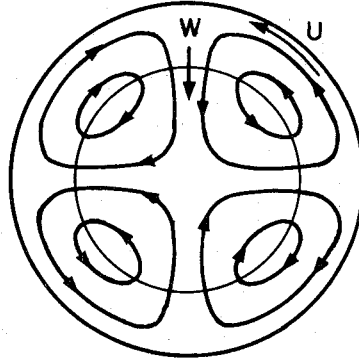


Fig.1

Let ν_e be an appropriate eddy viscosity for the convective zone. Then if we neglect coriolis effects we have in the convection zone

$$\nu_e \nabla^2 \underline{u} = - \frac{1}{\rho} \nabla P \quad (7)$$

where P is the deviation from the hydrostatic value. Then if U is a characteristic meridional velocity in the convective zone (of Fig.1) and if R is the characteristic distance over which this velocity varies appreciably we have:

$$\frac{\nu_e}{R^2} U \sim \frac{1}{\rho} \frac{1}{R} \delta(\rho R^2 \Omega^2) \quad (8)$$

$$U \sim \frac{R^2}{\nu_e} \Omega \delta \Omega \quad (9)$$

If W is a characteristic radial velocity and h the depth over which this velocity varies appreciably, then U and W must be related by continuity as follows:

$$WR^2 \sim URh \quad (10)$$

Combining (9) with (10) we obtain

$$W \sim \frac{R^2 h \Omega \delta \Omega}{\nu_e} \quad (11)$$

Now consider a ring of matter in the interior (concentric with rotation axis) as it moves out toward the edge. Then by conservation of angular momentum:

$$\delta(r^2 \Omega) = 0 \quad \text{so that} \quad (12)$$

$$\delta \Omega \sim \frac{\Omega}{R} \delta r \quad (13)$$

Then the time scale for this process T_{SD} (i.e., the spin down time) is given by:

$$T_{SD} \sim \frac{\delta r}{W} \sim \frac{V_e}{Rh\Omega^2} \quad (14)$$

Next we consider the effect of stratification on the penetration depth h . In the presence of stratification, the flow appears more like that shown in Fig.2 below. Now let V be a characteristic azimuthal velocity in the

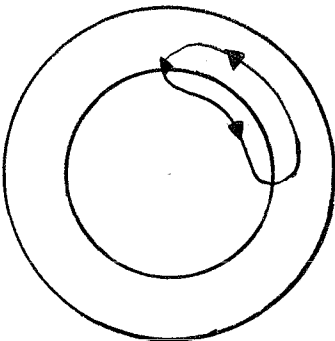


Fig.2

interior, and W a characteristic radial velocity. Also let z be the penetration depth and t a characteristic time for this penetration. Then continuity requires:

$$U \sim \frac{R}{z} W \quad (15)$$

and the momentum equation requires:

$$\frac{V}{t} \sim U \Omega \quad \text{and} \quad (16)$$

$$\frac{\delta P}{R} \sim \Omega V. \quad (17)$$

Now let $\alpha \equiv \frac{1}{T}$ where T is a characteristic temperature, $\beta \equiv \frac{dT}{dz} - \left(\frac{dT}{dz}\right)_{AD}$, and let θ be the perturbation temperature due to the motion. Then the buoyancy force is $g \alpha \theta$ and from the momentum equation we obtain:

$$\frac{\delta P}{z} \sim g \alpha \theta \quad (18)$$

In addition, the energy equation requires:

$$\frac{\theta}{t} \sim \beta W - \frac{K}{z^2} \theta \quad (19)$$

where K is the thermal conductivity.

Combining (15) and (16) we obtain:

$$V \sim \frac{\Omega t W R}{z} \quad (20)$$

From (17) and (18) we also obtain the thermal wind equation:

$$\Omega V R \sim g \alpha \theta z \quad (21)$$

Then if we eliminate V from (20) and (21) we obtain:

$$\frac{W}{\theta/t} \sim \frac{g \alpha}{\Omega^2} \frac{z^2}{R^2} \quad (22)$$

Let $S \equiv N^2/\Omega^2$

Equations (19) and (22) then yield an equation for the penetration depth z :

$$S \sim \frac{R^2 t}{z^2} \left(\frac{1}{t} + \frac{K}{z^2} \right) \quad (23)$$

where $N^2 \equiv g \alpha \beta$ is the square of the Brünt frequency. Then upon solving for z we obtain finally:

$$z^2 \sim \frac{R^2}{2S} \left\{ 1 + 1 + \frac{4KS}{R^2} t \right\} \quad (24)$$

where in the case of the sun $S \gg 1$.

From (24) we deduce the following:

$$\text{If } t \sim 0, \quad z = R/\sqrt{S} \quad (25)$$

whereas when $t \sim t_E \equiv S L^2/K$, then $z = R$ where t_E is the Eddington-Sweet time. Thus if $T_{SD} \ll t_E$, stratification is important since the penetration depth h then lies between R and R/\sqrt{S} .

Finally we ask what happens at the depth h when stratification is important. First of all we would expect the formation of a shear layer where the diffusive effect of kinematic viscosity becomes important. Now Yih² has shown that if Γ is the circulation at a given distance r from the center, then in the presence of viscosity the system may become less stable or even unstable if Γ increases but ρ decreases outward even though $\rho \Gamma^2$ increases with radial distance. We would therefore expect that the shear layer goes to neutral stability with weak turbulence. Thus a new convection layer is produced and spins the fluid down to a new depth h_1 , which

is smaller than h because of the larger S value. The process is repeated step by step until the center is reached.³

²Yih, C.-S. 1961 The Physics of Fluids 4: 806-811.

³Howard, L.N., D. Moore and E.A. Spiegel, 1967 Nature 214: 1297-1299.

Notes submitted by
Joseph M. Buschi

WAVES IN GALACTIC DISKS

Alar Toomre

We discuss wave motions in galactic disks with the intention of investigating the structure of spiral galaxies. To do this, we shall linearize our equations about a basic state of rotation $\Omega(r)$ (i.e. we assume the material in the galaxy to be in almost circular motion with an angular velocity which may depend on radius). In so doing, we automatically exclude discussion of such intrinsically non-linear phenomena as barred spirals.

To start with, let us consider the motion of a single particle moving in a force field (F_r, F_θ) in polar coordinates. The exact equations of motion are

$$\begin{aligned} \ddot{r} - r\dot{\theta}^2 &= F_r \\ \frac{d}{dt}(r^2\dot{\theta}) &= rF_\theta \end{aligned}$$

We now assume that the motion is a small perturbation of a circular orbit in which the angular velocity may be a function of the radius, i.e.

$$\left. \begin{aligned} r &= r_0 + x \\ \theta &= \theta_0 + \Omega(r_0)t + \frac{y}{r_0} \end{aligned} \right\} \begin{aligned} \frac{x}{r_0} &\ll 1 \\ \frac{y}{r_0} &\ll 1 \end{aligned}$$

where r_0 is the "home radius" of the particle and θ_0 its initial polar

angle. We also suppose that $F_n = -\Omega^2 r + f_x$, $F_\theta = f_y$ where f_x and f_y are both small. The equations of motion become

$$(i) \quad \ddot{x} - (x+r_0)\left(\Omega_0 + \frac{\dot{y}}{r_0}\right)^2 = -\left(r_0+x\right)\left(\Omega_0^2 + \frac{d}{dr}\Omega^2\Big|_{r=r_0} x + \dots\right) + f_x$$

$$(ii) \quad \frac{\ddot{y}}{r_0}(r_0+x) + 2\left(\Omega_0 + \frac{\dot{y}}{r_0}\right)\dot{x} = f_y$$

where $\Omega_0 = \Omega(r_0)$

Retaining only the first-order terms we have

$$\begin{aligned} \ddot{x} - 2\Omega_0 \dot{y} + \left[r \frac{d}{dr}\Omega^2\right]_{r=r_0} x &= f_x \\ \ddot{y} + 2\Omega_0 \dot{x} &= f_y \end{aligned}$$

These are the galactic dynamicists' equivalent of the well-known Coriolis equations. The coefficient of the additional term in the first equation is typically negative and so it represents a repulsive force. A trivial solution occurs in the case

$$f_x = f_y = 0, \quad \ddot{x} = \ddot{y} = 0, \quad \text{viz.} \quad \dot{x} = 0, \quad \dot{y} = x \frac{r_0}{2\Omega_0} \left[\frac{d}{dr}\Omega^2\right]_{r=r_0}$$

which represents a steady shearing motion. A less trivial and extremely important solution is that of epicyclic motion to which we now turn.

Epicyclic Motion: Here we assume only that $f_x = f_y = 0$. The equations then admit the first integral $\dot{y} + 2\Omega x = \text{constant}$. If we suppose for our particle that $\dot{y} = 0$ when $x = 0$ we obtain:

$$\ddot{x} + \chi^2 x = 0, \quad \dot{y} = -2\Omega_0 x$$

where the frequency χ is given by: $\chi^2 = r_0 \frac{d}{dr}\Omega^2\Big|_{r=r_0} + 4\Omega_0^2$.

This has the solution

$$x = c \cos \chi t$$

$$y = -\frac{2\Omega_0 c}{\chi} \sin \chi t$$

which represents a vibration of the particle about its "home radius". We observe that if $\Omega(r) \sim r^{-\eta}$ then the motion is unstable or stable accord-

ing as $n \geq 2$. For a typical galaxy, we have a distribution like that shown in Fig.1, so this motion is stable.

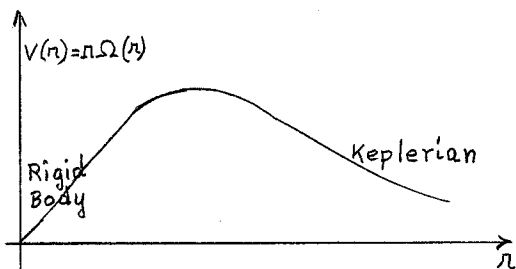


Fig.1

If Ω is constant (rigid body):

$$\chi_o = 2 \Omega_o$$

If $\Omega \sim \frac{1}{r^{3/2}}$ (Keplerian):

$$\chi_o = \Omega_o$$

The idea of epicyclic motion

can also be used to explain the obser-

vational fact that the radial velocity dispersion of nearby stars as seen from Earth is greater than their tangential velocity dispersion. To do this, let us follow a single star in its epicyclic motion. An orbiting observer would measure the velocities as

$$\dot{x}_m = -\chi c \sin \chi t$$

$$\dot{y}_m = -2 \Omega_o c \cos \chi t - \frac{r_o}{2 \Omega_o} \frac{d}{dr} (\Omega^2) c \cos \chi t$$

Hence $\left| \frac{v_m}{u_m} \right| = \left| \frac{\dot{y}_m}{\dot{x}_m} \right| = \frac{2 \Omega_o + \frac{r_o}{2 \Omega_o} \frac{d}{dr} (\Omega^2)}{\chi} = \frac{\chi_o}{2 \Omega_o} \leq 1$

with equality only for rigid body rotation.

In the 1950's Lindblad recognized that epicyclic motion was central to the discussion of waves in disks. To illustrate this, consider eight non-interacting particles orbiting with angular velocity Ω and executing epicyclic motions. Assume that, at some instant, the motion is as shown in Fig.2. One-eighth of a period later, Fig.3 will depict the configuration.

The angular velocity Ω_p of the pattern is therefore $\Omega_p = \Omega + \frac{\chi}{2}$.

There is also the possibility

$$\Omega_p = \Omega - \frac{\chi}{2}$$

Had we considered 4 m particles with a phase difference of 90° between

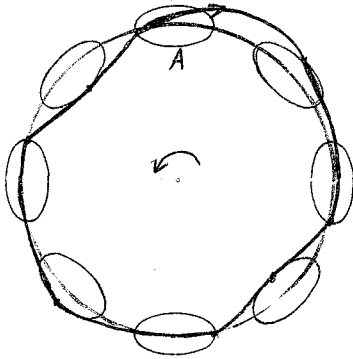


Fig.2

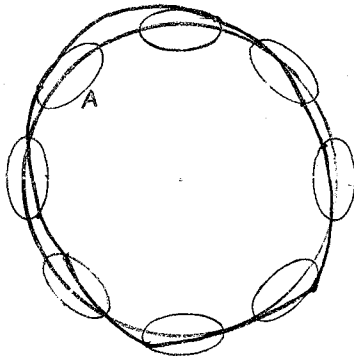


Fig.3

adjacent particles, we would have found

$$\Omega_p = \Omega \pm \frac{\chi}{m}$$

(The wave pattern then has multiplicity m .)

Lindblad recognized the simple fact that

$\Omega - \frac{\chi}{2}$ is very nearly constant over much

of an actual galaxy (except near the

centre). This is of course just the con-

dition needed for the existence of sim-

ple wave solutions.

Thus far, no account has been

taken of the mutual attractions of the

particles in the galaxy. To include this

effect in its full generality is a diffi-

cult task. We will consider only axisymmetric motions for which χ is independent of n and will further suppose that the phase of the epicyclic motion is a function of radius only.

Consider an initially flat sheet of matter with uniform surface density μ_0 and impose a perturbation $x = C \cos kr \cos \omega t$. The contin-

uity equation $\mu' = -\mu_0 \frac{dx}{dn}$ implies $\mu' = \mu_0 C k \sin kr \cos \omega t$. The

gravitational potential corresponding to this change in mass distribution is

$$\phi = -C 2\pi G \mu_0 e^{-|kz|} \sin kr \cos \omega t$$

and hence

$$f_x' = - \left. \frac{\partial \phi'}{\partial n} \right|_{z=0} = C 2\pi G \mu_0 k \cos kr \cos \omega t$$

Substituting into the equation $\ddot{x} + \chi^2 x = f_x$ we obtain

$$\omega^2 = \chi^2 - 2\pi G \mu_0 k$$

We observe that there is instability for $k > k_{crit} = \frac{\chi^2}{2\pi G \mu_0}$ i.e. the

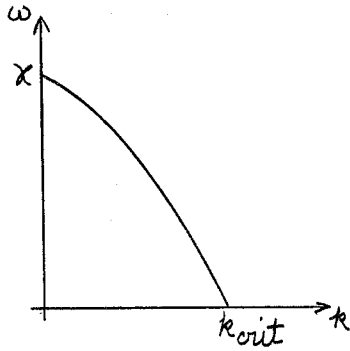


Fig.4

galaxy is unstable to sufficiently small wavelengths - a worrying situation. This can be remedied by considering the compressibility of the matter. Had we considered a rotating layer of gas between two rigid planes we would have

found $\omega^2 = \chi^2 - 2\pi G\mu_0 k + c^2 k^2$ where c is the sound speed. In the case of no rotation this gives a critical wavenumber $k_J = \frac{2\pi G\mu_0}{c^2}$ below which there is instability. When we have rotation, self-attraction and compressibility there is a critical sound speed $c_{crit} = \frac{\pi G\mu_0}{\chi}$ such that all wavelengths are stable if $c > c_{crit}$. In numerical work it is often convenient to force stability by using a modified gravity $\phi \sim \frac{1}{\sqrt{\lambda^2 + a^2}}$ instead of $\frac{1}{\lambda}$. The dispersion relation becomes $\omega^2 = \chi^2 - 2\pi G\mu_0 k e^{-ak}$ which is always positive if a is large enough. Collective vibrations are also at the core of Lin and Shu's

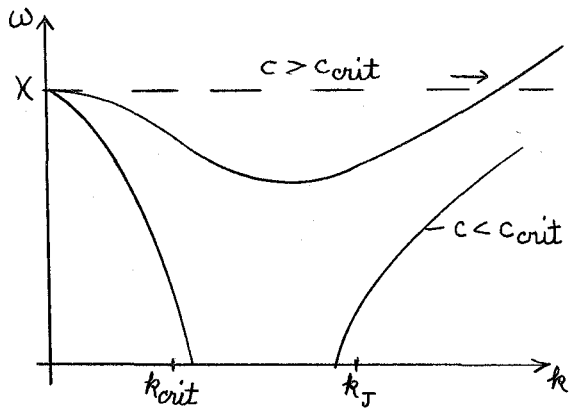


Fig.5

efforts to explain spiral arms as density waves in disks. Of course a galactic disk is more complicated than just a "thin gas sheet", or a "thin star sheet", but these approximations seem unavoidable in order to make a mathematical model tractable, and very often results

show that the approximation is not unreasonable. What Liu and Shu do is a WKBJ analysis on such a model, aimed at explaining the persistence (rather than the origin) of spiral arms.

They assume a spiral pattern and determine the response of the disk to the resulting perturbed gravity field. They note that such patterns are described by functions of the form $F(r, \theta, t) = u(r) \exp i(\omega t - m\theta + \Phi(r))$ where $u(r)$ is slowly varying, ω is a constant and $\Phi(r)$ is a slowly varying monotonic function multiplied by a large parameter. Lines of constant $\text{Re}(F)$ are approximately given by $m(\theta - \theta_0) = \Phi(r) - \int(r_0)$ which represents a spiral pattern with m arms. The pattern obviously rotates with angular velocity $\Omega_p = \frac{1}{m} \text{Re}(\omega)$ and the radial wavenumber is given by $|\Phi'(r)|$. The resulting perturbation of the gravitational potential will be of the form $\phi_1 = A(r) \exp i(\omega t - m\theta + \Phi(r))$. Lin, Yuan and Shu calculated the response of a stellar disk (in which the unperturbed state was time independent and approximately Gaussian) to this perturbation and showed that the dispersion relation became

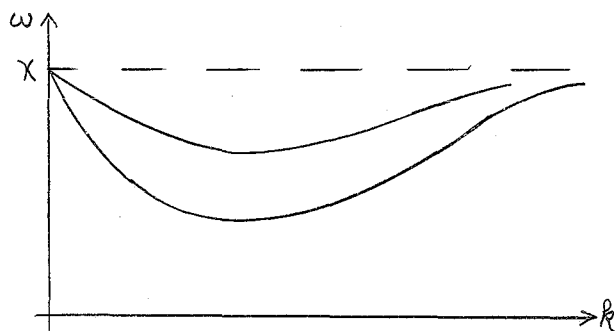


Fig.6

$$\omega^2 = \chi^2 - 2\pi G \mu_0 k \mathcal{F}_k,$$

where the reduction factor \mathcal{F}_k is unity for $k = 0$ and decreases as k increases. The important result of their model is that $\omega < \chi$ for all k (see Fig.6). They

repeated the calculation for a gaseous disk and then combined the answers to get the result for a galaxy consisting of both stars and gas. They further showed that the minimum velocity dispersion consistent with stability was given by $\langle u^2 \rangle_{\text{min}}^{1/2} = 3.36 \frac{G \mu_0}{\chi}$, in agreement with a result obtained earlier by Toomre.

The waves described above are confined to the regions of the galaxy for which $\Omega - \frac{\chi}{m} < \Omega_p < \Omega + \frac{\chi}{m}$. For the well-known Schmidt model of

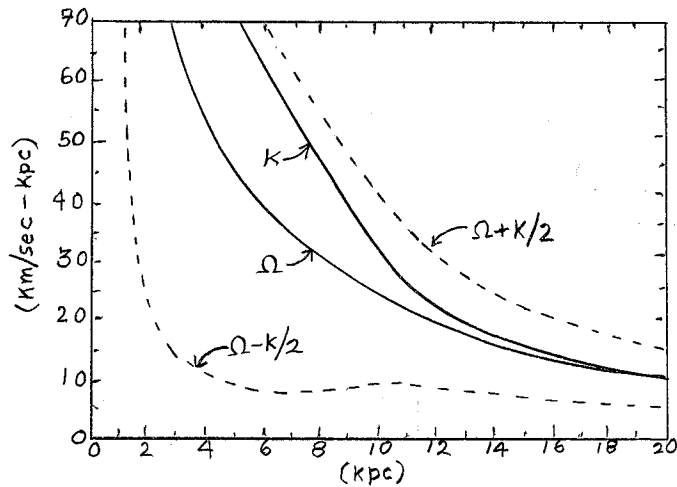


Fig.7

(or perhaps only one) spiral arm. Lin, Yuan and Shu also showed that many features of their model agreed well with observational evidence. However, none of their WKBJ calculations really proves that a complete disk would admit spiral modes.

our galaxy (Fig.7). The $m = 2$ wave would extend from $r = 4$ kpc out to beyond 20 kpc. For $m > 2$ the region would be very limited in extent. Hence, galaxies obeying this rotation curve will have two

Notes submitted by
William D. McKee

WORLDS IN COLLISION (ALMOST)

Alar Toomre

Twenty-one-centimeter observations have shown that the plane of the galaxy, although quite flat over the disk interior to the sun, outside that shows a warp amounting to about 1 kpc, upward and downward on opposite sectors (Burke 1957, Kerr 1957). From above it looks like Fig.1a where the (+) and the (-) indicate upward and downward deflection. Viewed from the side it looks like Fig.1b.

At least 4 explanations have been proposed for this curious effect.

- (1) It was thought that it might be a tidal distortion due to the

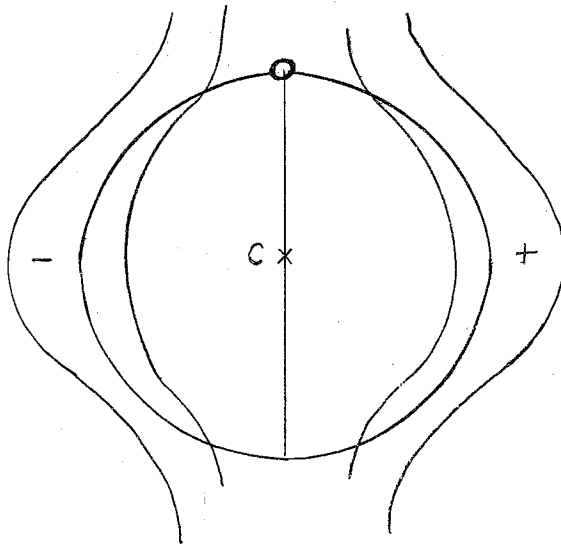


Fig.1a

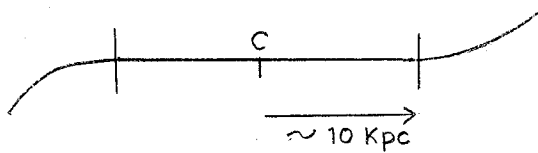


Fig.1b

Magellanic clouds at their present distance. Burke and Kerr themselves considered this possibility, but dismissed it on the ground that the force would not be enough. Later Elwert and Hablick (1965) and Avner and King (1967) did some calculations that showed better results.

(2) Kahn and Woltjer (1959) suggested that it might be the result of an intergalactic wind blowing past the galaxy and its halo.

However in order to get the pres-

sure required for the observed distortion one would need velocities of ~ 100 km/sec, and no evidence exists for such a wind.

(3) Kahn and Woltjer suggested (and dismissed) the possibility of it being a free mode of oscillation, presumably of primeval origin. Lynden-Bell (1965), however, showed that a highly flattened Maclaurin ellipsoid at least would show one such oscillation, similar to the mutation of a coin thrown spinning into the air.

(4) The effect might be due to a (past) close passage of the LMC near our galaxy, and the warp might be a remnant of this (Idlis 1959, Habing and Visser 1966).

In order to check mathematically these different possibilities, we make the idealization that the galaxy is an infinitesimally thin, smooth,

axysymmetric and cold (i.e. no random velocities) disk of finite radius, composed of self-gravitating material revolving in concentric orbits.

In this model in the linear approximation the motions \perp and \parallel to the plane are decoupled. It is further assumed that a) the surface mass density $\mu(r)$ on the unperturbed disk vanishes for $r > R$; b) that the angular velocity of the material $\Omega(r)$ is such that the centrifugal force compensates self-gravitation along the disk and c) that any slopes resulting from vertical displacements $h(r, \theta, t)$ are infinitesimal. One can take for instance

$h(r, \theta, t) = \text{Re} \left\{ e^{im(r)} H(r, t) \right\}$. If one neglects the gravitational effects of the perturbation itself, the vertical acceleration of a particle at r, θ is

$$\left[\frac{\partial}{\partial t} + \Omega(r) \frac{\partial}{\partial \theta} \right]^2 h(r, \theta, t)$$

and obeys the dynamical equation

$$\left[\frac{\partial}{\partial t} + \Omega(r) \frac{\partial}{\partial \theta} \right]^2 h(r, \theta, t) - F = F_{\text{imp}}$$

where F_{imp} is the externally imposed (distortion) force per unit mass and F is the vertical force due to the distorted disk itself. The detailed treatment can be found in Hunter and Toomre (1969), and here we present only the results. For hypothesis 3), the modes were calculated for various disk models differing in their rotation curves, for instance 1, 4, and 16. (Fig.2)

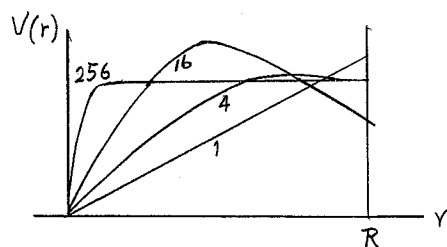


Fig.2

The $m = 1$ modes that advanced in the sense of rotation of the galaxy were labeled D1, D2, etc. in order of increasing frequency, and those in opposite sense as R1, R2, . . .

On the normalized scale, they look like Fig.3.

The behaviour of these modes can be understood qualitatively by considering a perturbing force that acts in the z-direction. For instance,

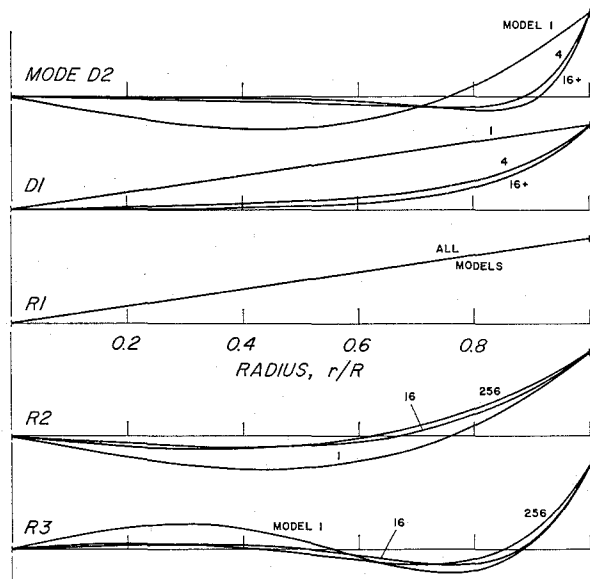


Fig.3

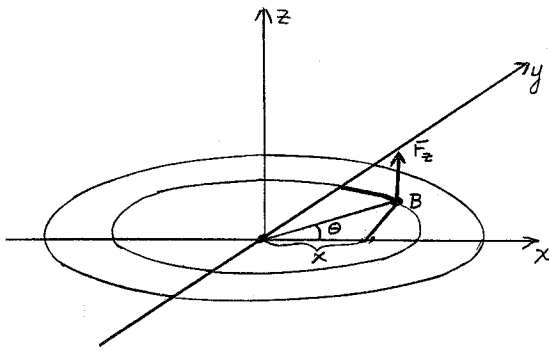
suppose one had a massive object situated at the point A. Let it act on a disk of non-interacting test particles initially moving in circular orbit for a certain (short) amount of time, and then let's switch it off. At a point of the disk like B, it will produce a force in the z-direction which will be approximately pro-

portional to the x-coordinate of point B, (i.e., F_z is proportional to x alone). The dynamics can be represented by

$$\left(\frac{\partial}{\partial t} + \Omega \frac{\partial}{\partial \theta}\right)^2 h = \cos \theta \delta(t) - \Omega^2 h$$

where the first term on the right is the disturbing force, and the second is the reaction to the displacement h caused by that force. We seek solutions of the type $e^{i(m\theta - \omega t)}$. If we substitute this in the equation, for $m = 1$, we find $h(\theta, t) = \frac{1}{2} \sin \theta - \frac{1}{2} \sin(\theta - 2\Omega t)$, where Ω is the angular velocity of the disk. This solution can be visualized if we consider the disk as composed of a central circle, and an outer ring that is tilted by the disturbing force, both rotating with Ω . It is seen that the ring will precess, in a similar way to the Eulerian wobbles of a coin thrown spinning into the air.

The assumed mass-distribution law is an important factor in determining the characteristics of the spectra. For instance the discrete modes in



•A

Fig.3 were obtained for (theoretical) models like 1, 4, 16 and 256 (see Fig.4), which have quite a

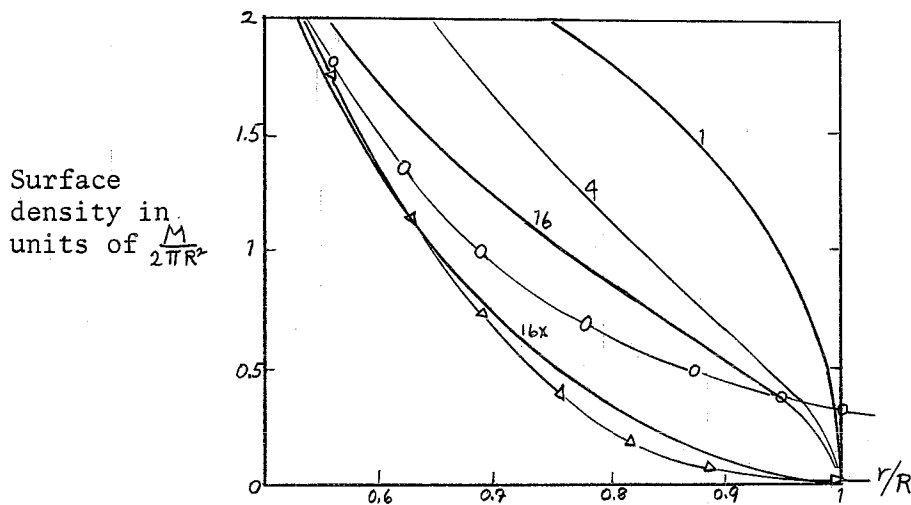


Fig.4

lot of mass at the edge, as compared with the semiempirical mass distribution models of Schmidt (—○—) and Innanen (—▷—), based partly on 21-cm observations. Thus a flared-out model like 16x is perhaps more realistic.

What happens with such flared-out models is that the modes tend to become a continuum. In Fig.5 the frequency of the first few modes ($m=1$) has been plotted for several models of decreasing density at the edges, labelled 16, 16/36, 16/64, etc. It is seen that as the model is made more and more flared-out, the spectrum becomes continuous, the tilt-over mode R1 remaining the only truly discrete $m=1$ mode. Now these are the free modes of the disks. If one applies to the disk a non-axisymmetric impulse as we did before, the

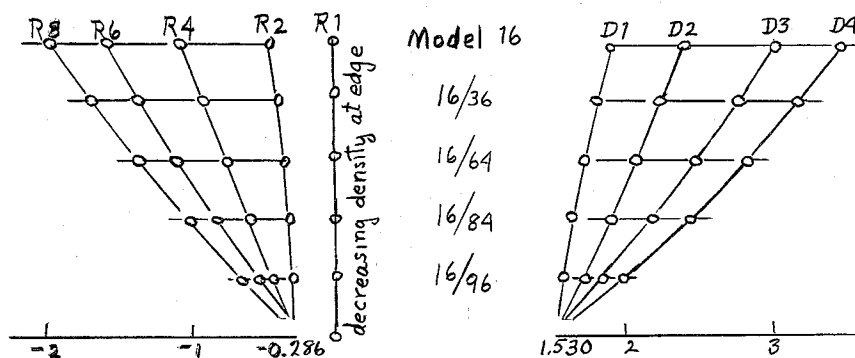


Fig.5

response of the disk (for example taking only the $m=1$ modes) is a combination of i) the tilt-over, ii) a relatively slowly evolving retrograde part, and iii) high-frequency nutations due to the direct half of the continuous spectrum. If one takes a double cross section of the disk for $m=1$ modes (i.e., two cross sections at right angles to each other), one gets for the time evolution of the response the behaviour shown in Fig.6.

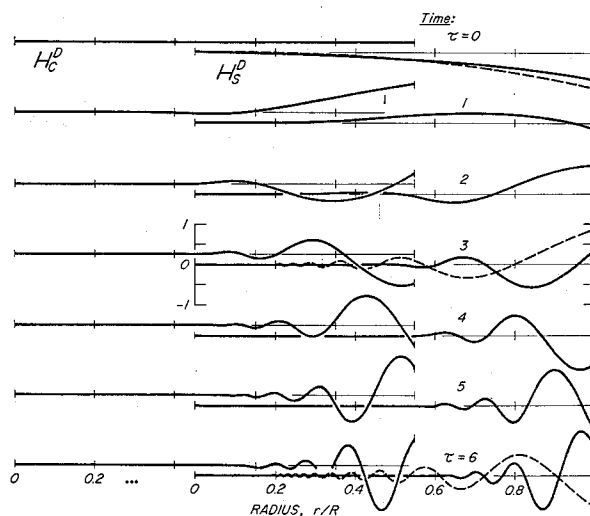


Fig.6

Radial cross sections through Model 16x, showing the "direct" part of its $m=1$ response to the unit impulse. Broken curves indicate the same for a disk of non-interacting test particles.

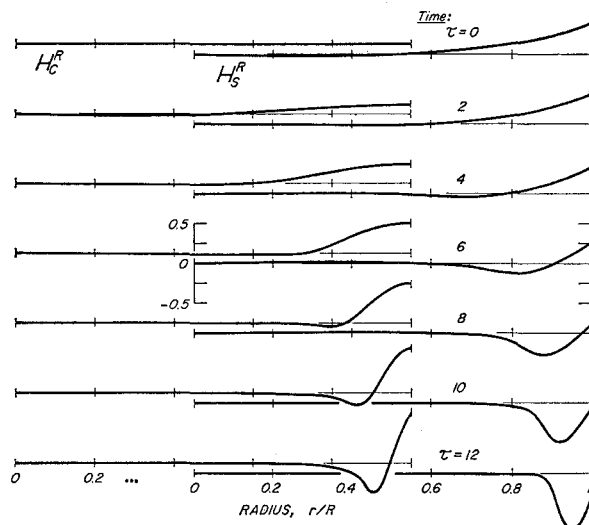


Fig. 7

Radial cross sections through Model 16x, showing the "retrograde" part of its $m=1$ response to the unit impulse.

Similarly for the retrograde part, get Fig. 7. Both Figs. 6 and 7 imply that material rings of different radii precess with different angular speeds, the total effect being that at the center they start smoothing themselves out, and this quiet zone moves steadily outwards toward the edges, whereas at the edges themselves the amplitude of the oscillations becomes bigger and bigger. This can be seen better in Fig. 8 where the abscissae refer to the sine tilt of a ring, and the ordinates to the cosine tilt. The thin lines describe the tilt history of some specific ring, while the heavy lines connect the instantaneous (constant-tilt) loci of different rings. One sees that the displacements of different rings grow increasingly out of phase with one another and that the central tilt decreases with time, whereas the amplitude at the edges increases.

Up to now we have studied only free modes, and responses to short-lived impulses. The response to a steady force can be found, for instance,

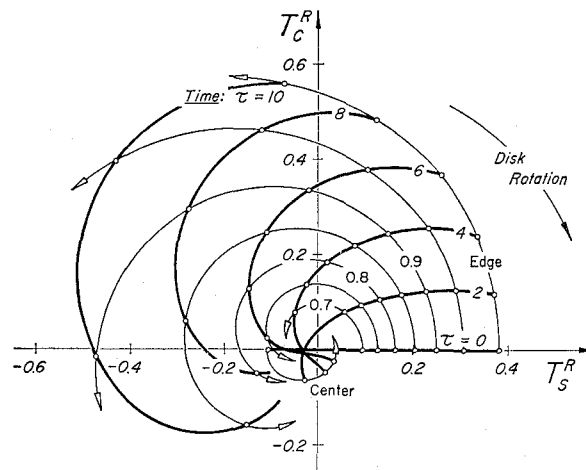


Fig.8 "Polar" version of Fig.7

by assuming a superposition of short impulses. We are now in a position to discuss the four theories that were cited originally as candidates for explaining the warp of the Milky Way.

a) Quasi-steady tidal distortion

If one uses the roughly known mass, distance and position of the Magellanic Clouds, and appraises their effect on the Milky Way in the light of the present theory, one finds that the overall precessing warp obtained for all the models (both those having discrete and continuous spectra) is not nearly large enough to reproduce the actual observations.

b) Free modes of oscillation

They could be the explanation only in the case of a discrete spectrum. However we have seen that the spectrum becomes continuous for all disks in which density dies off sufficiently gradually (i.e., where there is no sharply defined disk boundary), and most galaxies seem to be of this

type. But if the spectrum is continuous, no simple initial deformation can endure for long, and as we have seen, the different modes simply "iron" themselves out.

c) Intergalactic wind

It may work, but lacks observational evidence.

c) Close passage of the Magellanic Clouds

This seems to be the most promising explanation, so it will be developed in some detail. Upon correction for solar motion and galactic rotation, the observed radial motion of the LMC seems to be ~ 50 km/sec with respect to the galactic center. Thus if it passed close, that time of passage could have been no more than 5.8×10^8 years ago, for any reasonable orbit. Since the free fall velocity is 4.1×10^8 years, these two bounds leave only the relatively slowly evolving $m=1$ retrograde modes as plausible candidates.

Of course, we know only one component of the velocity of the LMC, and we do not know the plane of the orbit, nor the perigalacticon. But even in the most favorable case of a grazing collision (see Fig.9), it turns out that the amplitude of the warp at the edge obtained as response of the impulse received during the short time of collision seems to fall short of the observations by a factor of two, if we use the presently adopted value of the mass of the LMC. This mass, however, is by no means well determined, and if it were twice what it is usually believed to be, it could cause the observed warp.

At the time of the passage, the disk would have tilted as shown in Fig.10a and the subsequent retrograde motion would have carried this tilt

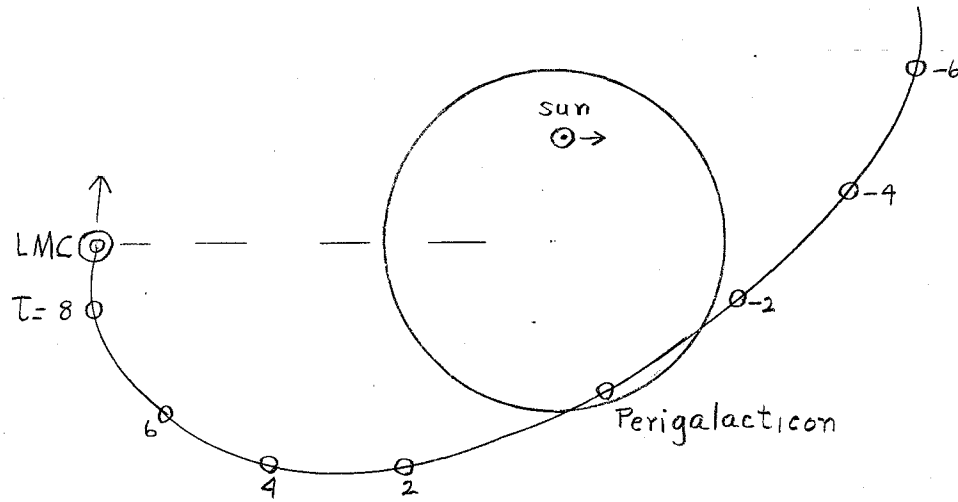


Fig.9

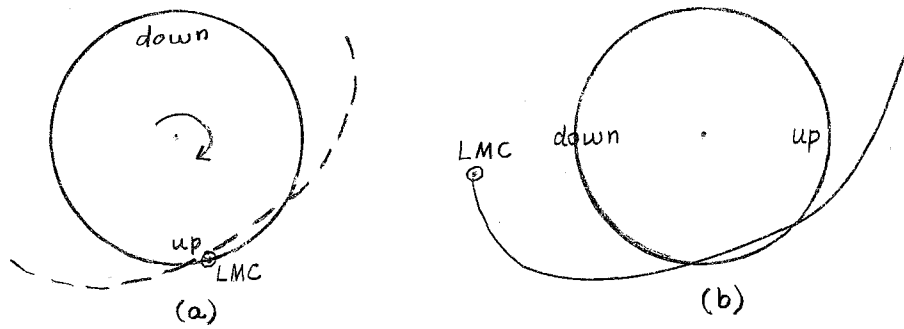


Fig.10

roughly to the position seen at present (Fig.10b). Unfortunately, if one calculates the velocity of precession of the retrograde distortion for any of the theoretical model galaxies described above, it seems it would have carried the tilt somewhat farther than the position at which it is presently seen. Thus, further work seems obviously called for. But, the present prognosis is that those chosen galaxy models were simply not realistic enough.

The effect of this close passage on the Magellanic Clouds themselves is interesting to speculate upon. Observations show that they are farther apart than their Roche limit, and that there is material in between them, which could well be the remains of any disruptive action of the Milky Way on the Clouds during the close passage. Another interesting thing to note is that the tidal force of the LMC in a direct orbit is an ideal generator of $\Omega - \frac{1}{2}k$ waves in the Milky Way, of multiplicity $m = 2$, in the context of the epicyclic theory. Thus that could have given rise to a double armed spiral pattern, as shown in the sequence of Fig.11.

Finally as a result of a close passage of the LMC one would also expect debris to be strewn roughly along the orbit described. It is interesting to

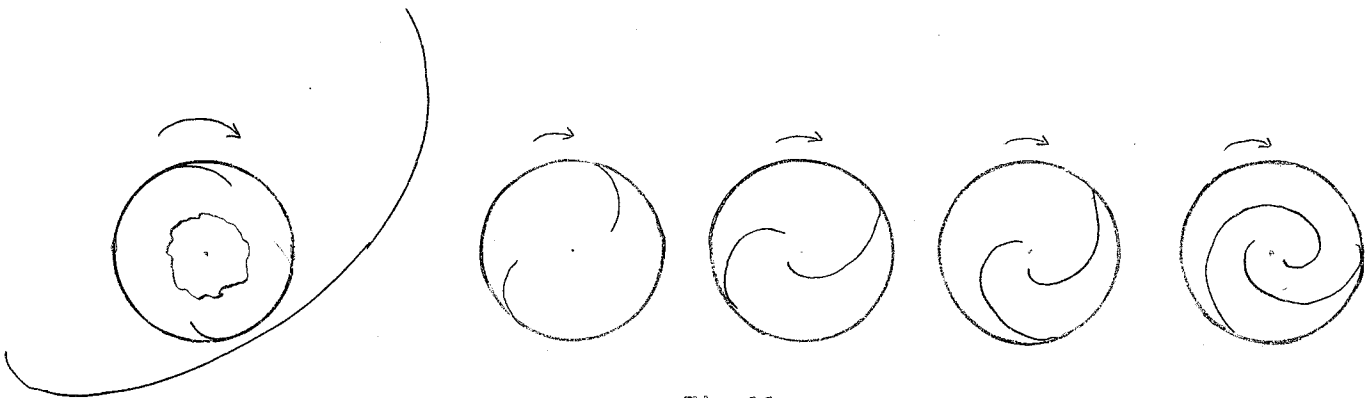


Fig.11

note that there exists an abnormal concentration of high-velocity clouds in just the plane of what we have taken as the most probable orbit, and that could be this debris.

References

- Avner, E.S. and I.R.King, 1967. Astronomical Journal 72: 650.
Burke, B.F. 1957. Astronomical Journal 62: 90.
Elwert, G. and D.Hablick, 1965. Zeitschrift für Astrophysik, 61: 273.

- Habing, H.J. and H.C.D. Visser, 1966. (unpublished report).
Hunter, C. and A. Toomre, 1969. Astrophysical Journal, 155: 747.
Kahn, F.D. and L. Woltjer, 1959. Astrophysical Journal, 130: 705.
Kerr, F.J. 1957. Astrophysical Journal, 62: 93.
Lynden-Bell, D. 1965. Monthly Not. of the Royal Astr. Soc. 129: 299.

Notes submitted by
Pedro Mészáros

TIDAL EFFECTS IN DOUBLE STARS

Jean-Paul Zahn

I Non-Radial Free Oscillations in the Stars

At first, we want to study the non-radial oscillations of a star without external forces. The equations which describe the linearized perturbation are:

Conservation of momentum:

$$-\sigma^2 \underline{\delta n} = -\underline{\nabla} \phi' + \frac{\rho'}{\rho} \underline{\nabla} p - \frac{1}{\rho} \underline{\nabla} p' \quad (1)$$

Conservation of mass:

$$\rho' + \underline{\nabla} \cdot (\rho \underline{\delta n}) = 0 \quad (2)$$

Poisson's equation:

$$\nabla^2 \phi' = 4\pi G \rho' \quad (3)$$

A perturbed quantity is written:

$$\chi = x + x' e^{i\sigma t} \quad (4)$$

x is the equilibrium quantity

x' is the Eulerian perturbation

p is the pressure, ρ the density, $\underline{\delta n}$ the displacement, ϕ the gravitational potential, G the gravitational constant.

1) Incompressible, homogeneous sphere

This case is analytically solvable (Kelvin). The system of equations become:

$$-\sigma^2 \underline{\delta r} = -\underline{\nabla} \left(\phi' + \frac{p'}{\rho} \right) = -\underline{\nabla} \chi \quad (5)$$

$$\underline{\nabla} \cdot \underline{\delta r} = 0 \quad (6)$$

$$\nabla^2 \phi' = 0 \quad (7)$$

If ψ is the potential of displacements ($\underline{\delta r} = \underline{\nabla} \psi$)

$$\sigma^2 \psi = \phi' + \frac{p'}{\rho} \quad (8)$$

$$\nabla^2 \psi = \nabla^2 \phi' = 0 \quad (9)$$

The solution is regular at the origin. ϕ' and ψ are expanded in spherical harmonic functions:

at the origin:

$$\psi = \psi_0 Y_n^m(\theta, \varphi) x^n \quad (10)$$

$$\phi' = \phi'_0 Y_n^m(\theta, \varphi) x^n \quad (11)$$

with:

$$x = 2/R \quad (12)$$

$$Y_n^m(\theta, \varphi) = P_n^m(\cos \theta) e^{im\varphi} \quad (13)$$

θ, φ are spherical coordinates, P_n^m is an associated Legendre's polynomial. At the surface (free boundary at $x = 1$):

$$\delta p = p' + \underline{\nabla} p \cdot \underline{\delta r} = 0 \quad (14)$$

δp is the Lagrangian perturbation of pressure

$$\rho(\sigma^2 \psi_0 - \phi'_0) = \rho \frac{GM}{R^2} \psi_0 n \frac{x^{n-1}}{R} \quad (15)$$

Condition of surface density:

$$\delta m = 4\pi R^2 \rho \delta r \quad (16)$$

$$\phi' = \frac{4\pi G \rho}{(2n+1)} \psi_0 n Y_n^m \quad (17)$$

$$\sigma^2 \psi_0 + \frac{4\pi G \rho \psi_0 n}{(2n+1)} - \frac{GM}{R^3} \psi_0 n = 0 \quad (18)$$

$$\sigma^2 = \frac{4\pi}{3} G \rho n \left[1 - \frac{3}{(2n+1)} \right] \quad (19)$$

$-\frac{3}{(2n+1)}$ is the term due to the perturbation of ϕ .

The case $n = 1$ ($\Rightarrow \sigma^2 = 0$ $\nabla \psi = 1$) is a linear displacement of the sphere. If the sphere has a hard core (oceans) with the same density

(χ_0 is the radius of the core)

$$\psi = \psi_0 \left[\frac{\chi^n}{n \chi_0^n} + \frac{\chi_0^{n+1}}{(n+1) \chi^{n+1}} \right] Y_n^m \quad (20)$$

$$\sigma^2 = \frac{4\pi}{3} G \rho n \left[1 - \frac{3}{(2n+1)} \right] \frac{1 - \chi_0^{2n+1}}{1 + \frac{n}{(n+1)} \chi_0^{2n+1}} \quad (21)$$

If $\chi_0 \rightarrow 1$

$$\sigma^2 = \frac{4\pi}{3} G \rho n (n+1) \left(1 - \frac{3}{(2n+1)} \right) (1 - \chi_0) \quad (22)$$

$n = 1$ is always a translation

If ρ fluid is different from $\bar{\rho}$ total

$$\sigma^2 = \frac{4\pi}{3} G \rho n (n+1) \left(1 - \frac{3}{(2n+1)} \frac{\rho}{\bar{\rho}} \right) (1 - \chi_0) \quad (23)$$

One sees that the perturbation of the potential can be neglected when

$\rho \ll \bar{\rho}$, which is the case in stars.

Phase velocity at the equator:

$$V_{eq}^2 = \frac{\sigma^2 R^2}{n^2} = \frac{G M R^2}{R^3} \left(\frac{n+1}{n} \right) (1 + \chi_0) (1 + \xi) \quad (24)$$

where ξ is again the correction due to the perturbation of the potential.

$$V_{eq}^2 = g_{surf} \cdot h \left(\frac{n+1}{n} \right) (1 + \xi) \quad (25)$$

g_{surf} gravity at the surface

h height of the fluid layer

2) Compressible case:

The variable separate in the perturbations which can be written:

$$f' = f^*(z) Y_n^m(\theta, \varphi) \quad (26)$$

$$\underline{\partial}_n = (a(n) Y_n^m, b(n) \frac{\partial Y_n^m}{\partial \theta}, \frac{b(n)}{\sin \theta} \frac{\partial Y_n^m}{\partial \varphi}) \quad (27)$$

The equations (5), (6), (7) become:

$$-\sigma^2 a = -\frac{d\phi^*}{dn} + \frac{\rho^*}{\rho} \frac{d\rho}{dn} - \frac{1}{\rho} \frac{d\rho^*}{dn} \quad (28)$$

$$\rho^* + \frac{2}{n^2} \frac{d}{dn} (n^2 \rho a) - \frac{n(n+1)}{n} \rho b = 0 \quad (29)$$

$$\frac{1}{n^2} \frac{d}{dn} (n^2 \frac{d\phi^*}{dn}) - \frac{n(n+1)}{n^2} \phi^* = 4\pi G \rho^* \quad (30)$$

We study an adiabatic perturbation:

$$\left(\rho^* + \frac{d\rho}{dn} a \right) = \frac{1}{\Gamma} \left(\rho^* + \frac{d\rho}{dn} a \right) \quad (31)$$

Introducing, following Ledoux, the function A:

$$A = \frac{d \log \rho}{dn} - \frac{1}{\Gamma} \frac{d \log \rho}{dn} \quad (32)$$

$$\frac{\rho^*}{\rho} = \frac{1}{\Gamma} \frac{\rho^*}{\rho} - a A \quad (33)$$

If we neglect here, for simplicity, the Eulerian perturbation of the gravity (Cowling's approximation good if $\rho_{ext} \ll \bar{\rho}$) and define:

$$y = \frac{\rho^*}{\rho} \quad (34)$$

we get the following second-order differential system:

$$\frac{da}{dn} + \frac{2a}{n} + \frac{1}{\Gamma} \frac{d \log \rho}{dn} a = \left(\frac{n(n+1)}{\sigma^2 n^2} - \frac{\rho}{\Gamma} \right) y \quad (35)$$

$$\frac{dy}{dn} + A y = (\sigma^2 + g A) a \quad (36)$$

Introducing the functions:

$$v = a n^2 \rho^{1/n} \quad (37)$$

$$w = y \rho p^{-1/n} \quad (38)$$

This system is transformed in:

$$\frac{dv}{dn} = \left(\frac{n(n+1)}{\sigma^2 n^2} - \frac{\rho}{\Gamma} \right) \frac{\rho^{2/n}}{\rho} n^2 w \quad (39)$$

$$\frac{dw}{dn} = (\sigma^2 + g A) \frac{\rho}{n^2 \rho^{2/n}} v \quad (40)$$

If $\sigma^2 \rightarrow \infty$

$$\frac{d}{dn} \left(\frac{\rho \Gamma}{n^2 p^{2/n}} \frac{dv}{dn} \right) + \sigma^2 \frac{\rho}{n^2 p^{2/n}} v = 0 \quad (41)$$

it is a Sturm-Liouville equation where σ^2 is the eigenvalue.

If $\sigma^2 \rightarrow 0$

$$\frac{d}{dn} \left(\frac{n^2 p^{2/n}}{\rho g A} \frac{d\omega}{dn} \right) - \frac{n(n+1)}{\sigma^2} \frac{p^{2/n}}{\rho} \omega = 0 \quad (42)$$

where here $n(n+1)/\sigma^2$ plays the role of the eigenvalue. In order to fulfill the boundary conditions, ω must have an oscillatory character with an increasing number of nodes when $\sigma^2 \rightarrow 0$ by positive values. The sign of σ^2 is thus determined by that of A:

$$\begin{aligned} \text{If } A > 0 \quad \sigma^2 < 0 \\ A < 0 \quad \sigma^2 > 0 \end{aligned}$$

Remembering that

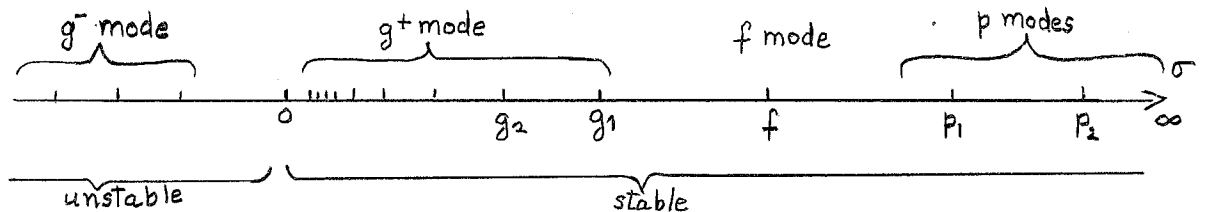
$$A = \frac{1}{H_p} \left[\left(\frac{\partial \log p}{\partial \log p} \right)_{\text{adiab}} - \left(\frac{\partial \log p}{\partial \log p} \right)_{\text{star}} \right] \quad (43)$$

where H_p is the height scale of pressure

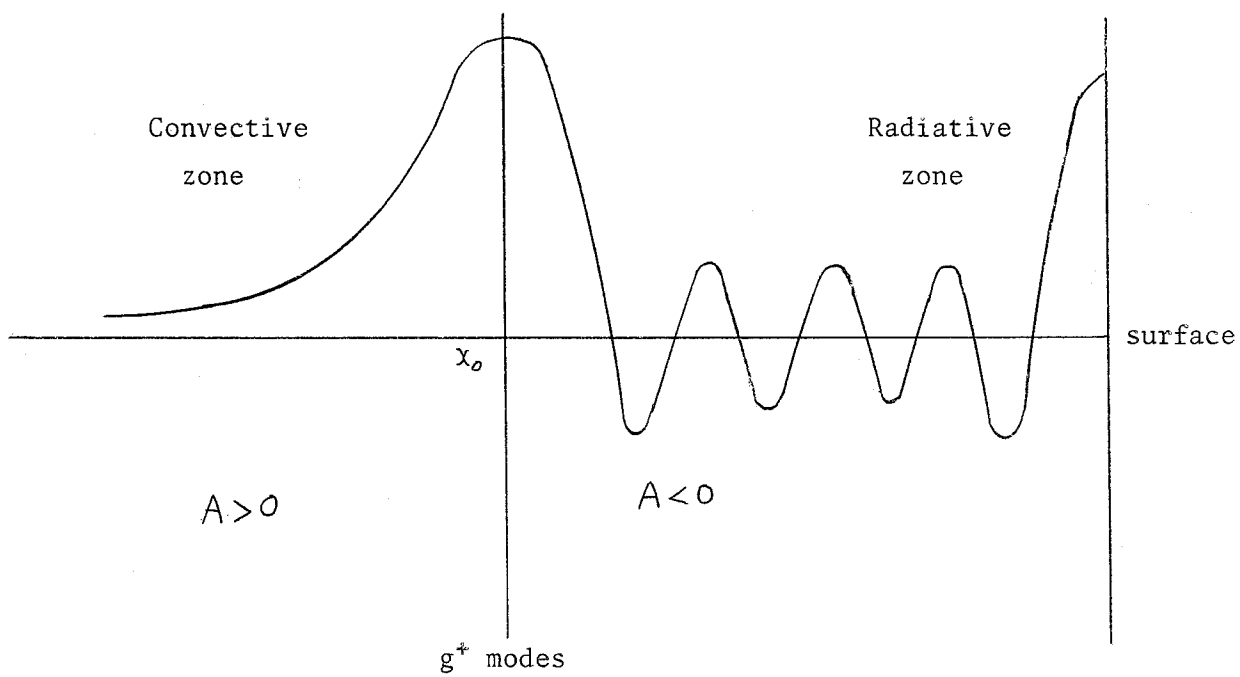
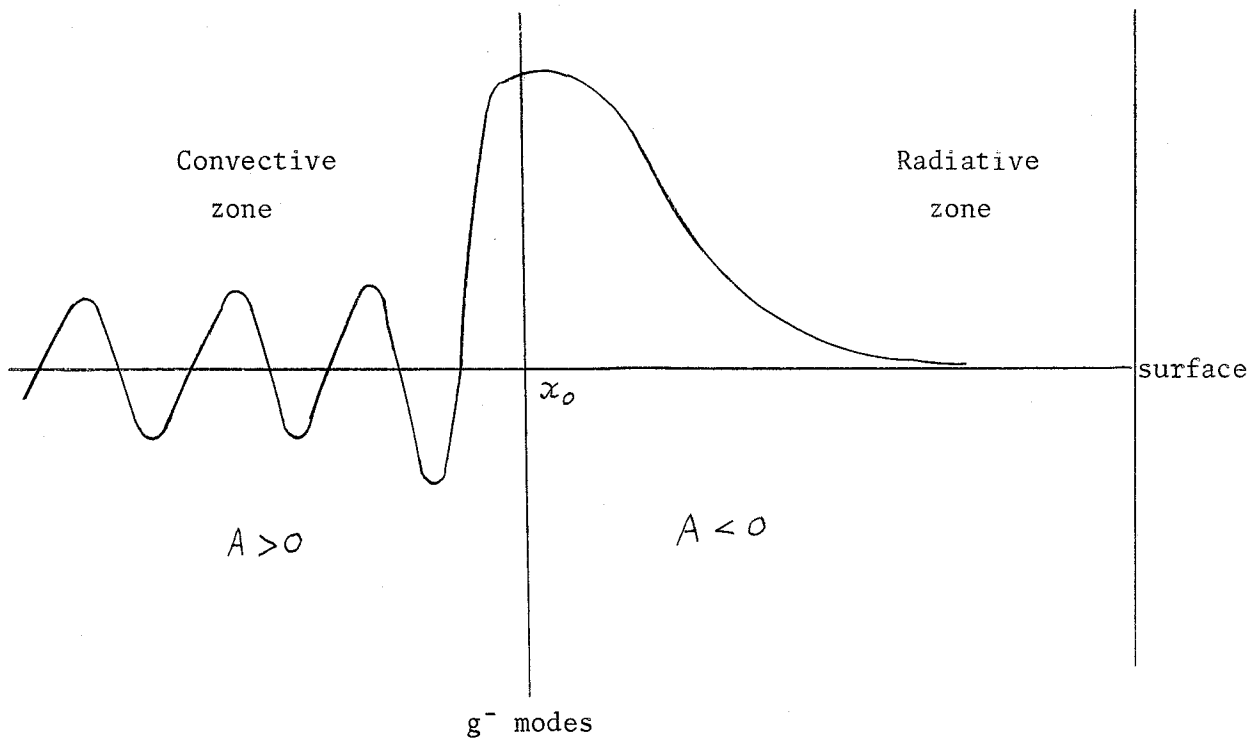
$$H_p = - \left(\frac{\partial \log p}{\partial r} \right)^{-1} \quad (44)$$

One sees that the condition above is nothing else than the Schwarzschild criterion of dynamic stability.

Thus one has three kinds of modes, which are plotted here along the frequency scale, and labeled according to Cowling:



The f-mode is the fundamental mode, or Kelvin's mode. The eigenfunctions of g^- modes and g^+ modes (gravity modes) are:



3) Asymptotic behaviour of the gravity modes

The equation (42) has singularities near the boundaries, which complicate the solution. We show here the treatment of one of them, the surface ($\chi = 1$), following a method given by Olver (1954-1955), which is an extension of that given by Langers (1935).

We define a new function $\omega(\chi)$ by:

$$\omega(\chi) = \left[- \left(\frac{\sigma^2 + gA}{\rho \nu^2} \right) \right]^{-1/2} y(\chi) \quad (45)$$

where y is the same function as previously. This function obeys to the second-order equation:

$$\frac{d^2 \omega}{d\chi^2} - \omega \left[\frac{n(n+1)}{\sigma^2 \chi^2} gA + \frac{1}{4} \frac{n_e^2 - 1}{(1-\chi)^2} + O \left(\frac{1}{1-\chi} \right) \right] = 0 \quad (46)$$

n_e : polytropic index near the surface

$$\frac{n_e + 1}{n_e} = \lim_{\chi \rightarrow 1} \left(\frac{\partial \log p}{\partial \log \rho} \right)_{star} \quad (47)$$

Near the surface, A is equivalent to $1/(1-\chi)$, thus near the singularity, the term in $1/\sigma^2$ ceases to be the leading term in the brackets of (46).

We introduce now a new variable η and a new function $W(\eta)$:

$$W(\eta) = \left(\frac{d\chi}{d\eta} \right)^{1/2} \omega(\chi) \quad (48)$$

with $\frac{\partial}{\partial \eta}$ designated by $\dot{}$, e.g. (46) becomes:

$$\dot{W} - W \left[\dot{\chi}^2 \frac{n(n+1)gA}{\sigma^2 \chi^2} + \dot{\chi}^2 \left(\frac{1}{4} \frac{n_e^2 - 1}{(1-\chi)^2} + \dots \right) + \dot{\chi}^{1/2} \frac{d^2}{d\eta^2} (\dot{\chi}^{-1/2}) \right] = 0 \quad (49)$$

Near the singularity, the relation between η and χ is chosen as follows:

$$\frac{d\eta}{d\chi} = \left[- \frac{n(n+1)}{U\sigma^2} \frac{gA}{\chi^2} \right]^{1/2} \quad (50)$$

where the choice of U is free. We choose:

$$\frac{d\eta}{d\chi} = \frac{1}{(1-\chi)^{1/2}} \left[1 + a_1(1-\chi) + \dots \right] \quad (51)$$

which defines the parameter U .

$$\dot{W} - W \left[-U + \frac{1}{\eta_e} \left(n_e^2 - \frac{1}{4} \right) + g(\eta) \right] = 0 \quad (52)$$

where

$$g(\eta) = O(1) \quad (53)$$

Olver gives the solution of this equation in the form of an expansion with respect to U :

$$W = P(u, \eta) \sum_{s=0}^{\infty} \frac{A_s(\eta)}{u^s} + \frac{\dot{P}}{U} \sum_{s=0}^{\infty} \frac{B_s(\eta)}{u^s} \quad (54)$$

where $P(u, \eta)$ is the solution of the simplified equation:

$$\ddot{P} - P \left[-U + \frac{\gamma}{\eta_e} \right] = 0 \quad (55)$$

the constant γ being here $\gamma = n_e^2 - \frac{1}{4}$. Putting the expansion of W in the equation (52), one gets two relations between the functions A_s and B_s .

$$2\dot{A}_{s+1} - \dot{B}_s - B_s g = 0 \quad (56)$$

$$\ddot{A}_s - 2\dot{B}_s - g A_s = 0 \quad (57)$$

For $s = 0$:

$$A_0 = 1 \quad B_0 = - \int_0^{\eta} \frac{1}{2} g(t) dt \quad (58)$$

$$A_1 = f(B_0) \rightarrow B_1 \rightarrow A_2 \quad \text{etc.} \quad \dots$$

These whole series may be computed.

Here:

$$P(u, \eta) = \eta^{1/2} J_{n_e}(u^{1/2} \eta) \quad (59)$$

J_{n_e} is the Bessel function of index n_e

$$y = \frac{p^*}{\rho} = K p^{-1/2} \left(-\frac{gA}{x^2} \right)^{1/4} \tau_s^{1/2} \left[J_{n_e}(\tau_s) - \left(\frac{1}{2Ux} \int_0^{\eta} g(t) dt \right) J_{n_e+1}(\tau_s) + \dots \right] \quad (60)$$

where

$$\tau_s = U^{1/2} \eta = \int_x^1 \left[-\frac{n(n+1)}{\sigma^2} \frac{gA}{x^2} \right]^{1/2} dx \quad (61)$$

Near the surface $\tau_s \sim (1-x)^{1/2}$ and $\rho \sim (1-x)^{n_e}$, and one verifies that $y \rightarrow \text{constant}$.

Far enough from the surface:

$$y = K p^{-1/2} \left(-\frac{gA}{x^2} \right)^{1/4} \left(\frac{2}{\pi} \right)^{1/2} \cos \left(\tau_s - n_e \frac{\pi}{2} - \frac{\pi}{4} \right) \quad (62)$$

This solution can be connected to that which comes from the interior and

which can be derived by the same method near the singular point which is there the boundary of a convective zone ($x = x_c$)

$$\eta = K_1 \rho^{-1/2} \left(-\frac{gA}{x^2} \right)^{1/4} \left(\frac{2}{\pi} \right)^{1/2} \cos \left(\tau_c - \frac{2\pi}{6} - \frac{\pi}{4} \right) \quad (63)$$

with here

$$\tau_c = \int_{x_c}^x \left[-\frac{n(n+1)gA}{\sigma^2 x^2} \right]^{1/2} dx \quad (64)$$

The continuity condition yields $K = \pm K_1$ and:

$$\left(\frac{n(n+1)}{\sigma^2} \right)^{1/2} \int_{x_c}^1 \left(-\frac{gA}{x^2} \right)^{1/2} dx = k \pi + \left(n_e + \frac{2}{3} + 1 \right) \frac{\pi}{2} \quad (65)$$

which gives the asymptotic value for the high frequencies:

$$\frac{1}{\sigma_0} \approx \frac{(k + k_0)}{\sigma_0 \sqrt{n(n+1)}} \quad \text{when } \sigma \rightarrow 0 \quad (66)$$

(k_0 and σ_0 are constants depending only on the structure of the star.)

II Non-Radial Forced Oscillations

In a double star, the tidal forces caused by one component produce forced oscillations in the other star. The equation of motion is then written:

$$\frac{D}{Dt} \underline{v} = -\frac{1}{\rho} \underline{\nabla} p - \underline{\nabla} (\phi + u) \quad (67)$$

where ϕ is the gravitational potential of the star, and u the potential of the external forces. A general theory of the tides in a rotating star is still lacking. We give here some properties of the equilibrium tides in a rotating star, and of the dynamical tides in a non-rotating star.

1) General properties of the equilibrium tides

We neglect the inertial terms $D\underline{v}/Dt$

$$-\frac{1}{\rho} \underline{\nabla} p = \underline{\nabla} (\phi + u) \quad (68)$$

Consequently, the pressure and the density are constant on an equipotential

surface. The entropy, depending only from p and ρ is also constant on an equipotential. If we assume that the transformation following the motion is adiabatic, we see that the fluid particles must stay on the same equipotential. Thus the motion is also isochoric, and the continuity equation yields:

$$\underline{\nabla} \cdot \underline{v} = 0 \quad (69)$$

The Lagrangian perturbations of the density and the pressure are equal to zero. We consider U as a perturbation ($\underline{\nabla} U_0 = 0$)

$$\frac{\partial}{\partial t}(\phi' + U') + \underline{v} \cdot \underline{\nabla} \phi_0 = 0 \quad (70)$$

to the first order, the vertical component of the velocity is thus given by:

$$v_R = -\frac{1}{g} \frac{\partial}{\partial t}(\phi' + U') \quad (71)$$

This holds only for a non-rotating star; if we take the rotation into account:

$$\frac{\partial}{\partial t} \rightarrow \left(\frac{\partial}{\partial t} + \Omega \frac{\partial}{\partial \varphi} \right) \quad (72)$$

$$v_R = -\frac{1}{g} \left[\frac{\partial}{\partial t} + \Omega \frac{\partial}{\partial \varphi} \right] (\phi' + U') \quad (73)$$

Ω is the angular velocity of rotation, and the z-axis is assumed to be the rotation axis.

We expand the outer potential in a Fourier series:

$$U = \sum_{n,m,l} u_{n,m,l} P_n^m(\cos \theta) \cos(m\varphi - l\omega t) \quad (74)$$

ω is the orbital angular velocity of the perturbing component. If the rotation axis is perpendicular to the orbital plane, the most important case is $n = 2$. Order of expansion terms (e: excentricity of the orbit):

$m \backslash l$	0	1	2	3
0	1	e	e ²	---
2	e ²	e	1	e

With this form of the outer potential, and neglecting for simplicity, the perturbation of the inner potential:

$$V_R = \frac{U_{e,m,m}}{g} (m\Omega - l\omega) x^n P_n^m(\cos\theta) \sin(m\varphi - l\omega t) \quad (75)$$

Now we have to construct also the θ and φ components of the velocity.

Let us try at first a poloidal field of velocity

$$\underline{v}_p = \underline{\nabla} \times \underline{\nabla} \times (\chi_p \underline{r}) \quad (76)$$

If $\underline{\Omega}$ is constant:

$$\chi_p = \frac{v_R}{n(n+1)} \quad (77)$$

But this poloidal field does not conserve the angular momentum. The equation of motion can be written:

$$\frac{D}{Dt} \underline{v}_p + 2\underline{\Omega} \times \underline{v}_p + \underline{\omega} \varphi (n \sin\theta \underline{v}_\theta \cdot \underline{\nabla} \underline{\Omega}) = -\frac{1}{\rho} (\underline{\nabla} p' - \frac{\rho'}{\rho} \underline{\nabla} p + \rho \underline{\nabla} v')$$
(78)

with

$$\frac{D}{Dt} = \frac{\partial}{\partial t} + \underline{\Omega} \cdot \frac{\partial}{\partial \varphi} \quad (79)$$

(We neglect $\underline{\nabla} \phi'$: Cowling's approximation.) Let us take the curl of this equation:

$$\underline{\nabla} \times \left[\frac{D}{Dt} \underline{v}_p + 2\underline{\Omega} \times \underline{v}_p + \underline{\omega} \varphi (2 \sin\theta \underline{v}_\theta \cdot \underline{\nabla} \underline{\Omega}) \right] = -\underline{\nabla} \cdot \frac{1}{\rho} \times \underline{\nabla} p' + \underline{\nabla} \cdot \frac{\rho'}{\rho^2} \times \underline{\nabla} p \quad (80)$$

There are no radial components in the second side of (80), but the Coriolis force introduces a radial component in the first side. We have thus to add a toroidal field to the poloidal field above:

$$\underline{v}_T = \underline{\nabla} \times [\chi_T \underline{r}] \quad (81)$$

(Any solenoidal field can be separated in the sum of a poloidal field and a toroidal field.) Let us expand this toroidal field into its Fourier components:

$$\begin{aligned} & 0 \\ & \sum c_s(r) \frac{m}{\sin\theta} Y_{s+1}^m \\ & \sum c_s(r) i \frac{dY_{s+1}}{d\theta} \end{aligned} \quad (82)$$

and try to connect these functions c_s with those which describe the poloidal field. More generally, we shall relate the toroidal field to a

field which is given by the expansion (such a field occurs in the dynamical tides, because the velocity field is then not divergence-free:

$$\begin{aligned} & \sum a_s(r) Y_s^m \\ & \sum b_s(r) \frac{dY_s^m}{d\theta} \\ & \sum b_s(r) \frac{\sin Y_s^m}{\sin \theta} \end{aligned} \quad (83)$$

Introducing (82) and (83) in the equation of motion, one gets:

$$\begin{aligned} & [(s+1)(s+2)(m\Omega - l\omega) - 2m\Omega] c_s = \\ & = \frac{(s-m+1)(s+2)}{2s+1} \left[2_s \Omega b_s - \frac{1}{r} \frac{d}{dr} (r^2 \Omega) a_s \right] + \frac{(s+m+2)(s+1)}{2s+1} \left[2(s+3) \Omega b_{s+2} - \frac{1}{r} \frac{d}{dr} (r^2 \Omega) a_{s+2} \right] \end{aligned} \quad (84)$$

In general, the poloidal field computed from the outer potential by Eq.(76) yields a non-zero right side in this equation, thus, there is a kind of resonance if the brackets multiplying c_s vanish; this occurs when:

$$\frac{\Omega}{\omega} = \frac{l}{m} \frac{(s+1)(s+2)}{s(s+3)} \quad (85)$$

If $n = 2$ $l = 2$ $m = 2$ there is resonance for:

$$\frac{\Omega}{\omega} = \frac{6}{5} \quad (86)$$

which is a very plausible value in a double star, for the rotation period and the orbital period tend to become equal. This result is true only if Ω is constant. If Ω depends on r , the resonance is confined in the correspondent spherical layer. If Ω depends also on θ , the resonances are given by the eigenvalue of the operator D:

$$D(\chi) = m M(\chi) - l\omega L(\chi) \quad (87)$$

where:

$$L(\chi) = \left[-\frac{m^2}{\sin^2 \theta} + \frac{1}{\sin \theta} \frac{\partial}{\partial \theta} \sin \theta \frac{\partial}{\partial \theta} \right] \chi \quad (88)$$

$$M(\chi) = - \left[\frac{\Omega m^2}{\sin^2 \theta} + \frac{2}{\sin \theta} \frac{\partial}{\partial \theta} (\Omega \cos \theta) \right] \chi + \frac{1}{\sin \theta} \frac{\partial}{\partial \theta} (\Omega \sin \theta) \frac{d\chi}{d\theta} \quad (89)$$

If Ω depends only on r :

$$D(\chi) = (m\Omega - l\omega)L + 2m\Omega \quad (90)$$

which, after splitting in spherical harmonics, is the same as Eq.(84).

In general, for a given rotation law the eigenvalues ω can be calculated from the extremum principle:

$$\frac{l\omega_{res}}{m} = \text{minimum} \frac{\int_0^\pi \chi M(\Omega, \chi) \sin\theta d\theta}{\int_0^\pi \chi L(\chi) \sin\theta d\theta} \quad (91)$$

ω resonance is only a function of Ω . Therefore, those resonances are confined in discrete spherical shells. If we take the inertial terms into account, the problem becomes very complicated. Formal solutions can be given, but they must be computed numerically. The Coriolis force is then going to connect the toroidal field to the poloidal field, through the equation of motion:

$$U_{ext} \longrightarrow V_G \xrightarrow{\text{Coriolis force}} V_T$$

whereas in the equilibrium tides there is no feed-back from the toroidal field.

2) Dynamical tides without rotation:

We can expand the functions describing the forced oscillation into a series of eigenfunctions f_i :

$$f = \sum c_i f_i \quad (92)$$

where c_i is connected to the Fourier component of the outer potential by

$$c_i = \frac{U_{n,m}}{g} \frac{1}{\sigma^2 - \sigma_i^2} C_i \quad (93)$$

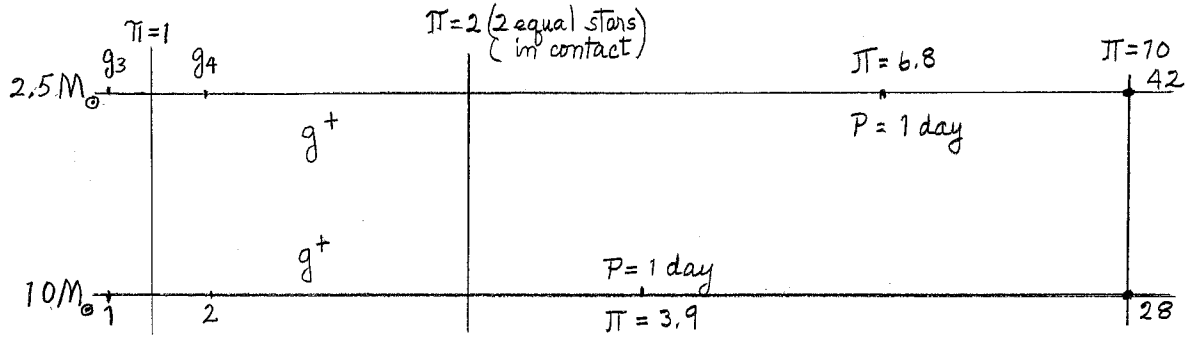
C_i depends only on the structure of the star:

$$C_i = R^2 \frac{\int_m \nabla [x^n Y_n^m] \cdot \delta r_i dm}{\int_m (\delta r_i \cdot \delta r_i) dm} \quad (94)$$

Let us show that the interesting frequencies are small enough to be treated by the asymptotic method: If \mathcal{T} is the dimensionless period

$$\Pi = \left(\frac{GM}{\sigma^2 R^3} \right)^{1/2} \quad (95)$$

One can sketch the period-spectrum of two typical main-sequence stars as follows:



The numbers give the rank of the harmonics. (These values are given without rotation.) If one tries to calculate C from Eq.(94), one has to push the expansions at least to the second order in σ , but this can be avoided by transforming the numerator:

$$I = \int_V \nabla \cdot (x^n Y_n^m \rho \underline{\delta r}) dv - \int_V x^n \cdot Y_n^m \nabla - (\rho \underline{\delta r}) dv \quad (96)$$

One finds the following asymptotic behaviour when $\sigma^2 \rightarrow 0$ (g^+ modes)

$$C_i = (-1)^i C_R(n, \text{structure of the star}) \left(\frac{\sigma^2 R^3}{GM} \right)^{1/2} (4 + \frac{1}{3} - n_e) \quad (97)$$

when the eigenfunctions a_i are taken equal to 1 at the surface. Introducing the non-dimensional variable s :

$$s^2 = \frac{\sigma^2 R^3}{GM} \quad (98)$$

The amplitude at the surface, $a(1)$, is

$$a_i(1) = \frac{U_{n,m}}{gR} \left[A_j(1) + C_R \sum_{i=j}^{\infty} \frac{(-1)^i}{s^2 - s_i^2} s_i^{(4 + \frac{1}{3} - n_e)} \right] \quad (99)$$

where j is taken large enough so that one can replace C_i by its asymptotic value above.

If $s^2 > 0$ the series converges if $n_e > 4 + \frac{1}{3}$

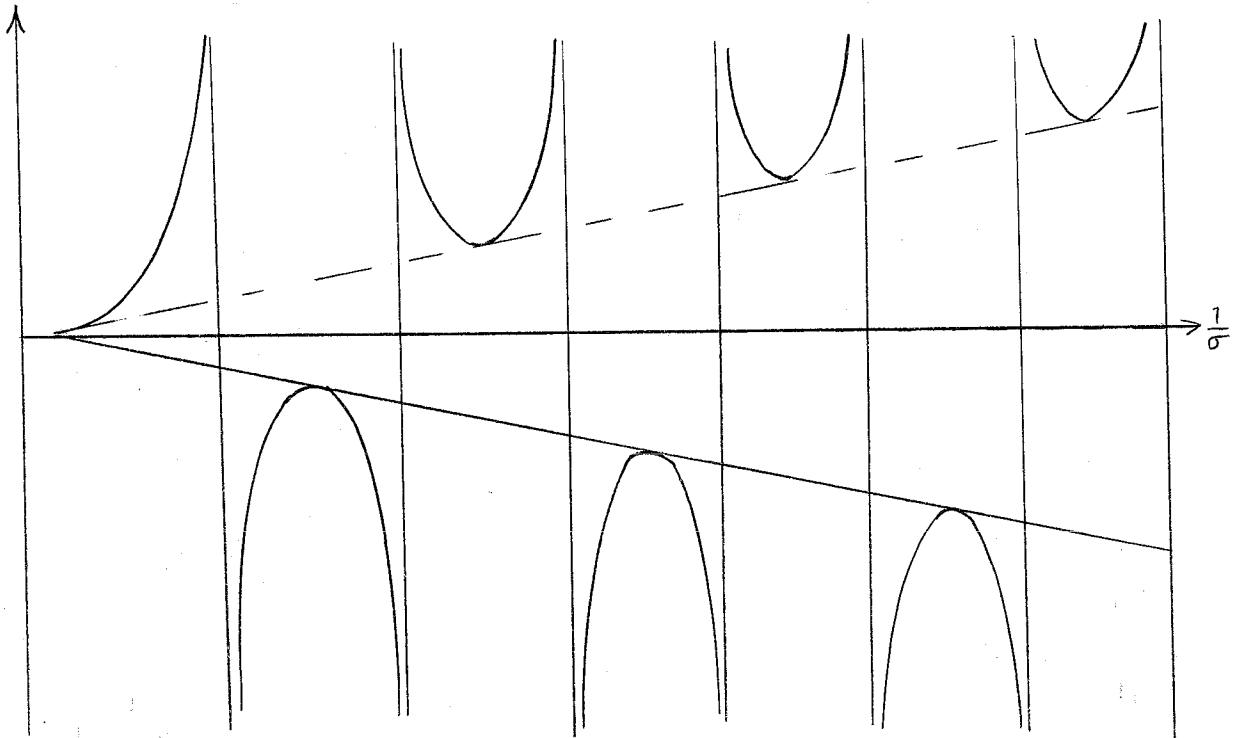
If $s^2 = 0$ the series converges if $n_e > 2 + \frac{1}{3}$

Between the resonances k and $k + 1$:

$$a(1) = \frac{U_{n,m}}{gR} \left[A_j(1) - (-1)^k \frac{\pi}{2} C_k s_0 s_k \left(\frac{4}{3} - n_e \right) \right] \quad (100)$$

where $1/s_0$ is the distance between two eigenperiods.

Thus, the amplitude at the surface grows with decreasing s , because $n_e > \frac{4}{3}$. It is like a multi-resonance phenomenon.



In the real stars, the radiative damping, important near the surface, reduces the amplitude of the oscillation.

3) Effects due to the radiative damping and viscosity

This study has only been done so far in the case of the equilibrium tides. The major causes of dissipation are the radiative damping in the radiative zones, and the eddy viscosity in the convective zones. There, one can take for the coefficient of eddy viscosity:

$$\nu = \frac{1}{3} \bar{\ell} \cdot \bar{v} \quad (101)$$

where $\bar{\ell}$ is the mean free course (\simeq scale height of the pressure in a mixing-length theory) and \bar{V} the mean convective velocity.

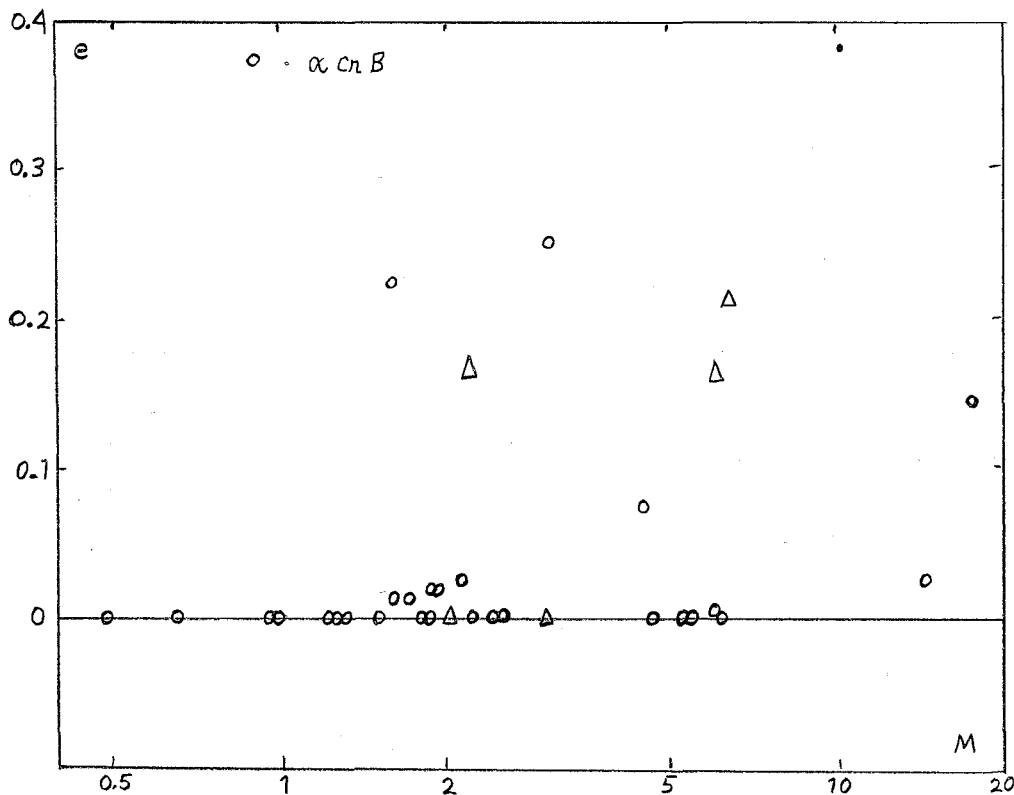
In the double stars, the existence of an outer convective zone seems to be important for the circularization of the orbits. The e -folding time for the synchronization of the rotation in the convective zone with the orbital motion is then:

$$\tau_R \sim (1 \text{ day}) P^4 \quad (102)$$

(P : period in days)

The e -folding time of the circularization of the orbits is:

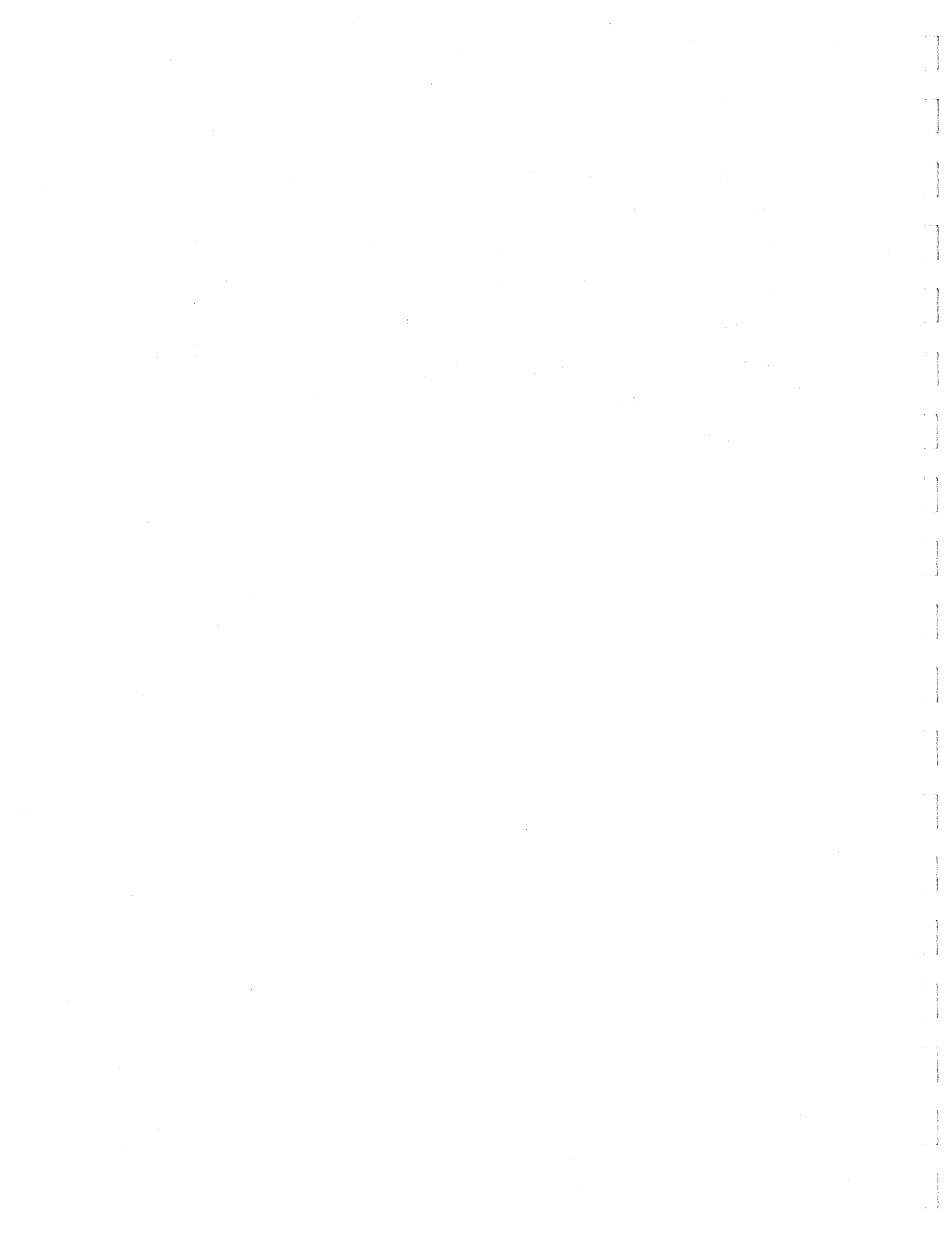
$$\tau_c \sim (1000 \text{ days}) P^{\frac{16}{3}} \quad (103)$$



The eccentricity of the orbits of eclipse binaries versus the mass of their secondary component. The elements come from the Kopal and Shapley catalog (1956).

This agrees with the observations. Close binaries with components of mass less than 1.6 solar mass show circular orbits, with only one exception, α Cr B, for which however the theory predicts a synchronization time of several billions of years, according to its high orbital period (17 days). The radiative damping strongly depends on the position in the meridional plane; thus it leads to a differential rotation which may be unstable. The associated e-folding time is however much longer (fraction of the lifetime of a star).

Notes submitted by
Jean-Luc Auré



ABSTRACTS



GEOPHYSICAL INVERSE PROBLEMS

George E. Backus

Abstract

A gross Earth datum is a single measurable number describing some property of the whole Earth, such as mass, moment of inertia, or the frequency of oscillation of some identified elastic-gravitational normal mode. We suppose that a finite set \mathcal{G} of gross Earth data has been measured, that the measurements are inaccurate, and that the variance matrix of the errors of measurement can be estimated. We show that some such sets of measurements determine the structure of the Earth within certain limits of error and except for fine-scale detail. That is, from some sets \mathcal{G} it is possible to compute localized averages of the Earth structure at various depths. These localized averages will be slightly in error, and their errors will be larger as their resolving lengths are shortened. We show how to determine whether a given set \mathcal{G} of measured gross Earth data permits such a construction of localized averages, and, if so, how to find the shortest length scale over which \mathcal{G} gives a local average structure at a particular depth if the variance of the error in computing that local average from \mathcal{G} is to be less than a specified amount. We apply the general theory to the linear problem of finding the depth variation of a frequency-independent local elastic dissipation (Q) from the observed damping rates of a finite number of normal modes. We also apply the theory to the nonlinear problem of finding density versus depth from the total mass, moment and normal-mode frequencies, in case the compressional and shear velocities are known.

THE OPTIMAL STRUCTURE OF TURBULENT TRANSPORT PROCESSES

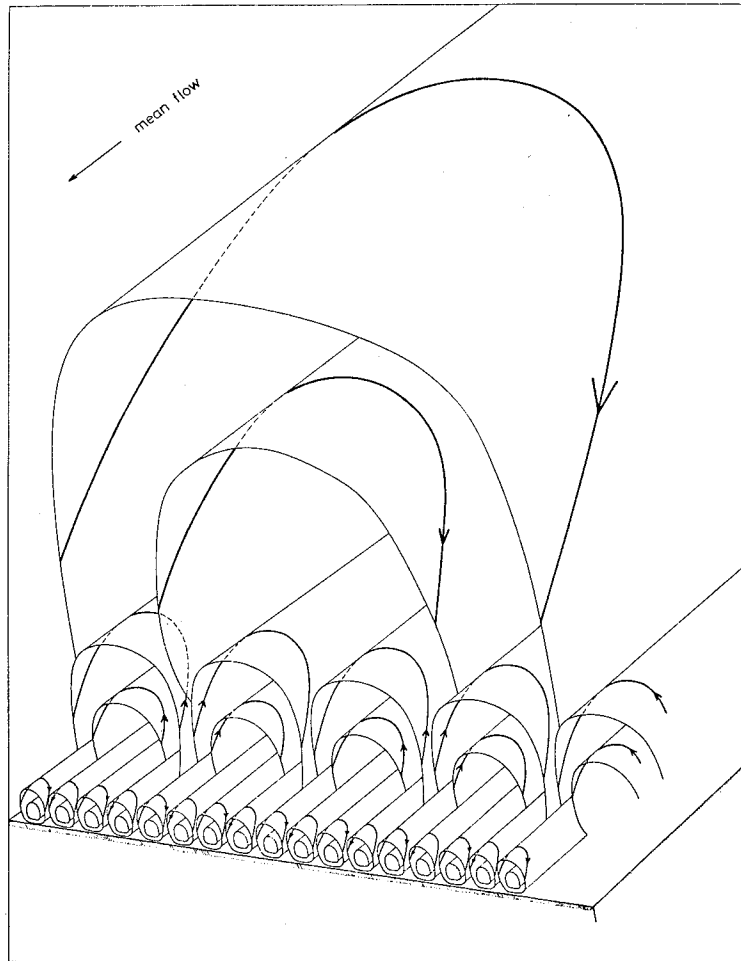
Freidrich Busse

The basic difficulty of the theory of turbulence is the fact that expressions for averaged quantities can not be derived without the detailed knowledge of the fluctuating velocity field. Bounds, however, for averaged quantities can be derived without the detailed knowledge of the turbulent velocity field. This approach to the problem of turbulence was first used by Howard (1963) when he deduced an upper bound for the heat transport by turbulent convection. It has been shown (Busse, 1967, 1969) that analogous bounds for the momentum transport can be obtained in turbulent Couette, pipe, and channel flow. The idea of the bounding method is to find the maximum of the transport property among a manifold of vector fields, which contains among others all turbulent velocity fields which are solutions of the basic Navier-Stokes equations of motion. Such a manifold can be defined by the requirement that the vector fields satisfy the boundary conditions and the energy balance for the fluctuating part of the velocity field which can be derived from the basic equations. The determination of the maximum of the transport property among this manifold leads to a variational problem the solution of which provides the upper bound for the physically realized transport property. By adding more constraints for the admissible vector fields better bounds can be obtained and, in principle, a systematic way of constraining the manifold of vector fields to the manifold of solutions of the basic equation is possible. An obvious step in this direction is the use of the equation of continuity as constraint.

The solutions of the Euler equations corresponding to an extremum of

the variational functional have physical significance beyond their purpose of providing the upper bound. When the equation of continuity is used as constraint the Euler equations resemble the Navier-Stokes equations in many respects. They can be regarded for this reason as model equations of turbulence. There appears to exist, however, an even closer relation between the solution of the variational problem and the observed turbulence. The comparison with the experimental data indicates that the turbulent transport tends to approach the upper bound rather closely. A strong similarity is found between the observed structure of turbulence and the extremalizing vector field. For example, the profile of the mean flow corresponding to the asymptotic extremalizing vector case seems to be approached by the realized turbulent mean flow. The boundary layer structure of the extremalizing vector field in the case of shear flow consists of a sequence of streamwise orientated eddies which take turns in transporting the momentum to the boundary as shown in the Figure. The scale of subsequent eddies differs by a factor of Ψ which allows the approximate description of the extremalizing field by boundary layer techniques. The observations indicate the predominance of streamwise orientated eddies, although the velocity field necessarily has to be three-dimensional in contrast to the extremalizing vector field. Peaks in the spectrum of turbulence corresponding to the property that the optimal transport is attained by vector fields with discrete scales have been found by Deardorff and Willis (1967) in the case of turbulent convection.

The tendency of the physically realized turbulence to approach the structure of the optimal transport process is caused by the fact that the



laminar boundary layer close to the wall is unstable unless the transport of heat or momentum is sufficiently high. The application of a stability criterion of the form $Re < Re_c$ for laminar shear flow with the Reynolds number Re shows that the momentum transport has to grow at least like Re^2 which is the same dependence as the upper bound. Hence the physically realized momentum transport should exhibit this dependence asymptotically.

DIFFERENTIAL ROTATION IN STELLAR CONVECTION ZONES

Freidrich Busse

The dynamical effects of rotation on thermal convection in a fluid layer of spherical shape induce an equatorial acceleration. Special properties of the convection zone which have been assumed in earlier theories on the differential rotation of the sun are not required. To demonstrate the mechanism all properties of stellar atmospheres which are not essential for the mechanism are neglected. The mathematical problem of convection in a rotating Boussinesq fluid subject to temperature and gravity fields of spherical symmetry is considered. An expansion in powers of the convection amplitude \mathcal{E} is introduced. The first order of this expansion describes the onset of the thermal instability of the static fluid shell. In order to simplify the analysis an additional expansion in powers of the basic rotation rate λ is used. In the case of no rotation convective modes corresponding to the spherical harmonics $P^m_e(\cos\theta)e^{im\varphi}$ with $m = -\ell, \dots, +\ell$ are equally possible. The value ℓ is determined by the requirement that the Rayleigh number has to assume the minimum value as a function of ℓ . It is shown without using specific models that in the case of rotation the mode with $|m| = \ell$ is distinguished as the mode with the lowest critical Rayleigh number. When this mode is realized a mean flow in azimuthal direction is generated by the action of the non-linear advection terms in the order $\mathcal{E}^2\lambda$ of the equation of motion. A more specific model using the limit of a thin shell shows that the induced azimuthal flow agrees with respect to form and sign with the observed differential rotation on the sun. An order of magnitude estimate using the velocity observed in the

giant convection cells on the sun (Bumba, 1967) and an eddy viscosity of about 10^{12} cm²/sec representing the influence of the small scale convective motions gives reasonable agreement with the value of the solar equatorial acceleration.

References

- Busse, F. H., 1969 Report MPI-PAE/Astro 15, Max-Planck-Institut für Physik, Munich.
Bumba, V., 1917 Proc.Int.School of Physics Enrico Fermi, Course XXXIX, ed. P.A.Sturrock, Academic Press, New York and London.

AN APPROACH TO THERMAL CONVECTION

Douglas O. Gough

A method of solution of the equations for thermal convection has been investigated in collaboration with E. A. Spiegel and J. Toomre: For a plane parallel layer of fluid each physical variable is expressed as a sum of a horizontal average and a fluctuation, and the horizontal structure of the fluctuation at each height is expanded in a series of orthogonal solutions of the equation $\nabla^2 f = -a^2 f$. By projecting the equations of motion onto the functions f , a sequence of differential equations is obtained for the height and time dependence of the coefficients of the series. The series are then truncated. It is hoped that even if the truncation is severe, a suitable choice of these functions f that are retained will yield a good approximation to the gross features of the flow, even at high Rayleigh numbers. The motivation for this approach was the desire to obtain a tractable technique for describing convection in natural circumstances; convection in the presence of mean shear, rotation or composition gradients, for example, and penetration into stable regions can all be studied by this method for

laboratory conditions, so that some idea of the accuracy of the description can be obtained, and extrapolation to natural conditions can be made without recourse to supplementary physical assumptions.

Attention is restricted to Boussinesq convection in a horizontally infinite fluid layer, and only one term in the series expansion is retained. Provided the horizontal average of f^3 is not zero, nonlinear fluctuation interactions are represented and even the time independent equations contain the Prandtl number. Finite amplitude solutions for marginally supercritical Rayleigh numbers, asymptotic solutions at high Rayleigh numbers and numerical solutions for a wide range of Rayleigh numbers and Prandtl numbers are discussed, and a brief comparison with experiment is made.

BARYON INHOMOGENEITY IN THE EARLY UNIVERSE

Edward R. Harrison

Various topics are discussed concerning galaxy formation; in particular the nature of the initial conditions. In the early high-density high-temperature universe, matter and antimatter are in equilibrium and exist in almost equal quantities. In a co-moving element of volume the ratio of the baryon number ΔB to the number of baryons B is small. We must explain why initially there is a slight excess of matter over antimatter and why finally after annihilation, matter is concentrated into objects of galactic size. By proposing that the initial conditions consist of spatial variations in the baryon number rather than variations in density (i.e., the number of baryons), we can link together the survival and aggregation of matter or antimatter as closely related subjects.

REPORT ON THE BOEING TURBULENCE SYMPOSIUM

Robert H. Kraichnan

On 23-27 June 1969, a Symposium on Turbulence was held in Seattle under sponsorship of the Boeing Company. It brought together a substantial fraction of the active workers on fundamental aspects of the subject and may be viewed as a successor to the meetings held in Marseilles in 1961 and in Kyoto in 1966. The proceedings of the Seattle meeting will appear as a special issue of the Journal of Fluid Mechanics. The following comments have to do with the state of research in turbulence theory, as reflected in the talks and discussions of this Meeting.

The primary reaction of this observer is that no revolution has taken place since the Marseilles meeting in 1961. There is an increased interest in the higher statistical structure of turbulence, particularly the intermittency effects in the small scales at high Reynolds numbers (papers by Gibson and Stewart), statistics of high-order velocity derivatives in decaying turbulence (Frenkiel), and the structure of the turbulent-nonturbulent interface, together with the entrainment process (a whole Session). A Session on the so-called deductive turbulence theories showed that proponents of the various formal schemes presented during the past fifteen years are still, for the most part, going their separate ways. Papers by Bradshaw and Saffman illustrated an increasing interest in developing statistical equations, for shear flows, which do not pretend to derive from first principles but which are a cut above the mixing-length level and deal with the detailed point-to-point transport processes. This observer is dismayed by the variety of competing models which seem feasible. Busse reported on

the application to shear flow of the optimal-transport approach developed by himself, Malkus, and Howard. This work still seems to stand apart from the directions taken by most workers in turbulence theory, despite the fact that the rigorous bounds on heat transport in turbulent convection are about the only rigorous results in all of turbulence theory. Finally, three topics of special interest, and relatively recent vintage, were non-Newtonian turbulence (Lumley), the demonstration of a turbulent dynamo mechanism in hydromagnetic turbulence that has a net velocity-vorticity correlation (Moffatt), and turbulence in stratified fluids (Pao).

CONVERGENTS TO TURBULENCE FUNCTIONS*

Robert H. Kraichnan

Analytical formulations for turbulence are characterized by infinite, usually divergent series of one sort or another. An important example is the Taylor-series development in time of turbulence averages that is obtained by repeated differentiation of the Navier-Stokes equation. The coefficients of these series embody prescribed properties of the turbulence; for the Taylor series, they are the initial moments of the velocity field. This talk presents some techniques for constructing converging, uniformly valid approximations for turbulence functions by combining qualitative information with the quantitative data provided by the first few coefficients of series like the Taylor series in time. We start by establishing, or assuming on physical grounds, a sufficiently healthy integral representation for the unknown function. Usually, this will be simply a spectral

* Presented at the Boeing Turbulence Symposium, Seattle, 1969.

representation, and we assume this case for what follows. The coefficients of the original Taylor series then give the moments of the spectrum function. The unknown spectrum function is then expanded in a set of complete continuous orthogonal functions, and it is found that the first n coefficients of the Taylor series fix the first n coefficients of the orthogonal-function expansion, provided that the latter are of the form $P_n(a)w(a)$, where a is frequency, and the P_n are orthogonal polynomials with respect to the positive weight function $w(a)$. We find that this expansion results in uniformly convergent approximations to the original time function under very broad conditions. The speed of convergence depends on how well the choice of $w(a)$ matches the unknown spectrum. We shall illustrate the power of such manipulations by setting up the Taylor series for the Lagrangian velocity correlation of a particle that follows a random velocity field and obtaining numerically accurate approximations, valid for all t , from the first three non-vanishing terms. The results are checked against a computer experiment. The weight $w(a)$ may be taken either arbitrarily (Gaussian $w(a)$), or, better, it may be taken as the direct-interaction approximation to the unknown spectrum function. The expansion procedure then gives higher corrections to the direct-interaction approximation. We shall also outline the use of the orthogonal-expansion method to obtain successive approximations to Kolmogorov's constant and the constant in Batchelor's k^{-1} law for a convected passive scalar. Finally, these methods can be used as an extrapolation device for extending to steady-state, or long times, the results of computer experiments, or of integrations of approximate equations like the direct-interaction equations, that have been carried for only a few time steps.

THE GENERATION OF LONGSHORE CURRENTS

Michael Longuet-Higgins

It is well known that when sea waves or swell approach a straight coastline at an oblique angle, a mean current tends to be set up parallel to the coastline. Such longshore currents and the associated longshore transport of sand and other sedimentary material, are of prime importance for both the coastal engineer and the submarine geologist.

Many hypotheses, of a very rough kind, have been put forward to account for this phenomenon. But a recent review of the subject by Galvin (1967) arrives at the justifiable conclusion that: "A proven prediction of longshore current velocity is not available, and reliable data on longshore currents are lacking over a significant range of possible flows".

It has often been suggested (as for example by Putnam, Munk and Traylor (1949) that the magnitude of the longshore current is related in some way to the energy or to the momentum of the incoming waves. Of these two approaches, that employing momentum is the more promising since momentum is conserved, whereas energy may be dissipated by breaking and other processes not immediately associated with sediment transport.

It goes without saying that any momentum theory must be correctly formulated. The estimate of the momentum made by Putnam, Munk and Traylor (1949) has been already criticised on theoretical grounds by Galvin (1967). Moreover Inman and Quinn (1949) showed that in order to make the theory fit the observations, the friction coefficient C would have to be assumed to vary over a wide range of 3-1/2 orders of magnitude. A modified version of Putnam, Munk and Traylor's theory due to Galvin and Eagleson (1965) also

requires a large variation in C .

The aim of this paper is to introduce a more satisfactory estimate of the momentum of the incoming waves, based on the concept of the radiation stress as developed by Longuet-Higgins and Stewart (1960, 1961, 1962, 1963, 1964). This estimate of the excess transfer of momentum due to the waves has already proved remarkably successful in the prediction of several wave phenomena, particularly the wave set-up, or change in mean level of the sea surface in the breaker zone (Longuet-Higgins and Stewart 1963, 1964).

In the present paper it is pointed out, first, that there exists a simple and precise relationship between the total longshore thrust exerted by the incoming waves on the one hand, and their direction and amplitude in deep water on the other. This result may be derived either from the concept of the radiation stress mentioned earlier, or by a direct evaluation of the momentum flux due to the waves.

Next it is shown that the local longshore stress due to the waves is very simply related to the local rate of dissipation of wave energy, regardless of whether this is due to wave breaking or to bottom friction. Hence, using the known relation of breaker height to local depth in the surf zone, one can estimate accurately the local longshore stress due to the waves.

Knowing the local longshore wave stress, it is then possible to write down an equation of motion for the longshore current which involves in general both the bottom friction and lateral mixing between horizontal eddies. To make further progress in predicting the longshore current, one must make some assumption about the nature of the horizontal mixing in the surf zone. This we do by adopting a certain form for the coefficient μ_e of the hori-

zontal eddy viscosity, as a function of distance from the shoreline.

In fact we assume in the following that μ_e is proportional to the offshore distance $|x|$ multiplied by a typical velocity \sqrt{gh} , where h denotes the local depth. When the bottom slope \mathcal{J} is uniform, this particular form for the eddy viscosity yields a very simple analytical form for the longshore current profile, which is found to be in remarkably good quantitative agreement with the detailed laboratory measurements by Galvin and Eagleson (1957). In particular, the position and magnitude of the maximum current appear to be correctly predicted.

While this paper was in preparation, the author's attention was drawn to an unpublished manuscript by Dr. A. T. Bowen (1969) in which the concept of radiation stress was also applied to the same problem. Dr. Bowen also takes into account both bottom friction and horizontal mixing, though in a somewhat different way. The two approaches, and the differences between them, are discussed. It appears that the present formulation of the theory is both simpler analytically and better in agreement with available observations.

ON MULTI-VARIABLE ASYMPTOTIC EXPANSIONS*

Edward L. Reiss

1. Introduction

The multi-time or multi-variable method is extensively used to obtain asymptotic expansions of the solutions of a variety of fluid mechanics and other physical problems (1). A typical problem involves a small

* This work was supported by the Office of Naval Research, U.S. Navy.

parameter ϵ . An asymptotic expansion of the solution is desired that is valid as $\epsilon \rightarrow 0$. In the multi-variable method, this expansion is usually a power series in ϵ . The coefficients in the series are assumed to be functions of the independent variables and new "auxiliary" independent variables. The auxiliary variables are functions of the genuine independent variables and ϵ . The auxiliary variables give the method its flexibility but they also introduce a certain amount of indeterminacy. It is thus frequently necessary to appeal to a variety of intuitive mathematical and physical arguments in order to determine the expansion coefficients. The application of the multi-variable method therefore relies on the cleverness of the practitioner.

In this talk we indicate, for an initial value problem for a simple linear ordinary differential equation, how to eliminate the need for intuitive arguments in applying the multi-variable method. We present a systematic and rational procedure to determine the expansion coefficients and prove the uniform asymptotic convergence of the expansion. The procedure and technique of proof are clearly applicable to a wide class of problems.

2. Formulation

We consider the initial value problem for the damped linear oscillator:

$$Ly \equiv y'' + 2\epsilon y' + y = 0, t > 0; \quad y(0; \epsilon) = 0, \quad y'(0; \epsilon) = 1 \quad (2.1)$$

A prime denotes differentiation with respect to t and $\epsilon > 0$ is proportional to the damping coefficient. We wish to obtain an asymptotic expansion of the solution $y(t; \epsilon)$ that is uniform in t as $\epsilon \rightarrow 0$.

The solution of (2.1) is

$$y(t; \epsilon) = (1 - \epsilon^2)^{-1/2} e^{-\epsilon t} \sin \left[(1 - \epsilon^2)^{1/2} t \right]. \quad (2.2)$$

For any $\epsilon > 0$ we have, $\lim_{t \rightarrow \infty} y(t; \epsilon) = 0$. However, if we formally set $\epsilon = 0$ in (2.1) or in (2.2), then

$$y(t; 0) = \sin t. \quad (2.3)$$

Thus $\lim_{\epsilon \rightarrow 0} y(\infty; \epsilon) \neq \lim_{t \rightarrow \infty} y(t; 0)$ and if $y(t; \epsilon)$ converges as $\epsilon \rightarrow 0$ to (2.3), the convergence is not uniform in t for $t \geq 0$. There is a "boundary layer at $t = \infty$."

The non-uniform convergence can also be detected when we attempt to solve (2.1) by a regular perturbation expansion*. If we insert

$$y = \sum_{j=0}^M y_j(t) \epsilon^j + R_M \quad (2.4)$$

in (2.1), where $R_M(t; \epsilon)$ is the remainder after $M+1$ terms, and equate to zero the coefficients of ϵ^j , $j = 0, 1, \dots, M$, we obtain

$$y_j'' + y_j = -2y_{j-1}; \quad y_j(0) = 0, \quad y_j'(0) = \delta_{j0}, \quad j = 0, 1, \dots, M. \quad (2.5)$$

Here δ_{j0} is the Kronecker delta. We solve (2.5) with $j = 0$ and then $j = 1$ and insert the results in (2.4) with $M = 2$. This gives

$$y = \sin t + [-\sin t + t \cos t] \epsilon + R_2. \quad (2.6)$$

Because of the factor t in the bracketed term, (2.6) clearly does not give a uniform expansion for $t \geq 0$.

3. The Two-Time Method

We define the auxiliary independent variable t_1 by

$$t_1 = \epsilon t. \quad (3.1)$$

We seek a representation of the solution in the form,

$$y = \sum_{j=0}^M y^j(t, t_1) \epsilon^j + R_M. \quad (3.2)$$

The superscript in y^j is an index and $y^{-1} \equiv 0$. The equations for y^j , which are determined in the usual way by substituting (3.2) into (2.1) are,

* In the terminology of this paper, the regular perturbation expansion is the one-time method.

$$y_{tt}^j + y^j = Z_1^{j-1}, \quad y^j(0,0) = 0, \quad y_t^j(0,0) = -y_{t_1}^{j-1}(0,0) + \delta_{j0} \quad (3.3)$$

$j = 0, 1, \dots, M,$

and the equations for R_M are,

$$L R_M = r_M \equiv Z_1^M \in^{M+1} + Z_2^M \in^{M+2} \quad (3.4)$$

$$R_M(0) = 0, \quad R'_M(0) = Y_M \equiv -y_{t_1}^M(0,0) \in^{M+1},$$

where Z_k^j are defined for $j = 0, 1, \dots, M$ by

$$Z_2^j \equiv -y_{t_1, t_1}^j - 2y_{t_1}^j, \quad Z_1^j = Z_2^{j-1} - 2(y_{t_1}^{j-1} + y_{t_1}^j). \quad (3.5)$$

Since R_M satisfies (3.4) it is easy to prove the estimate,

$$|R_M(t; \epsilon)| \leq \alpha |Y_M| + \beta \|r_M\| / \epsilon, \quad \|r_M\| \equiv \max_{0 \leq t \leq t_1} |r_M(t)|, \quad (3.6)$$

where α and β are constants independent of t and ϵ .

We obtain y^0 by setting $j = 0$ in (3.3) and solving the resulting initial value problem. This yields,

$$y^0(t, t_1) = A^0(t_1) \sin t + B^0(t_1) \cos t, \quad (3.7)$$

where A^0 and B^0 are to be determined subject to the conditions

$$A^0(0) = 0, \quad B^0(0) = 1. \quad (3.8)$$

We wish to choose A^0 and B^0 to make R_0 as small as possible as $\epsilon \rightarrow 0$. We conclude from (3.4) and (3.6) with $M = 0$, that A^0 and B^0 must satisfy,

$$Z_1^0 \equiv 0 \quad (3.9)$$

We insert (3.7) in (3.9) and use the definition (3.5) of Z_1^0 and find that

(3.9) implies that

$$A_{t_1}^0 + A^0 = B_{t_1}^0 + B^0 = 0 \quad (3.10)$$

The solution of (3.10) and (3.8) combined with (3.7) gives

$$y^0 = e^{-t_1} \sin t. \quad (3.11)$$

Since Z_2^0 is uniformly bounded in t we conclude from the definition of r_0

in (3.4) that $r_0 = O(\epsilon^2)$. Since $Y_0 = 0$ for y^0 given by (3.11), we obtain

from (3.6) that as $\epsilon \rightarrow 0$,

$$R_0 = O(\epsilon) = O(1). \quad (3.12)$$

In (3.12) and in the remainder of the paper the "o" symbol implies that the estimate is uniformly valid in t for $t \geq 0$.

The higher order coefficients are obtained in the same way from (3.3) and the condition that $Z_1^j = 0$. For example,

$$y^1 = -(t_1/2)e^{-t_1} \cos t, \quad R_1 = o(\epsilon) \text{ as } \epsilon \rightarrow 0. \quad (3.13)$$

In fact, we can prove that $R_M = o(\epsilon^M)$ as $\epsilon \rightarrow 0$ for any integer $M \geq 0$ and hence (3.2) is a uniform asymptotic expansion of the solution of (2.1).

4. The Three-Time Method

The auxiliary variables are, t , defined in (3.1) and $t_2 \equiv e^2 t$.

We seek an expansion in the form,

$$y = \sum_{j=0}^M y^j(t, t_1, t_2) e^j + R_M. \quad (4.1)$$

Thus we obtain, as in the two-time method,

$$y_{tt}^j + y^j = Z_1^{j-1}, \quad y^j(0,0,0) = 0, \quad y_{t_1}^j(0,0,0) = -y_{t_1}^{j-1}(0,0,0) - y_{t_2}^{j-1}(0,0,0) + \delta_{j0}, \quad (4.2)$$

$j = 0, 1, \dots, M,$

$$L R_M = r_M \equiv \sum_{k=1}^4 Z_k^M \epsilon^{M+k}, \quad R_M(0) = 0, \quad R_M'(0) = Y_M, \quad (4.3)$$

where the Z_k^j and Y_M are now defined for $j = 0, 1, \dots, M$ by

$$\begin{aligned} Z_4^j &\equiv -y_{t_2 t_2}^j, \quad Z_3^j \equiv -2(y_{t_1 t_2}^j + y_{t_2}^j) + Z_4^{j-1}, \\ Z_2^j &\equiv -2y_{t t_2}^j - y_{t_1 t_1}^j - 2y_{t_1}^j + Z_3^{j-1}, \quad Z_1^j \equiv -2(y_{t t_1}^j + y_t^j) + Z_2^{j-1}, \\ Y_M &\equiv -[y_{t_1}^M(0,0,0) + y_{t_2}^{M-1}(0,0,0)] \epsilon^{M+1} - y_{t_2}^M(0,0,0) \epsilon^{M+2}. \end{aligned} \quad (4.4)$$

From (4.2) with $j = 0$ we conclude that y^0 is given by (3.7) where A^0 and B^0 are now functions of t_1 and t_2 . They are determined so as to make R_0 as small as possible as $\epsilon \rightarrow 0$. We therefore find that A^0 and B^0 must satisfy

$$Z_1^0 = Z_2^0 = 0 \quad (4.5)$$

and hence that y^0 and R_0 are given by

$$y^0 = e^{-t_1} \sin(t - t_2/2), \quad R_0 = O(\epsilon^2) = o(\epsilon), \text{ as } \epsilon \rightarrow 0. \quad (4.6)$$

The greater flexibility provided by the additional variable t_2 allows us to make Z_2^0 vanish in addition to Z_1^0 . The remainder R_0 is smaller for the three-time method than the two-time method, c.f. (3.12) and (4.6). It is easy to prove by induction that, $y^j \equiv 0$ for j an odd integer, (4.1) is a uniform asymptotic expansion of the solution of (2.1) for every even integer $M \geq 0$ and $R_M = O(\epsilon^{M+1})$ as $\epsilon \rightarrow 0$.

5. The N-Time Method

The solution y of (2.2) is independent of ϵ^j for $j > 1$ and odd. Thus the four-time method involves the variables t, t_1, t_2 and $t_3 \equiv \epsilon^4 t$. By applying the same reasoning as in the two and three-time methods, we obtain

$$y^0 = e^{-t_1} \sin(t - t_2/2 - t_3/8), \quad R_0 = O(\epsilon) \text{ as } \epsilon \rightarrow 0. \quad (5.1)$$

The estimates for R_0 are the same for the three and four-time methods, see (4.6) and (5.1), since $Y_0 = O(\epsilon^2)$ in both cases.

The leading term of the N-time expansion is

$$y^0 = e^{-t_1} \sin [P_N(\epsilon)t], \quad P_N(\epsilon) \equiv \sum_{j=0}^{N-2} a_j \epsilon^{2j}, \quad (5.2)$$

where P_N is the binomial expansion to $N-1$ terms of $(1 - \epsilon^2)^{1/2}$. Since $Y_0 = O(\epsilon^2)$ for $N \geq 3$, $R_0 = O(\epsilon)$ and no improvement is obtained in the estimates of R_0 using more auxiliary variables. The uniform asymptotic convergence of the N-time expansion to M-terms can also be proved.

6. Expansion of the Solution

The results of the multi-time methods can be obtained by appropriately expanding the explicit solution (2.2). If we let

$$(1 - \epsilon^2)^{1/2} = P_N(\epsilon) + \phi(\epsilon), \quad (6.1)$$

where P_N is defined in (5.2) and ϕ is the remainder in the binomial expansion of $(1 - \epsilon^2)^{1/2}$, then

$$\sin[(1 - \epsilon^2)^{1/2} t] = \sin P_N t \cos \phi t + \cos P_N t \sin \phi t \quad (6.2)$$

We insert (6.2) in (2.2) and expand $\cos \phi t$, $\sin \phi t$ and $(1 - \epsilon^2)^{-1/2}$ in power series in ϵ . This yields the expansion

$$y = \sin P_N t \sum_{j=0}^{\infty} \alpha_j \epsilon^j + \epsilon^{2N-1} \cos P_N t \sum_{j=0}^{\infty} \beta_j \epsilon^j. \quad (6.3)$$

The coefficients α_j and β_j depend on a_j and the coefficients in the expansion of $(1 - \epsilon^2)^{-1/2}$. It can be shown that the M-term expansion for the N-time method is obtained by appropriately truncating the series in (6.3). The leading term of the N-time method is thus equivalent to the N^{th} Rytov approximation (2) of y .

7. Concluding Remarks

There are a minimum number of auxiliary variables, namely one, that are required to obtain a uniform asymptotic expansion. There are a maximum number of auxiliary variables, namely two, that give uniform asymptotic expansions with the smallest estimate of the remainder. The higher time methods give different expansions of the solution which may be more desirable for certain purposes. The same estimate of the remainder is achieved by either using a two-term expansion with the two-time method, see (3.13) or a one-term expansion with the three-time method, see (4.6). However, it is computationally simpler to determine the last expansion.

In previous approaches to multi-time methods it is necessary to analyze the equations for the higher order coefficients in order to determine the lower order ones. The procedure we employ has the important

practical advantage that y^0 is completely determined by the problem satisfied by y^0 , y^1 is completely determined by y^0 and the problem satisfied by y^1 , and so forth. However, the main practical contribution of our analysis is a precise recipe to determine y^j without resorting to intuitive and other arguments.

The present methods have been successfully applied to other less trivial linear ordinary differential equations of higher order and to a class of initial boundary value problems for partial differential equations.

References

1. Cole, J.D., 1968 Perturbation Methods in Applied Mathematics, Blaisdall, New York.
2. Keller, J.B., 1969 Accuracy and Validity of the Born and Rytov Approximations, to appear in the J. Optical Soc.

ACOUSTIC WAVES IN RAPIDLY VARYING INHOMOGENEOUS FLUIDS

Edward L. Reiss

An ideal, inviscid and inhomogeneous fluid occupies a region in X, Y, Z space. The density and the constant pressure of the fluid in static equilibrium are denoted by $\rho_0(\underline{X})$ and $p_0 = \text{constant}$. Here \underline{X} is the radius vector with components (X, Y, Z) . The additional pressure, $p(\underline{X}, T)$, that is caused by a small disturbance of the fluid satisfies the linear equation (1),

$$p_{TT} - c_0^2 \Delta p + c_0^2 [\nabla \ln \rho_0 \cdot \nabla p] = 0 \quad (1)$$

Here T is time, ∇ is the spatial gradient, Δ is the Laplace operator and $c_0^2(\underline{X})$ is the adiabatic sound speed in the equilibrium state.

We define new dimensionless independent variables $\underline{x} = (x, y, z)$ and t by

$$x, y, z = X/L, Y/L, Z/L, \quad t = CT/L, \quad (2)$$

and a new dependent variable v by

$$v(\underline{x}, t) \equiv p(\underline{x}, t) / [\rho_0(\underline{x})]^{1/2} \quad (3)$$

Here L is a reference length and C is a reference speed. We insert (2)

and (3) in (1) and find that v must satisfy the Klein-Gordon equation

$$v_{tt} - c^2 \Delta v + H v = 0, \quad (4)$$

where

$$c^2(\underline{x}) \equiv c_0^2(\underline{x})/C^2, \quad H(\underline{x}) \equiv C^{-2}[-\Delta \ln \rho^* + \frac{1}{2}(\nabla \ln \rho^*)^2], \quad \rho^*(\underline{x}) \equiv \rho_0(\underline{x}) \quad (5)$$

and Δ and ∇ are now the Laplacian and gradient with respect to \underline{x} .

A fluid is defined to be rapidly varying if $|\nabla \rho^*|$ is "large" compared to ρ^* . More precisely, the fluid is rapidly varying if

$$H(\underline{x}) = \lambda^2 h(\underline{x}) \quad (6)$$

and $\lambda^2 \gg 1$ for an appropriately defined λ . For example, $\lambda^2 \equiv \max_{|\underline{x}| \leq L_0} |H(\underline{x})|$

where L_0 is a space scale over which the solution is to be studied or it is the radius of the region if the region is finite.

In this talk we shall consider only one-dimensional motions.

Thus c and h are functions of x only, $v(x, t)$, $\Delta = \partial^2/\partial x^2$ and (4) is the one-dimensional Klein-Gordon equation. In particular we study the signalling or impact problem for (4). We refer to it as Problem I. It is to determine a solution $v(x, t)$ of (4) for $x, t > 0$ which satisfies the initial and boundary conditions:

$$v(x, 0) = v_t(x, 0) = 0, \quad x \geq 0, \quad (7a)$$

$$v(0, t) = \psi(t), \quad t \geq 0. \quad (7b)$$

The prescribed function $\psi(t)$ is called the impact data. For simplicity we assume that it has the following properties.* $\psi(0) = 0$; $\psi(t)$ is bounded for all $t \geq 0$ and it is a $C^\infty[0, \infty]$ function; for some $n > 0$, $d^n \psi(0)/dt^n \neq 0$.

* More general data can also be treated by the present method.

The last condition and (4) and (7a) imply that a discontinuity propagates from $x = t = 0$ with speed $c(x)$ along the characteristic curve

$$t = D(x) \equiv \int_0^x \frac{d\xi}{c(\xi)}. \quad (8)$$

In the region $t < D(x)$, $v \equiv 0$ is the unique solution of Problem I. Thus we need only consider $t \geq D(x)$.

We investigate the solution of Problem I as $\lambda \rightarrow \infty$. We assume that for x bounded away from zero v has a formal asymptotic expansion,

$$v(x,t) \sim J_0(\lambda S) \sum_{n=0}^{\infty} v^n(x,t) \lambda^{-n} + J_1(\lambda S) \sum_{n=0}^{\infty} w^n(x,t) \lambda^{-n} \quad (9)$$

as $\lambda \rightarrow \infty$. Here $J_n(z)$ is the Bessel function of order n . The phase function $S(x,t)$ and the coefficients v^n and w^n satisfy first order partial differential equations. They are solved by a ray method. The primary rays are curves passing through the origin $x = t = 0$ and lying in the domain of the influence of the origin. We call them the corner rays. We refer to (9) as the corner expansion. The structure of the rays depends on the coefficients $c(x)$ and $h(x)$. If, for example, $h(x) \leq h(0)$, then the corner rays are monotonically increasing functions of x and t with bounded slope. If, however, $h(x)$ is monotone increasing, then for every corner ray there is an $x = x_T$ at which the ray has a vertical tangent. We call x_T a turning point. If $h'(x_T) \neq 0$, then there is no real continuation of the ray for $x > x_T$. The ray is continued for $x < x_T$ and increasing t by the turned ray issuing from the turning point. The turned ray will eventually reach and be reflected at the boundary $x = 0$; see Fig.1. If $h(x)$ has a local maximum at $x = x_S$, then there are three possible continuations of the ray. It may be continued as a corner ray for $x > x_S$, a turned ray for $x < x_S$, and a ray parallel to the

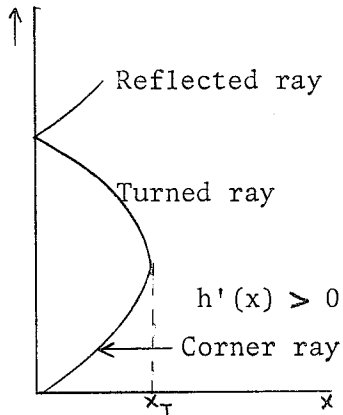


Fig. 1
Sketch of the rays at a turning point x_T .

t -axis at $x = x_S$. In this case a shadow region is formed with the lower part of the shadow boundary consisting of the turned ray for $x < x_S$ and the continued ray for $x > x_S$: see Fig. 2. No corner rays enter the shadow, and the expansion (9) is not defined in this region. Another expansion, involving diffracted rays is required in the shadow.

We shall not consider this expansion in the present lecture.

The canonical problem to evaluate the undetermined coefficients of the leading term in (9) is Problem I with constant coefficients. This problem is solved by studying an integral representation of the solution. We can prove that for fixed x and t with x bounded away from zero \mathcal{U} has

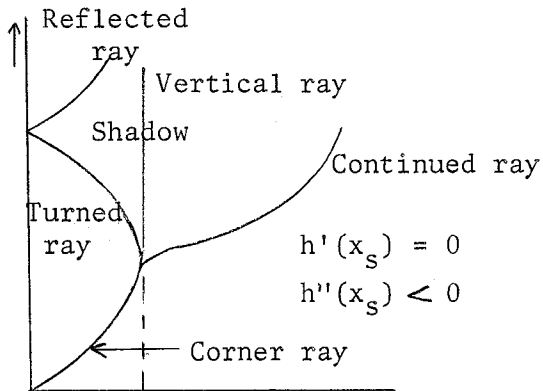


Fig. 2
Sketch of the rays at a splitting point x_S

the asymptotic expansion (9) as $\lambda \rightarrow \infty$. The coefficients v^j and w^j can be completely determined in the case of constant c and h . The expansion is not uniform in x and t in a region containing (8) since the estimate of the remainder is not uniformly valid. The zeros of J_n prevent a uniform estimate.

Another expansion which is valid near and at $x = 0$ is also obtained from the integral representation. It is called the end expansion. We can

prove that it is a uniform asymptotic expansion of the solution of Problem I with constant coefficients for $t > 0$ and $\lambda x \geq 0$ and bounded as $\lambda \rightarrow \infty$. It is of the form

$$v(x,t) \sim \exp[\lambda Q(x,t)] \sum_{j=0}^{\infty} W^j(x,t) \lambda^{-j}. \quad (10)$$

The end expansion for variable coefficients is obtained by assuming that near $x = 0$, v has an expansion in the form (10). The "phase" function Q and the coefficients are determined by solving phase and transport equations for Q and W^j by a ray method. The rays in this case are the lines $t = \text{const}$. The end expansion gives an exponentially small contribution in the shadow region.

The details of the analysis are given in (3).

References

1. Chernov, L.A. 1960 Wave Propagation in a Random Medium, McGraw Hill.
2. Reiss, E.L. One-Dimensional Impact Waves in Inhomogeneous Elastic Media, to appear in J.Appl.Mech.
3. Reiss, E.L. 1969 The Impact Problem for the Klein-Gordon Equation, S.I.A.M. J.Appl.Math. 17.

TIME-DEPENDENT CELLULAR CONVECTION

Juri Toomre

An approach for modelling non-linear convective motions in a thin horizontal layer of fluid has been discussed by Gough in the previous lecture. The model equations result from a truncated expansion of the velocity and temperature fields in terms of specified orthogonal horizontal eigenfunctions. The resulting system of non-linear partial differential equations capable of describing 3-D motions is parabolic in classification, involving the

vertical spatial coordinate and time. If a complete set of eigenfunctions is considered, these model equations would become analogous to the full Navier-Stokes equations within a Boussinesq approximation; all appropriate non-linear triad interactions are included. Gough has indicated that an expansion involving only one horizontal eigenfunction or planform, thereby representing motions such as simple rolls or hexagons, has always yielded steady-state numerical solutions. We consider here some consequences of the model equations as this expansion is truncated with two or three planforms, and indicate that the numerical solutions have some distinct points of contact with time-dependent laboratory convection.

The recent experiments by Deardorff and Willis (1967) and Krishnamurti (1969) have emphasized that the nature of the time-dependence and the spatial structure of laboratory convection is sensitive to both the Rayleigh number R and the Prandtl number σ . For $\sigma \gtrsim 6.8$, steady 2-D rolls persist up to $R \simeq 2 \times 10^4$, and then are replaced by steady 3-D approximately rectangular or hexagonal patterns. These detailed studies of the transition from 2-D to 3-D motions in the laboratory are consistent with the stability analysis of Busse. Periodic time-dependent 3-D motions are observed for $R \gtrsim 5 \times 10^4$, until aperiodic time-dependent motions are established at $R \approx 10^7$. These transitions occur at rapidly decreasing R for lower σ , with little evidence of any steady motions at the $\sigma \approx 2 \times 10^{-2}$ of mercury (Busse (1969)).

Numerical experiments with our model equations indicate the 2-D to 3-D transitions quite clearly. The principal results occur at higher R where periodic time-dependent solutions are obtained with both two or

three planform model equations, if the planforms are chosen so that the triad interaction terms are present. For instance a three planform set with a horizontal fundamental hexagon with wavenumber a_1 , and the two harmonic hexagons with $a_2 = \sqrt{3} a_1$ and $a_3 = 2a_1$, yields periodic time dependent solutions for $\sigma \geq 0(1)$. Similarly two planform sets of hexagons a_1 and a_2 (or a_3) indicate periodic time dependence, as do interacting rectangular planforms. As σ is decreased, transitions from periodic to aperiodic time-dependent motions are evident in the two planform solutions at R and σ values consistent with laboratory experiments.

The time-dependence however, occurs only within a narrow range of horizontal wavenumbers a_i for all these cases, with steady state solutions showing bifurcation features existing outside this time-dependent window. This window suggests a mechanism for predicting the preferred a_i . The periods of the time-dependent solutions are insensitive to position within the window, and are in close agreement with Krishnamurti's observed results for $2 \times 10^5 \lesssim R \lesssim 10^7$. This represents the first prediction of such periods by an energetically consistent non-linear model, and corresponds approximately to the orbit time of a fluid particle within the velocity field of the fundamental planform mode. The time mean Nusselt numbers for these solutions are about 5% higher than the laboratory results. A movie of these periodic computer solutions indicates significant temporal variations in the temperature and velocity fields which are approximately analogous to the observed laboratory results.

MAGNETIC BRAKING AND THE OBLIQUE ROTATOR MODEL

Leon Mestel

Gas flowing out from a non-magnetic rotating star remembers the angular momentum it had at the stellar surface, so that its angular velocity lags behind that of the star. If the star has a magnetic field, symmetric about the rotation axis, the non-uniform rotation of the out-flowing gas generates a twist in the magnetic field, which therefore exerts a torque on the gas, tending to restore co-rotation. In a steady state, as long as the gas flow is markedly sub-Alfvénic, the magnetic stresses do maintain approximate co-rotation, and most of the angular momentum transport is via the magnetic stresses. As the gas speed approaches the Alfvénic speed the non-uniform rotation becomes more marked, and roughly comparable proportions of angular momentum are carried by gas and field. Beyond the Alfvénic surface the gas feels less and less magnetic torque and so approaches a state of angular momentum conservation. In a strictly axisymmetric system it can be shown that the net outward flow of angular momentum, carried jointly by the gas and field, is equivalent to assuming strict co-rotation out to the Alfvénic surface, and strict angular momentum conservation beyond. The magnetically-controlled centrifugal forces assist the thermal pressure in driving out the gas; if the corona surrounding the star is comparatibely cool, it may be more correct to talk of a centrifugal pump rather than a thermal wind.

In the oblique rotator model for the magnetic variables the axis of the magnetic field no longer coincides with the rotation axis. The steady-state axisymmetric theory can be generalized by using a frame

rotating with the angular velocity $\alpha \underline{k}$ of the star. With the velocity \underline{V} in this frame parallel to the magnetic field \underline{B} , the total torque \underline{G} on the star can be written as

$$-\underline{G} = \alpha \underline{k} \times \int_{S_A-S} \underline{r} \times \rho (\underline{V} + \alpha (\underline{k} \times \underline{r})) d\tau + \int_{S_A} (\underline{r} \times \underline{n}) \left(p + \frac{B^2}{8\pi} \right) dS + \int_{S_A} \rho \underline{V} \cdot \underline{n} (\underline{r} \times (\alpha \underline{k} \times \underline{r})) dS,$$

where S is the stellar surface, S_A is the Alfvénic surface, defined by

$4\pi\rho \underline{V}^2 = \underline{B}^2$, p and ρ are pressure and density, and \underline{n} is the outward drawn unit normal. In the axisymmetric case only the last term survives, and the torque is parallel to the axis. In general all three terms survive. In addition to the braking component parallel to the rotation axis, there are now two extra components which cause the instantaneous axis to precess through the star, while the magnetic axis rotates in space.

The question of crucial interest for the oblique rotator is whether the angle between the two axes tends to increase or decrease. If the same magnetic braking process that is involved to explain the abnormally slow rotations of most of the magnetic stars will simultaneously reduce an initial obliquity to zero, then the oblique rotator model may be in trouble; but equally, if the obliquity is simultaneously increased to a large angle, the case for the model is strengthened. From computations done to date, it appears that the precessional torque can be of either sign, depending on the detailed flux distribution over the stellar surface. The tentative hypothesis is made that the same internal hydrodynamical processes that are presumably responsible for this flux distribution, may be also responsible - via dynamical coupling with a strong wind, flowing during at least part of the stellar lifetime - for the large mutual inclination of the magnetic and rotation axes.

References

- Mestel, L. 1966. Liège Symposium.
- Mestel, L. 1967. Stellar Magnetism in Plasma Astrophysics,
39th Enrico Fermi School, Varenna 1966.
- Mestel, L. 1968a. Mon.Not.R. Astr. Soc., 138: 359.
- Mestel, L. 1968b. Mon.Not.R. Astr. Soc., 140: 177.
- Mestel, L. and C.S.Selley. 1970 (in preparation)
- Selley, C.S. 1970 (in preparation)
- Weber, E.J., and L.Davis, Jr. 1967. Astrophys.J. 148: 27.